

Charité

UNIVERSITÄTSKLINIKUM MEDIZINISCHE FAKULTÄT DER HUMBOLDT-UNIVERSITÄT ZU BERLIN

Research Report
Trauma and Reconstructive Surgery
(Director: Prof. Dr. N. P. Haas)

2001 - 2002

Trauma and Reconstructive Surgery
- Research Laboratory -
Charité, Campus Virchow-Clinic
Humboldt-University of Berlin
Augustenburger Platz 1, D-13353 Berlin
Germany

Tel +49 (0)30 450 559079
Tel +49 (0)30 450 552012
Fax +49 (0)30 450 559969
email biomechanics@charite.de
http [//www.charite.de/unfallchirurgie](http://www.charite.de/unfallchirurgie)

Preface

It is indeed a pleasure to present our report of research activities 2001-2002. We thank you for your interest and your support during the last two years. We hope that this information is of use to you and look forward to continuing what has become excellent co-operation.

Berlin, January 2002

Prof. Dr. med. Norbert P. Haas

Table of Contents

Preface.....	3
Table of Contents	5
Introduction	8
Research Activities	10
<i>Accreditation according to DIN EN ISO/IEC 17025.....</i>	<i>10</i>
<i>Cartilage mechanics: A new device to diagnose cartilage degeneration.....</i>	<i>12</i>
<i>Bone straining of the intact and fractured proximal humerus under physiological-like loading.....</i>	<i>14</i>
<i>Radiofrequency treatment of partial-thickness cartilage defects in the sheep knee joint leads to cartilage injury.....</i>	<i>16</i>
<i>Mechanical conditions are essential in osteochondral defect healing.....</i>	<i>18</i>
<i>Does low-intensity pulsed ultrasound stimulate maturation of tissue engineered cartilage ?.....</i>	<i>20</i>
<i>Interfragmentary movements in the early phase of healing in distraction and correction osteotomies</i>	<i>22</i>
<i>Effect of partial weight bearing on fracture gap motion</i>	<i>24</i>
<i>New concepts in fracture stabilization: Comparison of different fixation principles and surgical approaches in an experimental ovine model</i>	<i>26</i>
<i>Time course of unstimulated and growth factor stimulated rat tibial healing</i>	<i>28</i>
<i>BMP-coating of titanium implants increases biomechanical strength and accelerates bone remodeling in fracture treatment.....</i>	<i>30</i>
<i>Quantification and localization of IGF-I and TGF-β1 during growth factor stimulated fracture healing</i>	<i>32</i>
<i>Differentiation but not proliferation of osteoblasts is stimulated by IGF-I and TGF-β1 in vitro.....</i>	<i>34</i>
<i>Antibiotic coated intramedullary titanium implants in prophylaxis of acute implant related osteomyelitis in rats</i>	<i>36</i>
<i>Osteogenesis and vascularization of the fracture callus are affected by local application of growth factors IGF-1 and TGF-beta 1</i>	<i>38</i>
<i>The influence of systemic GH- application on VEGF- expression and revascularisation during intramembraneous bone- healing</i>	<i>40</i>
<i>Locally administered Growth Hormone and it's mediator insulin-like growth factor exert similar effect on callus formation in a femur osteotomy model in rats.....</i>	<i>42</i>
<i>Poly(D,L-lactide) coating enhances osseous integration of mechanically loaded and unloaded Schanz' screws</i>	<i>44</i>

<i>Tibio-femoral loading during human gait</i>	46
<i>Kinematics of the in vivo sheep knee</i>	48
<i>Surgical approach in THA causes long term differences in periprosthetic femoral bone densities</i>	50
<i>THA loading arising from increased anteversion and offset may lead to critical cement stresses</i>	52
<i>Influence of muscle force simulation in vitro on the pre-clinical evaluation of the initial stem stability in THA</i>	54
<i>Influence of anchorage principle on the primary stability in cementless THA under physiologic-like loading conditions</i>	56
<i>The initial phase of Fracture healing is specifically sensitive to mechanical conditions</i>	58
<i>Capability of bone turnover markers to predict the course of bone consolidation during fracture healing</i>	60
<i>Influence of unreamed nailing and external fixation on the mechanical conditions during fracture healing</i>	62
<i>Mechanical Conditions in the Early Phase of Fracture Healing</i>	64
<i>Bone graft straining in Box and Cylinder Cervical Spine Interbody Fusion Cages</i> ..	66
<i>Biomechanical analysis of biodegradable interbody fusion cages augmented with Poly(propylene glycol-co-fumaric acid)</i>	68
<i>Biomechanical comparison of bioabsorbable cervical spine interbody fusion cages</i>	69
<i>Biomechanical comparison of cervical spine interbody fusion cages</i>	70
<i>Cage design significantly influences interbody fusion in a sheep cervical spine model</i>	71
<i>Biomechanical comparison of expandable cages for vertebral body replacement in the thoraco-lumbar spine</i>	72
<i>Biomechanical comparison of expandable cages for vertebral body replacement in the cervical spine</i>	73
<i>BMP-2 application by a Poly-(D,L-lactide) coated interbody cage In vivo results of a new carrier for growth factors</i>	74
<i>IGF-I and TGF-β1 application by a Poly-(D,L-lactide) coated cage promotes intervertebral bone matrix formation in the sheep cervical spine</i>	75
<i>Comparison of BMP-2 and combined IGF-I/TGF-β1 application in a sheep cervical spine fusion model</i>	76
<i>Dose-dependent effects of combined IGF-I and TGF-β1 application in a sheep cervical spine fusion model</i>	77
<i>Detection of alpha-smooth muscle actin (ASMA) containing contractile fibroblastic cells in knee arthrofibrosis tissue</i>	78
<i>Histologic comparisons of the ACL in humans, dogs, cows and sheep</i>	80

<i>Effect of Locally applied PDGF on cellularity, revascularisation and ultrastructural changes during ACL graft remodelling</i>	<i>82</i>
<i>Locally applied platelet derived growth factor-BB ameliorates structural properties of a free tendon graft after anterior cruciate ligament reconstruction</i>	<i>84</i>
<i>Comparison of tendon-to-bone healing using extracortical and anatomic interference fit fixation of soft tissue grafts in a sheep model of acl reconstruction</i>	<i>86</i>
<i>Crimp frequency is strongly correlated to myofibroblast density in human tendon tissue.....</i>	<i>88</i>
<i>Biocompatibility and osseous replacement of composite interference screws.....</i>	<i>90</i>
<i>Remodeling of the flexor tendon vs. bone patellar tendon bone graft after anterior cruciate ligament (ACL) reconstruction in a sheep model.....</i>	<i>91</i>
<i>Assessment and comparison of the tendon remodeling and the tendon-to-bone healing of a free allogenic and autologous graft for the reconstruction of the anterior cruciate ligament (ACL) in a sheep model.....</i>	<i>92</i>
<i>The impact of thermal radio-frequency shrinkage on the mechanical and histological properties of the chronically elongated ACL.....</i>	<i>94</i>
<i>Impact of tendon graft suturing on the interference fixation strength of quadrupled hamstring tendon grafts</i>	<i>96</i>
<i>Analysis of the tendon remodeling of a free allogenic and autologous graft for the reconstruction of the anterior cruciate ligament (ACL) in a sheep model.....</i>	<i>97</i>
<i>Comparison of the tendon-to-bone healing of free allogenic and autologous grafts for the reconstruction of the anterior cruciate ligament (ACL) in a sheep model</i>	<i>98</i>
<i>Immediate microcirculatory derangements in skeletal muscle and periosteum following closed tibial fracture.....</i>	<i>99</i>
<i>Fracture-induced periosteal microvascular injury: Characterizing the time course of changes in periosteum microcirculation.....</i>	<i>100</i>
<i>Temporal profile of microvascular dysfunction in tibial periosteum following closed soft tissue trauma in rats</i>	<i>102</i>
Peer Reviewed Publications	104
Awards.....	115
Research Guests	116
Students.....	116
Congresses – Symposia.....	118
Equipment.....	119

Introduction

It is a pleasure to present our report of research activities for the period 2001-2002. The last two years have been extraordinarily successful for the Research Laboratory of Trauma and Reconstructive Surgery, and we would like to use this opportunity to thank all our friends, scientific partners and sponsors, but also our research staff for their support during the last two years.

Our recent success was made possible only by the commitment of all those involved in our activities: Clinicians, scientists and technical staff have all performed their research in genuine partnership. Even though the research lab has provided "service" for those interested, our best results have come from partnerships and the tight interaction of groups from various scientific disciplines. This concept has helped to further streamline our research activities – specifically to meet the needs of our patients and to improve clinical treatment.

The research focal areas *Fracture Healing*, *Ligament Healing*, *Soft Tissue Trauma* and *Musculo-Skeletal Loading* were expanded considerably with regard to both personnel and space. The focal area *Spinal Research* has been installed and now provides a considerable contribution to our research output.

The research laboratory currently includes 27 employees from various scientific disciplines. In addition, three clinical colleagues are in "research rotation" and thereby strengthen the clinical expertise within the research staff.

The range of scientific activities described in this report were made possible by increasing third-party funding from 0.4 million in 1998 to 1.8 million in 2002. Specifically three major grants need to be mentioned:

In January of 2001, the Collaborative AO Research Center at the Charité was established, which will have a service life of up to six years and focuses on biological and mechanical factors that influence bone healing. The Collaborative AO Research Center is financed by the AO Foundation.

Secondly, and perhaps most outstandingly, the foundation of the Clinical Research Group "Bone Healing" was established in January, 2002. This Clinical Research Group is financed partially by the German Research Foundation (DFG) and partly by the medical faculty of the Charité. With this funding, the German Research Foundation intended to establish a structure that allows a long term commitment to research in a clinical setting, thereby strengthening clinical research. It is the intention of the DFG that upon a successful review after 3 years, the basic structure of the Clinical Research Group "Bone Healing" should be integrated in the research structure of the medical faculty.

Finally, we would like to acknowledge funding from the European Fund for Regional Development (EFRE) to establish the "Musculo-Skeletal Research Center Berlin (MRCB)". The MRCB was formally established in December 2002 and provides an open network of institutions engaged in musculo-skeletal research in the region of Berlin and Brandenburg. The initial focus is on improving bone healing by means of "Biotechnology" and "Information-Technology". In addition, the MRCB provides direct

support during the initial phase of start-up companies in the area of musculo-skeletal research.

Besides these large grants, a number of projects financed by the German Research Foundation, by federal funding (BMB+F, BfArM), as well as a series of foundation projects were awarded in 2001 and 2002. Details on all projects are given throughout this research report.

Finally, a considerable effort has been made to establish a quality control system throughout the research laboratory as a basis for the accreditation of the biomechanics laboratory. The laboratory was accredited in December 2002 according to the new DIN EN ISO/IEC 17025 standard. This effort in quality control shall provide our customers, as well as all scientists working in the lab, confidence in our work by defined internal standards.

Cooperative ventures are essential to our work and we would like to thank specifically all our academic and industrial partners on a national and international level. Close cooperation exists with various organizations of the Humboldt-University in Berlin, the biomechanics lab and the veterinary medicine department at the Free University, the Konrad-Zuse-Zentrum in Berlin, the engineering science departments of the Technical University in Berlin and the trauma surgery research department of the University of Ulm. International cooperative ventures with an exchange of scientific employees exist with the AO Research Institute in Davos, the Università degli Studi di Bologna, the Johns Hopkins University, the University of Pittsburgh and with Boston University.

A list of peer-reviewed original publications and both national and international academic prizes provide an impression of our research output. In addition to these, a multitude of conference contributions and patents have been awarded.

This report intends to give an overview of our activities and projects during the last years and may serve as initial information for those interested in a scientific exchange. For further information, please do not hesitate to contact us directly.

Berlin, January 2002

Prof. Dr.-Ing. Georg N. Duda

Research Activities

Accreditation according to DIN EN ISO/IEC 17025

Hoffmann JE, Zarnack F, Duda GN

In November 2002, our biomechanics laboratory received accreditation as a testing laboratory for medical products. Checked by the 'Central Office of the Countries for Health Protection with Medical and Medicine Products' (ZLG), the lab has been approved by the authority for the physical and mechanical examination of synthetic materials for medical products. After confirmation from the accreditation office, registration took place under the registration number: ZLG-P-671.02.08 .

Akkreditiert durch



Zentralstelle der Länder
für Gesundheitsschutz
bei Arzneimitteln und
Medizinprodukten

vertreten im



ZLG-P-671.02.08

The basis for the accreditation of service and research laboratories in Germany is the international standard DIN EN ISO/IEC 17025 "General requirements of the authority for test and calibration laboratories" which has been available since April 2000. In this standard, the relevant requirements from the ISO 9001 or 9002 test activities, have been implemented.

The accreditation is now valid for an initial period of 2 years, when the ZLG will supervise whether the lab fulfills the conditions for further accreditation. In addition, audits are to be carried out in the accredited department by the ZLG.

Each accredited laboratory must confirm that it operates according to the conditions layed down and upholds a quality management system that conforms with all the required standards. This creates confidence in the security and traceability of all results produced within the lab. This accreditation helps increase client confidence but also benefits the lab by helping it to receive international recognition. The accreditation of a test laboratory is a reliable confirmation of quality by an independent reviewer.

For the establishment of the quality management system, a quality manual of the research laboratory of trauma and reconstructive surgery has been prepared. Contained within it are the regulations concerning the quality management system and all relevant procedures. The co-workers are regularly trained in quality workshops on the basics of good laboratory practice. A basis for all relevant quality procedures

and responsibilities has also been created according to the quality management system.

With the accreditation of the biomechanics laboratory, the research department of trauma and reconstructive surgery has strengthened its position within the field of biomechanical and clinical research. The aim of a quality management system in our research lab is to ensure the transparency and effectiveness of all organizational and operational procedures for the execution and completion of analyses and investigations in accordance with previously validated test sequences. To examine the suitability of these processes, a professional system for the constant improvement of all processes and co-workers is to be developed. Co-operation with internal and external customers should be promoted in order to be able to offer an optimum research service.

Cartilage mechanics: A new device to diagnose cartilage degeneration

Kleemann R, Bluecher U, Weiler A, Duda GN

Repair of articular cartilage defects and the diagnosis of cartilage degeneration at an early stage remains a scientific challenge. During arthroscopy, cartilage quality can be determined from visual examination, manual palpation or histological analysis. While the first two methods hardly lead to quantifiable results, the last should be abandoned due to ethical considerations. In contrast to previous arthroscopical methods, mechanical testing clearly allows to quantify material strength. However, the procedure of indentation testing may cause damage to the healing tissue due to high contact forces and currently available testing apparatus appear to be highly sensitive in their readings to the handling of the individual user. Therefore, diagnostic procedures will benefit of a device which allows to determine cartilage stiffness a) without endangering the healing tissue and b) being user independent.

A method was developed to measure mechanical stiffness of biological materials arthroscopically. The device avoids rigid contact between the instrument tip and the examined object. Object deformation is produced by a defined flow of sodium chloride and measured optically with a coaxial lightfibre. The femoral condyles and the tibia plateaus of eight non-paired ovine knees were tested in a native and degenerated (0.1%-trypsin solution at 37°C for 48h) mode. Cartilage stiffness was non-destructively determined using the new water jet system and a standard indentation protocol using a materials testing machine.

The trypsin solution caused cartilage degeneration and consequently stiffness reduction. The reduction was measured at 30.8 % ($p < 0.002$) by the water jet system and 33.0% ($p < 0.001$) by the indentation test. A well correlation ($r = 0.69$) between the water jet system and the standard indentation procedure was observed. Intra- and inter-individual variabilities of the novel device were low (< 10%).

The stiffness values obtained from arthroscopical stiffness measurement (0.9 MPa for native and 0.55 MPa for degenerative cartilage) were well within the range of those previously reported by others. Only minor influences on the stiffness reading due to individual handling of the device were observed. Similarly to conventional testing, the reading of the new device allows to differentiate between native and degenerated cartilage probes ($p < 0.002$). Biphasic properties are excluded from in vivo diagnosis.

Compared to other arthroscopic devices, this new diagnostic technique appears to minimize the risk of surface damage of the cartilage during mechanical testing. The system is sensitive to testing of soft tissues in particular. Measurement results were relatively user-independent. The water jet system may therefore be considered a valuable tool in the arthroscopic diagnosis of cartilage lesions. Further evaluation in vivo is necessary to illustrate its beneficial effects.

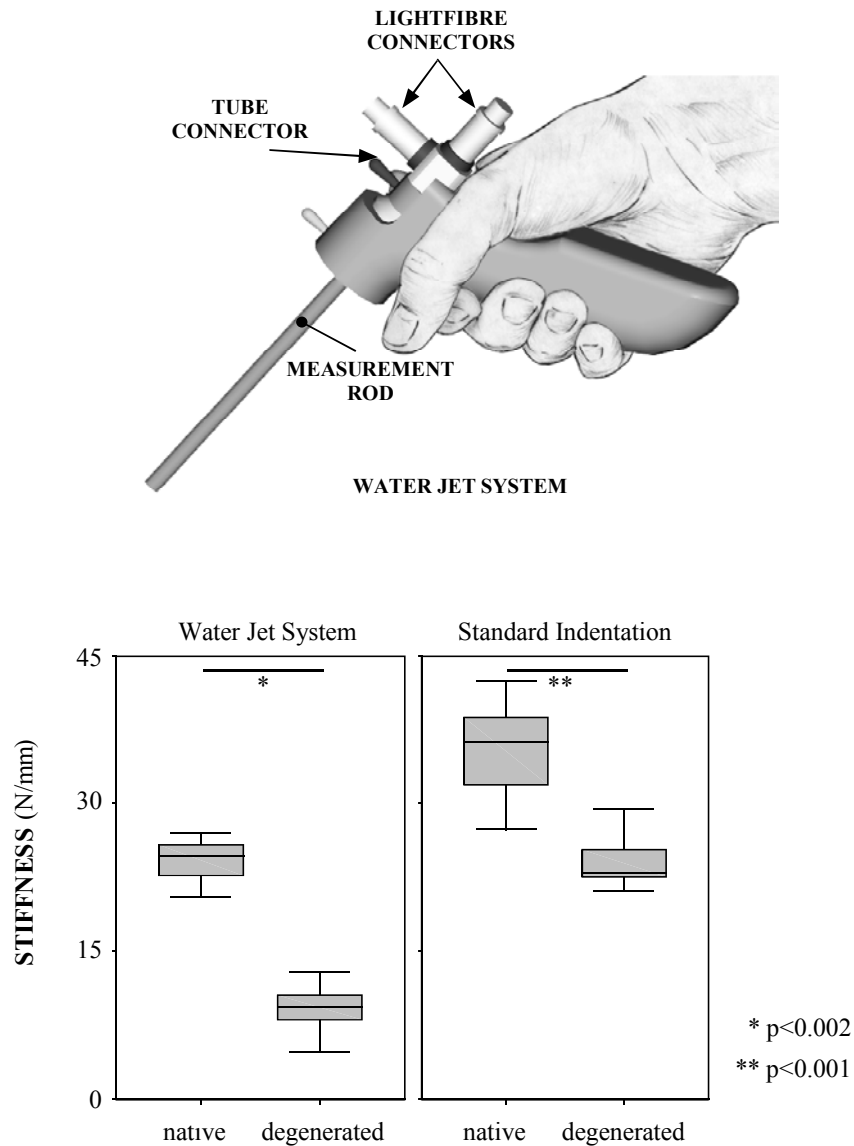


Fig. 1: (top) Arthroscopical cartilage tester with a component to apply the pressure and measure the distance. (bottom) Comparison of native and degenerated cartilage stiffness measured with the water jet system (left, * $p < 0.002$) and materials testing machine (right, * $p < 0.001$).

This study was partially supported by a grant of the Karl Storz GmbH & Co.KG, Germany

Bone straining of the intact and fractured proximal humerus under physiological-like loading

Maldonado Z, Seebeck J+, Heller M, Brand D*, Hepp P#, Lill H#, Duda GN

Surgical treatment of proximal humeral fractures in elderly patients is challenging, primarily due to insufficient implant-fixation. Knowledge regarding bone strength is important for the understanding of the origin of fractures, as well as for optimising fracture fixations in weak bone. The goal of this study was to determine the straining of the intact and fractured humerus under physiological-like loading conditions. Furthermore, the impact of bone quality on tissue straining was evaluated. Additionally, the effect of cement augmentation used in critical clinical cases is studied. The strain distribution in osteoporotic bones, its relationship to bone mineral density and mechanical properties, as well as the response to musculo-skeletal loading conditions were analysed.

In a related study, 24 paired fresh humeri from human cadavers were obtained for histomorphometric analysis of trabecular bone structure. Out of this total group, seven unpaired humeri were selected for biomechanical testing. A 5mm osteotomy was created at the surgical neck and stabilised by means of an angle stable plate (LCP-PH, Mathys). Mechanical testing (axial and torsional) was performed on a material testing machine and the resulting construct (implant and bone) stiffness determined. Before mechanical testing occurred, QCT scans with a slice distance of 1 mm were taken of the proximal humeri. From these QCT data sets, two representative specimens were selected for modelling: a reference bone and a specimen with poor bone quality (average BMD values of 0.49 g/cm² and 0.26 g/cm² respectively, as determined by DEXA). For each finite element model, the material properties of the matching voxel-based QCT data points were averaged, leading to the definition of 127 and 125 independent material properties in each finite element model respectively. The bone elements were modelled as linear elastic and isotropic with a $\nu = 0.3$. The implant (screws and plate) were modelled as isotropic, linear-elastic and homogeneous with an elastic modulus of 110 GPa and $\nu = 0.3$. Model validation was performed by comparison of stiffness data from Finite Element analysis and in vitro biomechanical testing results. Three physiological loading conditions: 0°, 90° forward flexion and 90° abduction, were studied. To simulate the effects of augmentation, the elastic cement properties were gradually decreased from a starting value of 2.4 GPa, which represents commercially available cements. The results obtained from the in vitro mechanical testing and the FE simulation differed in compression by a maximum of 13.0% and in torsion by maximum of 7.8%. Under physiological-like loading conditions the bone was loaded mainly in compression with superimposed bending and torsion. When the bone strain was compared for various arm positions, the largest strain magnitudes were found in the proximal humerus at 90° abduction (Fig. 1). For the identical loading configuration, the specimen with poor bone quality showed substantially increased cortical straining (38% of elements $\geq 1000 \mu\epsilon$). Strain patterns and magnitudes within the treated bone with a defect stabilised by the angle stable implant were similar to those in an intact bone. No marked differences in the strain orientations were observed between the two different quality bones. The strain magnitudes were, however, increased in the specimen with the lower average

density. The use of commercially available cement showed an overloading of the remaining trabecular bone. Local overloading of trabecular bone due to augmentation can be reduced with a more elastic bone cement (e.g. $E = 1.75$ GPa).

The findings of this study demonstrate a strong influence of bone quality on the bone strains in an intact and plate stabilised proximal humerus. The two extremes examined in this study demonstrate the possible strain limits to be expected in the proximal humerus. Strain was influenced to a lesser degree by specific musculo-skeletal activity. The loading of the shaft only slightly increases after osteosynthetic treatment of a proximal humerus defect (up to +15%). However, the influence of a defect on the overall straining was more pronounced in an osteoporotic bone compared to a healthy specimen (up to +20%).

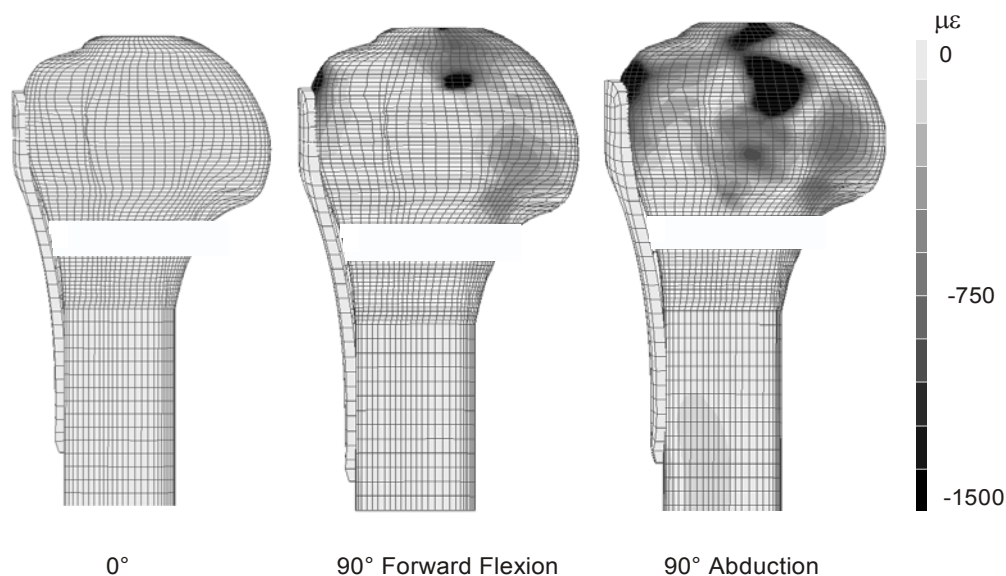


Fig. 1 Minimum principal strain distribution (microstrains) in the proximal humerus for a poor bone quality under different physiological loading

+AO Research Institute, Davos, Switzerland; *Paracelsus Klinik, Henstedt, Ulzburg, Germany; #Trauma and Reconstructive Surgery, University of Leipzig, Germany

This study was supported by a grant of the AO/ASIF Foundation, Switzerland

Radiofrequency treatment of partial-thickness cartilage defects in the sheep knee joint leads to cartilage injury

Kääh M.J., Bail H., Rotter A., Mainil-Varlet P., Südkamp N.P., Weiler A.

Use of Radiofrequency (RF) energy is recently gaining increasing popularity for treatment of articular cartilage partial-thickness defects. The rationale behind thermal treatment is to smoothen and stabilize the cartilage surface to retard the development of osteoarthritis. Goal of this study was to analyze the effect of RF-treatment on grade II partial-thickness defects in the sheep knee joint.

The left knee joint of 10 adult Merino sheep was arthrotomized under general anesthesia. Standardized grade II cartilage surface defects of 1x1 cm² were created in the main load bearing area on the medial and lateral femoral condyle using a specific scratching device consisting of 4 parallel K-wires. The cartilage lesions were treated randomized on either the lateral or the medial condyle, using a monopolar RF-electrode (4mm ball, K. Storz GmbH, Tuttlingen, Germany). RF-treatment was performed by sliding with the ball along the scratches under continuous rinsing for a few seconds until surface smoothening was seen without change of cartilage color (Power setting 60W, soft coagulation mode), reaching a temperature of between 52° and 58°C, as tested in previous in vitro trials. Another 10 samples of sheep femoral condyle cartilage were scratched in-vitro and half of the samples RF-treated, as well as 5 samples were only object to RF-treatment. 24 weeks after surgery the animals were sacrificed and samples were harvested and processed for macroscopic evaluation, histologic evaluation following haematoxylin/eosin and Safranin-O staining and surface analysis by Scanning Electron Microscopy. Furthermore, an in vitro study was done to determine the initial thermal damage using Radiofrequency. The previously scratched and RF-treated cartilage was stained by viability markers and analyzed under a Confocal Scanning Microscope.

24 weeks following surgery, macroscopic and histologic analysis revealed in the central area of all RF-treated samples an grade IV cartilage defect of average 1,8 cm² (1,4-2cm²)size (Fig.1). Histological findings confirmed the macroscopic impression showing these central ulcer and chondrocyte death in the RF-treated regions. Cartilage surface which was not subjected to RF-treatment showed partial surface irregularities with partial defect repair and no chondrocyte death 24 weeks postoperatively. After in vitro RF-treatment, chondrocyte death was found up to 50% of the cartilage thickness (Fig. 2)

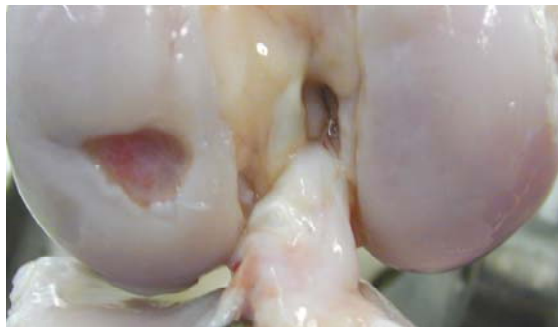


Fig. 1. All samples treated with RF showed grade IV cartilage defects after 24 weeks.

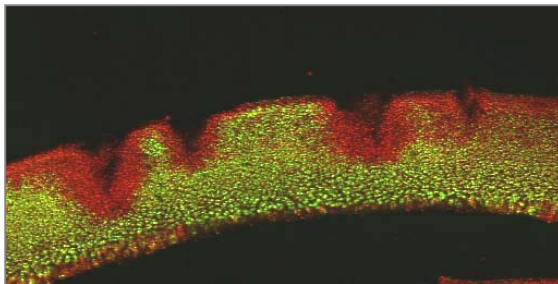


Fig. 2. Confocal Microscopy shows chondrocyte death (red staining) following in vitro RF-treatment.

In this study RF-treatment showed a deleterious effect on articular cartilage of sheep femoral condyle 24 weeks following surgery. In this study temperature measurement was not performed but RF-treatment controlled by time and visually (no change of color as under clinical conditions). It was shown that RF-treatment of partial-thickness cartilage defects leads to articular cartilage damage and therefore can not be recommended for clinical use if applied only by visual control.

This study was supported by a grant of the AO/ASIF Foundation, Switzerland, No. 2000-K69

Mechanical conditions are essential in osteochondral defect healing

Duda GN, Maldonady Z, Bail H, Klein P, Malayse F, Heller M, Haas NP

The traumatic destruction of a cartilage layer marks the onset of joint degeneration and may, in the long-term, lead to surgical intervention or joint replacement. Clinically, fibrous cartilage may re-establish a defect filling. Delay or failure of healing is usually associated with complications in the biological process of cartilage regeneration. Mechanical constraints are rarely considered of importance. The goal of this study was to compare the histological outcome with the initial strain environment of the tissue and the mechanical boundary conditions during healing of osteochondral defects.

18 healthy female Yucatan minipigs were included in this experiment. Ground reaction forces were measured (emed SF-4, novel) preoperatively, on the 3rd postoperative day and then in weekly intervals. Under general anesthesia, an osteochondral defect was created at the lateral surface of the trochlear groove of the left hindlimb. The osteochondral defect was 6 mm in diameter and 1.5 mm in depth from the osteochondral junction. 6 animals were sacrificed after 4 weeks, 9 after 6 weeks and the remainder after 12 weeks. 6 μ m sections were produced from a sagittal cut through the left lateral femoral condyle and stained. The amount of defect area, fibrous tissue, cartilage, and remodeled bone was determined (KS400 image analysis system, Zeiss). Mean intercept length (structural orientation) and trabecular volume fraction were measured in three ROI's within the subchondral bone. For comparison, both measures were also quantified at identical locations on the contralateral condyle.

The osteochondral defect was modeled by an axisymmetric, 2D FE model including a cartilage layer, subchondral bone plate, trabecular bone and defect area (Fig. 1). Load equilibrium was assumed between fluid and solid phase on one side and external loading on the other. Mechanical loading of the model was approximated from analytical analysis, resulting in a pressure of 1.35 MPa. Initially, the defect consisted of connective tissue only. Defect healing was modeled by gradually changing the element material properties from one iteration to the next. The minimum principal strain served as the remodeling stimulus and led to tissue development or resorption. Within 100 iterations, all analyzes had reached equilibrium of material distribution. The amount of fibrous tissue, cartilage, calcified cartilage and cancellous bone as well as the defect size was determined.

After 2 postop weeks, animals had returned to preoperative weight bearing. Qualitative analysis of the histological sections unveiled new bone formation on the defect edges while considerable bone resorption enlarged the defect depth. Major osteoclastic activity and bone resorption was found below the defect especially at 4 but also at 6 weeks (Fig. 1). Histomorphometric analysis showed an increase in cancellous bone and cartilage area. The organization of the subchondral trabeculae was, at all timepoints and locations, reduced ($p=0.001$) while the trabecular volume fraction was increased ($p=0.002$) compared to the contralateral side. The finite element analysis unveiled an initial unloading (-27%) of the defect base and an increased straining of the defect circumference (+200%). During simulated healing, filling occurred from the circumference and with resorption of the

defect base. After the initial resorption at the base, the adaptive analysis predicted a restoration of the tide mark and a complete defect filling. This pattern of healing appeared to be independent of the specific defect geometry or loading configuration. Only in the situation with reduced loading did adaptive finite element analysis predict substantial cartilage formation.

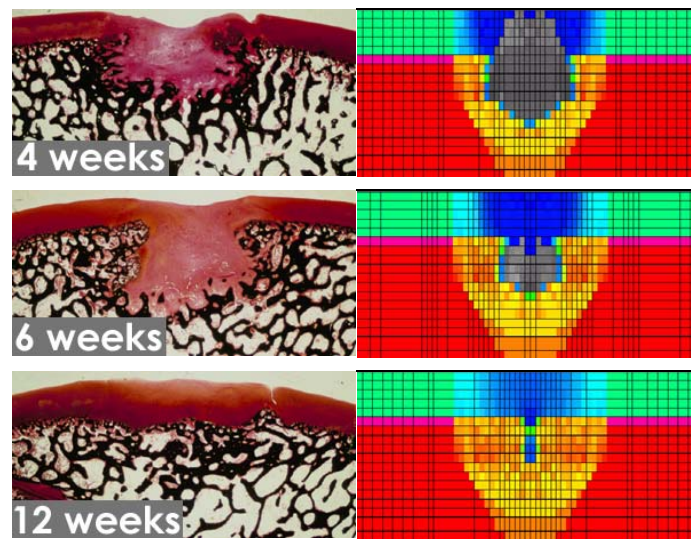


Fig. 1: Histological sections after 4, 6 and 12 weeks and corresponding simulated material distribution from FEA.

Osteochondral defect healing is a complex process involving biological and, as demonstrated, mechanical factors. Previous studies have shown that regeneration of cartilage is a demanding process and only rarely leads to a complete regeneration. It may be possible that a complete restoration of a hyaline-like cartilage layer may only be achieved under specific mechanical conditions, including a significant unloading of the joint. Further experimental studies are required to illustrate the potential of mechanical factors in supporting osteochondral regeneration. The employed adaptation relied on simple mechanical principles. The results, however, show a good qualitative and quantitative agreement to the histological findings. The findings of the present study imply that mechanical factors have – beside biological ones – a significant influence on the process of osteochondral healing.

Does low-intensity pulsed ultrasound stimulate maturation of tissue engineered cartilage ?

Duda GN, Haisch A*, Kliche A, Kleemann R, Hoffmann JE, Sittlinger M**

Traumatic events in sports or vehicle accidents are a main reason for local lesions of articular cartilage. With tissue engineering (TE) it is generally possible to supply sufficient amounts of cartilage tissue for defect filling. Critical to the clinical success is the time necessary for tissue maturation and the mechanical quality of the regenerate at implantation. Low-intensity pulsed ultrasound has proven to accelerate chondrogenesis *in vitro*. The goal of this study was to evaluate if low-intensity pulsed ultrasound would accelerate the process of cartilage maturation and thereby lead to increased regenerate stability.

Articular cartilage from adult bovine forelimbs was diced into pieces and enzymatically digested. Cell amplification was performed in culture flasks and 3D chondrocyte cultures were prepared. Cells were suspended in the fibrinogen solution. Bioresorbable co-polymer fleeces of vicryl served as a second component of the carrier system. Fibrinogen was polymerized by addition of 50µl thrombin solution per transplant. Tissues were cultured for 8 days *in vitro* before transplantation in subcutaneous pockets in the back of anaesthetized male homocytotic athymic nude mice (age: 60-80 days, 35-45g weight). 21 animals received low-intensity pulsed ultrasound stimulation, while 21 animals received a sham treatment. Animals were treated for 20 minutes per day, seven days a week. After 3, 6 and 12 weeks, the mice were sacrificed. Native bovine cartilage specimens served as control. Within 3 hours after sacrifice, biomechanical testing was performed on all TE and native probes. Mechanical indentation tests were performed under sterile conditions on a material testing machine. The Young's modulus was determined from the linear slope of the load-deflection curve. Deflection was defined as displacement divided by the thickness of the specimens. Non-parametric statistical analysis was performed on Young's modulus and failure load data. One half of each specimen was prepared for histological examination. For morphological measurements, haematoxylin and eosin staining was performed. Proteoglycan synthesis was analyzed by alcian blue staining. The other half of the specimen was placed on dry ice for RNA extraction (Col1, Col2, TGF-β1 expression) using RT-PCR techniques.

The TE specimens appeared a whitish color typical for hyaline cartilage. No infection was observed throughout the experiment. After 6 and 12 weeks, implants appeared flexible and of solid consistency. At sacrifice, the implants were attached to the subcutaneous pocket, due to a superficial infiltration of adjacent tissue. In biomechanical testing the 12 week implants proved to have superior mechanical properties compared to the 3 week ones ($p < 0.001$; Fig. 1). At 6 and 12 weeks, material properties of the TE specimens were comparable to those of native articular cartilage. No significant difference in stiffness was identified between the ultrasound treated and the control group at any time point.

All TE specimens showed neocartilage formation in macroscopical and histologic examination (HE) with increasing degree of tissue maturation. At 6 and 12 weeks, round shaped chondrocytes were homogeneously embedded within the cartilage matrix. No difference could be depicted in Col1 and Col2 expression in RT-PCR.

Only TGF- β 1 was reduced in the ultrasound treated group at 3 weeks postoperatively.

Macroscopical examination as well as histological staining proved the hyaline-like nature of the TE cartilage specimens at 6 as well as 12 weeks. The mechanical testing methods allowed clear differentiation between tissue types: The significant gain in mechanical stability between the 3 and 12 week groups showed a positive influence of the maturation process on the quality of the tissue. However, no positive effects of low-intensity ultrasound stimulation could be confirmed for cartilage maturation. Only the 3 week ultrasound group showed a reduced TGF- β 1 level indicating a reduced matrix synthesis in these specimens.

Previous analyses report stimulatory effects of low-intensity pulsed ultrasound on chondrogenesis within the first days and up to three weeks of stimulation. The results of the present study suggest that the stimulatory effect of low-intensity pulsed ultrasound may be limited to the very initial phase of chondrogenesis. Even though low-intensity pulsed ultrasound has been proven to be beneficial in accelerating chondrogenesis in fracture healing, it appears to have no positive effect in the maturation of tissue engineered cartilage structures.

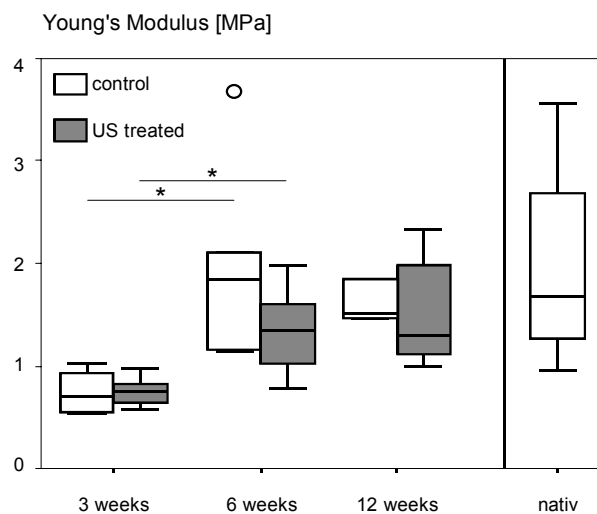


Fig. 1: Biomechanical stiffness at 3, 6 and 12 weeks and native articular cartilage (ultrasound and sham treated groups, * $p < 0.001$).

* Dept. Otorhinolaryngology, University Hospital Benjamin Franklin, FU Berlin,** German Rheumatism Research Center, Berlin, Germany

This study was supported by a grant of the AO/ASIF Foundation, Switzerland

Interfragmentary movements in the early phase of healing in distraction and correction osteotomies

Duda GN, Bartmeyer B, Hoffmann JE, Kassi J-P, Raschke M

Independent of the method of fragment fixation, bone healing is generally subjected to complex inter-fragmentary movements. It is well accepted that this movement influences the bone healing process in both type and rate of healing. Since axial and shear movements appear to influence the bone healing process differently, knowledge of the interfragmentary motion is essential in order to judge the appropriateness of the stabilization. In critical clinical cases such as distraction osteogenesis and correction osteotomies, the mechanical conditions may be even more demanding than those during experimental studies. The goal of this study was to characterize the gap movements in distraction and correction osteotomies and to draw conclusions on the suitability of initial fixation.

Interfragmentary movements were measured in eighteen patients with tibial osteotomies stabilized by Ilizarov-hybrid constructs until either bone union or conversion to internal fixation occurred (9 distraction treatments, 9 correction osteotomies). Prior to measurements, written consensus was obtained from all patients. Markers with reflective spheres were mounted via additional Schanz' screws to the proximal and distal bone fragments. During recording, these screws were unattached from the fixator. Using a 2-camera optical measurement system (accuracy 0.1 mm, 0.1°) the 3D interfragmentary movements were monitored during various patient activities. Initial measurements were performed within the first 2 weeks post-operatively. Ground reactions of the injured limb were also monitored: In a sitting position with the heel on the force plate, patients were asked to rest, to co-contract the muscles of the lower limb (2 contraction periods, 5 secs each), to stand up and to slowly walk over the force plate. Each activity was repeated four times. Patients were monitored until completion of the distraction phase or change to internal fixation occurred. The longest monitoring period was 340 days postoperative. Consolidation was determined by clinical evaluation and standard X-ray techniques. In addition, the 3D stiffness of representative ring fixator constructs were determined in vitro.

Clinically, all patients showed good postoperative fragment stabilization. Variations in ground reactions were negligible between different trails of a single activity. During the initial measurements, shear movements were significantly larger than axial motion ($p < 0.007$ t-test). In both groups, co-contraction led to gap movements comparable to level walking. Although the in vitro stiffness was slightly increased in the correction constructs, the in vivo interfragmentary movement was initially comparable between the groups. In the distraction group, the gap movements increased with treatment time, whilst in the correction group, movements steadily reduced (Fig. 1).

During the early healing period (up to 80 days postop), none of the cases showed consolidation and the ring fixator construct supplied the mechanical stability. The axial and bending stabilities appeared sufficient in the in vitro test and were comparable to those reported by others. The magnitude of in vivo axial movement was in the range of previously reported data. Shear clearly outweighed the axial movement component, the parameter that other studies have concentrated on. The presented data, however, suggests that judgment regarding the appropriateness of fixation is possible from the shear component (Fig. 1), both in a direct post-operative situation as well as during the long term performance of the fixation.

Co-contraction alone showed similar movements at the healing site to activities associated with high loading conditions (e.g. standing-up, walking). This in vivo data stresses the importance of muscle activity for the straining of a healing bone.

Interfragmentary movements may provide an additional means of quantifying healing progression besides conventional radiographic diagnosis. Mechanical conditions at the defect appear to be more critical in distraction than during correction osteosynthesis.

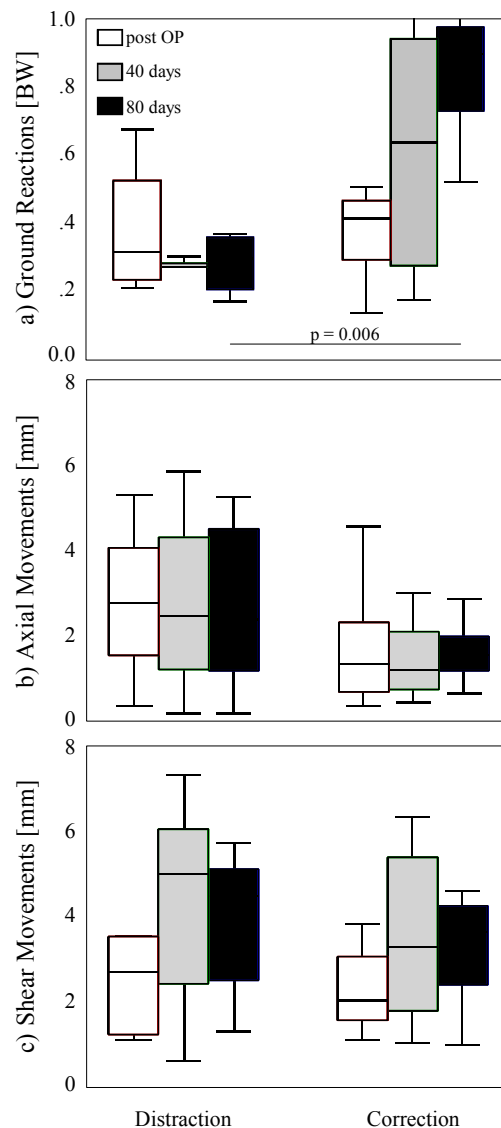


Fig. 1: a) Ground reactions in bodyweight [BW], b) axial movements in mm and c) shear movements in mm during walking for different time points and both osteotomy groups.

Effect of partial weight bearing on fracture gap motion

Bartmeyer B, Raschke M, Duda GN

The mechanical conditions significantly affect the biological process of healing. Experimental studies have identified numerous mechanical parameters such as gap size, strain rate and strain magnitude that affect the healing process. The nature of loading, the number of cycles and the timing of mechanical stimuli during healing are also important. Even muscle activity seems to have significant influence on the mechanical loading of the fracture zone and may thereby affect the healing outcome. Callus formation characterizes secondary bone healing. Experimental findings suggest that less callus formation is achieved with a generally stable fixation, whereas a larger callus forms with an unstable fixation. To what degree “unloading” of the limb influences the mechanical conditions at the fracture site remains so far unknown. The goal of this study was to determine the influence of partial weight bearing on the interfragmentary movement in complex tibial osteotomies.

22 patients with complex tibial shaft fractures (18 men, 4 women), all possessing an Ilizarov-hybrid fixator, were examined for the 3D fracture gap movement. All patients had at least two Schanz screws and a pair of crossed Kirschner wires for the proximal fracture fragments and two Schanz screws and a pair of crossed Kirschner wires for the distal fracture fragments. Interfragmentary movements were recorded in all patients immediately after surgery and continuously until consolidation.

Furthermore ground reactions of the treated limb were recorded in body weight during each patient activity. Ground reaction force and contact area were transferred to a personal computer for additional analysis. Gap movements and corresponding ground reactions were measured initially within the first 2 weeks after surgery. 6 patients (4 men, 2 women) took part in a partial weight bearing study, to show the influence of muscle activity on the interfragmentary movement. Patients were asked to rest, to co-contrast the gastrocnemii muscle, to stand up, to walk slowly over the force plate and to load the treated limb with 20 kg weight. To describe fracture gap movements, a right handed reference coordinate system was defined. A reference frame with reflective markers was attached to one of the carbon rings of the Ilizarov construct.

During the initial measurement sessions, interfragmentary movements as large as 4 mm were recorded. Compared with resting, co-contraction and standing up showed significantly increased motion in axial compression and shear. In all activities shear movement was increased significantly compared with axial compression.

Patients who were taking part in the partial weight bearing study showed that the same axial compression as during walking was achieved with a partial weight bearing of only 20 kg.

In the partial weight bearing group, ground reactions were significantly increased in activities such as walking, compared with resting. These results lead to the conclusion, that muscle activity seems to have greater influence on the fracture zone than expected.

This study suggested a strong relationship between movement magnitudes, ground reaction forces, muscle activity and healing progress. Knowledge of these mechanical conditions is essential to elucidate the mechanism of bone healing. In this view, measurements of complex interfragmentary movements might be an aid in finding appropriate fixation methods in complex osteotomies and thereby optimize the mechanical environment for bone healing.

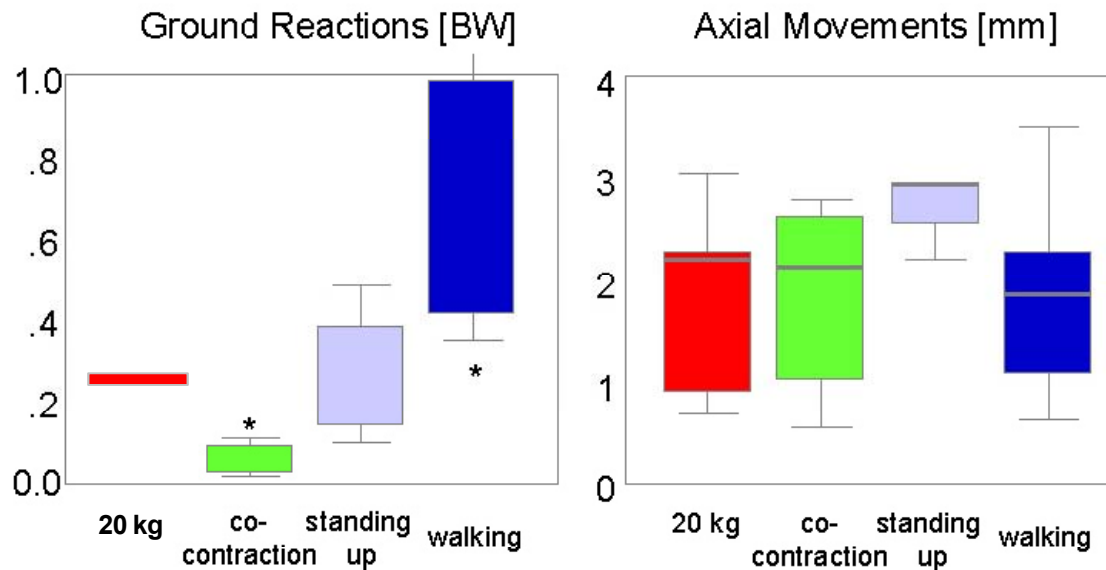


Fig.1: Ground reaction force in body weight (left) and axial compression (in mm) during various activities.



Fig. 2: To measure three-dimensional gap movement, triangles with three reflective markers each were mounted using custom-made clamps onto Schanz screws. The Schanz screws were detached from the fixator construct during the measurement sessions to allow direct measurement of fragment movements. The interfragmentary movements were determined from the rigid body movements of the triangles and the offsets toward the centre of the osteotomy gap.

This study was supported by a grant of the AO/ASIF Foundation, Switzerland

New concepts in fracture stabilization: Comparison of different fixation principles and surgical approaches in an experimental ovine model

Schmeling A, Ito K*, Käab M, Bodmann G, Grell D, Wolf C, Schütz M

Recently, internal fixators were developed. These devices can preserve vascularity of the fracture site by facilitating minimal invasive application and also by using angular-stable monocortical screws. The objective of this study was to compare fracture healing in a standardized sheep tibial shaft fracture with adjacent soft tissue injury treated by different operative approaches (minimal invasive surgical approach (MIS) versus conventional open technique (ORIF), Grp I) and different stabilization techniques (internal fixator versus conventional open plate-osteosynthesis (LCDCP, GrpII) or unreamed intramedullary nailing (UTN, GrpIII)).

A standardized ovine mid-shaft tibial fracture with an adjacent defined soft tissue contusion was developed. For Grp I, in both approaches, an internal fixator (PC-Fix II, Synthes) was used on the medial tibia for stabilization. For the MIS technique, the internal fixator was slipped beneath the submuscular fascia and applied on the periosteum through two 2cm skin incisions. For the ORIF technique, the fixator was applied through a 12cm medial skin incision. A 2cm band of muscle was circumferentially separated from the periosteum around the fracture, and reduction was maintained with a bone clamp under direct visualization during screw insertion. For Grp II & III, after closed reduction, the internal fixator (PC-Fix II, Synthes) was applied medially either in open conventional (PC-Fix/LC-DCP, Grp II) or in a minimal invasive technique (PC-Fix/UHN, Grp III). For direct comparison, a plate (LCDCP) in open technique or an unreamed intramedullary nail (UHN) in a closed technique was applied to the contra-lateral hind limb. Twelve sheep per comparison (6 in each group) were operated bilaterally. Biweekly x-rays and weekly weight bearing measurements were monitored. Half of the sheep were sacrificed after 6 and 12 weeks. Following hardware removal, tibiae were biomechanically tested and prepared for histological analysis. Sections from undecalcified MMA embedded specimens were stained with von Kossa/Safranin O, and callus histomorphometry was digitally analyzed (KS400, Zeiss). OP duration between treatment groups was compared and statistical analysis was done for all parameters. This study was approved by the Animal Experimentation Commission of the Veterinarians Office of the Canton Graubünden, Switzerland.

At 6 or 12 wks, no significant differences were found in biomechanical testing between MIS and ORIF tibiae (Grp I). The MIS treated fractures had a significantly smaller periosteal callus, which tended to have a higher percentage of mineralization than those treated with ORIF. OP duration for internal fixator stabilization was significantly less, compared to plating ($p < 0.008$) or nailing technique ($p < 0.001$). In the early postop period, the sheep in Grp II bore more weight on the plate-stabilized limb, whereas in the later period, the fixator side was preferred. In Grp III, the fixator-stabilized legs were preferred significantly. Biomechanical testing exhibited significant higher values in bending strength and torsional stiffness for fixator treated fractures compared to the plate-stabilized fractures at 12 wks post-op ($p = 0.04$), but there was no statistical difference between the fixator and nail treated fractures at 6 or 12 wks. Histologically, secondary fracture healing occurred in all sheep. Callus area was less in fixator treated fractures than in

plated fractures but quotient mineralized/total callus area was increased at 6wks post-op in some regions and at 12 wks post-op in most regions compared to the plated fractures (Grp II). Summarizing all regions, in Grp III, there is no difference between fixator and nail, neither in total callus area nor in mineralized callus area or quotient mineralized/total callus area.

This study did not show that MIS fracture treatment results in faster functional fracture healing compared to ORIF techniques in the chosen model. There was a trend toward a larger early callus in the ORIF fractures, but callus resorption and consolidation was accelerated in the MIS treated fractures. The internal fixator reveals advantages in fracture healing compared to conventional plating. Histological analysis showed qualitative superior fracture healing in terms of increased mineralized callus area, which seems responsible for increased early biomechanical stability after 12 wks. Compared to the golden standard technique of i.m. nailing, no objective difference could be evaluated in biomechanical or histological analysis. Internal fixators are an alternative for nailing techniques, i.e. at problematic regions like the metaphyseal regions or proximal tibia or in complex fracture types, respectively.

*AO/ASIF Research Center, Davos, Switzerland

This study was supported by a grant of the AO/ASIF Foundation, Switzerland

Time course of unstimulated and growth factor stimulated rat tibial healing

Schmidmaier G, Wildemann B, Haas NP, Raschke M

One of the main projects of our group is the development of a biodegradable drug carrier for local growth factor release. Previous studies were able to show, that the local release of IGF-I and TGF- β 1 from a poly(D,L-lactide) coating of titanium implants accelerates fracture healing in the early phase. However the long term effect of the locally applied growth factors is still unknown. Therefore, the aim of this study was to analyze the effect of growth factor treatment at different time points representing different phases of healing. The tibia and fibula of rats were fractured in a closed manner with a special developed guillotine-like device under standardized conditions. After closed reduction the tibia was intramedullary stabilized with a coated vs. uncoated titanium Kirschner wire. To evaluate the soft tissue trauma the compartment pressure was measured postoperatively. To follow the healing process, x-ray examinations were performed and the bridging of the calluses were scored throughout the experimental period. Four, six and twelve weeks after fracture were the tibiae prepared for biomechanical torsional testing or histological analyses.

A standardized closed fracture of the right tibia of five months old Sprague Dawley rats (n=180) was performed with a fracture device. The fractures were intramedullary stabilized with uncoated versus coated titanium K-wires. Following groups were examined:

Group I: uncoated, Group II: coated with PDLLA, Group III: coated with PDLLA & IGF-I (50 μ g)+ TGF- β 1 (10 μ g)

n=60 each group, sacrifice: 28, 42, and 84 days after fracture, PDLLA: poly(D,L-lactide)

x-ray examinations (p.a. and lat.) were performed throughout the experimental period. After sacrifice both tibiae were dissected for biomechanical torsional testing using a material testing machine (Zwick 1455, Ulm, Germany). For histological and histomorphometric analyses the tibiae were fixed and embedded in methylmethacrylate. 5 μ m sections were cut and stained with Safranin O/light green and v. Kossa. The histomorphometry of the calluses was performed using an image analyzing system (Zeiss KS 400).

Radiology

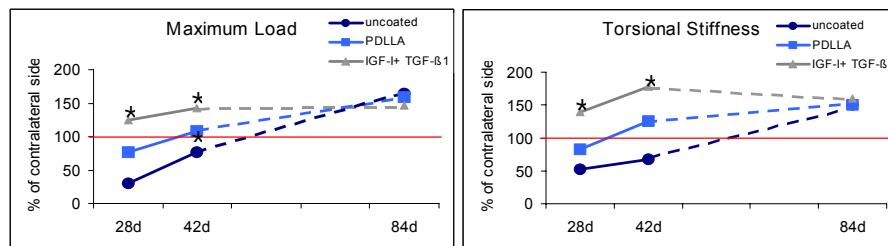
The animals revealed radiologically a transverse midshaft fracture of the tibia and a fracture of the fibula with a comparable soft tissue trauma.

The healing process showed differences in the radiology 28 and 42 days after fracture between the groups. The growth factor treated group revealed significantly more completely bridged fractures at this time points compared to the groups I and II. At the latest investigated time point (84 days) no differences in the radiology were detectable.

Biomechanics

The biomechanical strength increased with healing time and showed the highest values after 84 days in group I and II. In the growth factor treated group III a slight

reduction of strength was seen at day 84. Significant differences were seen between the three investigated groups at days 28 and 42 after fracture. The animals treated with growth factors revealed a significantly higher maximum load and torsional stiffness compared to the PDLLA and the uncoated groups. Even the PDLLA treatment showed an effect in the biomechanical testing compared to the control group I. 84 days after fracture no significant differences were detectable between the groups.



Results represent % to contra lateral side; red line: unfractured tibia (100%)

Histology

After 28 days the calluses were composed of soft tissue, cartilage and newly formed trabecular bone. At the later investigated time points a remodeling process of the callus was detectable with a decrease of cartilage and an increase of mineralized tissue. Significant differences in the callus composition were seen after 28 and 42 days. The growth factor treated group III revealed significantly less cartilage at both time points compared to the other groups. At the latest time point (84 days after fracture) almost no cartilage were detectable in the calluses of the investigated groups and a callus remodeling with a reduced callus size was seen.

Using this model a standardized fracture comparable to an accidental situation could be produced and the healing process was analyzed at different time points. The uninfluenced healing can be compared to the growth factor stimulated healing. The radiological, biomechanical and histological investigation revealed a significantly enhanced fracture healing in the growth factor treated group at days 28 and 42. However, 84 days after fracture the groups showed almost identical results. No influence of the growth factor on systemic parameter were found. This study clearly demonstrates an enhanced fracture healing due to growth factor application without alteration of the healing phases.

The time point when the bone is restored in rats seems to be longer than the investigated 84 days post fracture, because the biomechanical stability is still above the intact contra lateral side.

BMP-coating of titanium implants increases biomechanical strength and accelerates bone remodeling in fracture treatment

Schmidmaier G, Wildemann B, Raschke M

Bone morphogenetic protein-2 (BMP-2), a member of the TGF-beta superfamily is known to stimulate osteogenic cells. In vivo studies have shown that BMP-2 delivered from collagen sponges enhances fracture healing. This application technique requires the opening of the fracture and may have possible side effects due to the use of bovine collagen. A newly developed coating method for implants based on biodegradable poly(D,L-lactide) allows the incorporation of growth factors and the controlled release of these factors during the healing process without the need of further devices. The effect of BMP-2 (5% w/w, 50 µg) locally released from coated intramedullary implants on fracture healing was investigated with biomechanical and histological analysis in rats.

A standardized closed fracture of the right tibia of five months old Sprague Dawley rats (n=80) was performed with a fracture device (impulse p=1.12 Ns). The fractures were intramedullary stabilized with uncoated versus coated titanium K-wires. Following groups were examined:

- Group I: implant uncoated, 28 days (n=20)
- Group II: implant coated with PDLLA + rh-BMP-2, 28 days (n=20)
- Group III: implant uncoated, 42 days (n=20)
- Group IV: implant coated with PDLLA + rh-BMP-2, 42 days (n=20)

After fracture of the right tibiae, x-ray examinations (p.a. and lat.) were performed throughout the experimental period. After sacrifice both tibiae were dissected for biomechanical torsional testing using a material testing machine (Zwick 1455, Ulm, Germany). For histological and histomorphometric analyses the tibiae were fixed and embedded in methylmethacrylate. 5µm sections were performed and stained with Safranin O/light green and v. Kossa. The histomorphometry of the callus was performed using an image analyzing system (Zeiss KS 400).

The results demonstrated a progressed callus consolidation in the BMP-2 treated groups compared to the uncoated groups at both time points. The histomorphometrical analyses demonstrated a progressed callus remodeling with significantly higher mineralization of the cortices and higher mineralization and less cartilage of the periosteal callus.

After 4 and 6 weeks the local application of BMP-2 demonstrated a significantly ($p < 0.05$ ANOVA) higher maximum load and torsional stiffness in the biomechanical testing compared to controls (Fig 1).

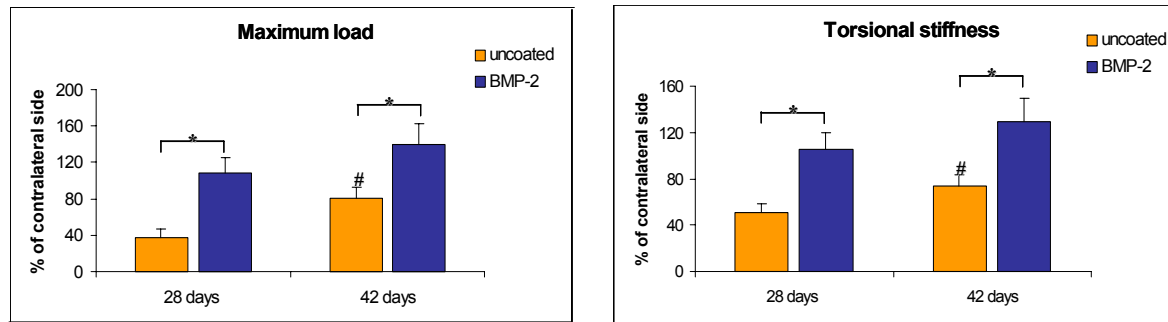


Fig 1: Biomechanical testing

The results clearly demonstrate that the local application of BMP-2 from PDLLA coated implants significantly accelerates fracture healing. Two time points were investigated to analyze the effect of the BMP-2 coating on the healing process. The biomechanical torsional testing after 28 and 42 days revealed a higher torsional stability compared to the control groups. These data were supported by the histomorphometrical results. The callus treated with BMP-2 demonstrated a progressed callus remodeling with significantly higher mineralization and less cartilage compared to controls.

These results are in accordance with other studies investigating the effect of BMP-2 on fracture healing. However, local administration of growth factors from coated osteosynthetic implants could reduce clinical problems in fracture treatment without opening of the fracture, implantation of further devices, injections with the risk of infection or side effects caused by the carrier.

This study was partially supported by a grant of Synthes, U.S.A.

Quantification and localization of IGF-I and TGF- β 1 during growth factor stimulated fracture healing

Wildemann B, Schmidmaier G, Raschke M

Local application of IGF-I and TGF- β 1 from Poly(D,L-lactide) coated titanium implants was able to stimulate fracture healing in rats. However, the distribution and expression pattern of these growth factors during the healing process is still unknown. The present study investigated the cellular distribution of IGF-I and TGF- β 1 and changes in the amount of total protein and the IGF-I and TGF- β 1 concentration (using ELISA) during normal and growth factor (IGF-I and TGF- β 1) stimulated fracture healing.

A standardized tibial fracture of 5-month-old female Sprague Dawley rats was performed and intramedullary stabilized with titanium Kirschner wires as described previously. Three different time points were investigated (days 5, 10 and 15 after fracture). The unfractured tibia served as control for normal levels.

Group 1: uncoated K-wire (n=39)

Group 2: IGF-I and TGF β 1 in PDLLA coated K-wire (n=39)

Control: unfractured tibia (n=24 for ELISA)

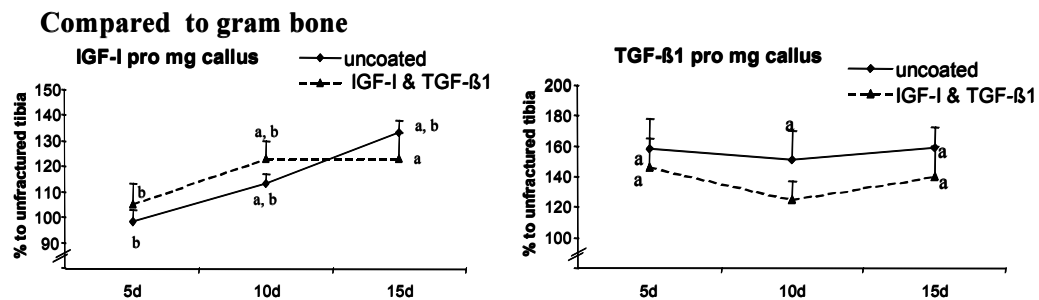
ELISA and protein quantification: n=8 each group and time point;
Immunohistochemistry: n=5 each group and time point.

Protein Extraction procedure: Using a cooled mill (Retsch, Germany) the bone was pulverized and the powder was diluted for 2 hours in 10 ml 1M acetic acid/g callus at 4°C (pH 3.8). Using acidic buffer IGF-binding protein artifacts were avoided. After the extraction the probes were centrifuged by 12 000 U/min and the supernatant was stored at -80°C. IGF-I and TGF- β 1 quantification: IGF-I and TGF- β 1 concentration in the extract was quantified using ELISA-methods (both Kits Brenzel Bioanalytic, Germany). The sensitivity of the ELISA kits was: TGF- β 1 = 1.9ng/l and IGF-I = 0.15 μ g/l. The TGF- β 1 kit showed no cross reactivity to TGF- β 2 or TGF- β 3 and the IGF-I kit to IGF-II. Interassay coefficient of variation was 7.5% (TGF- β 1) or 6.7% (IGF-I) and intraassay CV was 1% (TGF- β 1) or 2.31% (IGF-I). Immunohistochemistry: The tibiae were dissected, fixed in 10% buffered formaldehyde, decalcified in EDTA, and paraffin-embedded. For immunohistochemistry the sections were incubated with either goat polyclonal TGF- β 1 antibody (Santa Cruz Biotechnology, USA; 1:100) or goat polyclonal IGF-I antibody (R&D-Systems, USA; 1:50). Incubation of slices without the primary antibody served as negative control. The slices were analyzed with an image analysis system (Zeiss KS 400, Germany).

The immunohistological investigation showed an expression of the growth factors in mesenchymal cells, osteoblasts, osteocytes and chondrocytes during fracture healing without differences between the groups. The total protein quantification revealed a time depending increase in the control group (30-90%), whereas the growth factor group revealed a constant increase of about 30%. The IGF-I increased during the investigated time points starting at day 10. The TGF- β 1 level increased at day 5 and showed a steady level over the experimental period. An influence of the locally applied growth factors was only detectable in the increased IGF-I/protein level at day 15 compared to the control group. These results indicate,

that local application of growth factors did not lead to an alteration of cells expressing this factors or to significant changes in the measurable amount.

a: significant to unfractured tibia, b: significant to other time points



This study used different methods to investigate the temporal expression and localization of IGF-I and TGF-β1 during different phases of fracture healing. In addition to the normal fracture healing, the influence of locally applied IGF-I and TGF-β1 on these parameter was analyzed. The localization of the growth factors using immunohistochemistry revealed an expression of both factors in mesenchymal cells, osteoblasts, osteocytes and chondrocytes during fracture healing without differences between the groups.

The growth factor quantity measured with ELISA was normalized to the callus weight or the total protein content of the callus. The amount of growth factors per mg callus showed a significant increase of the IGF-I level during the healing process whereas the TGFβ1 level was significantly enhanced at day 5 and then revealed a steady state without significant differences between the two experimental groups. Normalizing the growth factor quantity to the total protein content revealed different results. At day 15 significantly more IGF-I/protein was measurable in the growth factor group 2 compared to the control group 1 and the amount of TGF-β1/protein increased significantly in the group 2 from day 10 to day 15.

The dimension of measured IGF-I and TGF-β1 in bone was comparable to concentrations found in other studies. The IGF-I concentration was higher than the TGF-β1 concentration in the analyzed bone tissue. The total TGF-β1 level increased at day 5 and showed a steady level. Compared to the protein concentration only a slight increase was detectable. These results are in accordance with the analyses of TGF-β1 RNA during murine bone healing with a constitutive expression of TGF-β1 RNA during fracture healing.

This study was supported by a grant of the German Research Foundation, DFG Schm 1436/1-1,2

Differentiation but not proliferation of osteoblasts is stimulated by IGF-I and TGF- β 1 in vitro

Wildemann B, Lübberstedt M, Stange R, Schmidmaier G, Raschke M

Growth factors are known to influence osteogenic and chondrogenic cells. In vitro and in vivo studies investigated the effect of various growth factors on different cell types, cellular processes and on bone formation. Previous studies of our group revealed a stimulating effect of locally applied IGF-I and TGF- β 1 from Poly(D,L-lactide) coated titanium implants on fracture healing in rat and ovine tibia healing. However, also the PDLLA coating seemed to effect healing processes. The purpose of the present study was to evaluate the effect of IGF-I (5% w/w) and TGF- β 1 (1% w/w) and the carrier PDLLA on osteoblasts in cell culture.

Recombinant human IGF-I (5% w/w, 30 μ g) and recombinant human TGF- β 1 (1% w/w, 6 μ g) (R&D-Systems, USA) were incorporated into Poly(D,L-lactide) used for implant coating. Following samples were investigated:

1. titanium kirschner-wires uncoated, 2. coated with PDLLA, 3. coated with PDLLA and IGF-1 + TGF- β 1

Cell culture: The osteoblast cell line *hFOB 1.19* (10.000 each well) was used for the experiments and cultured in DMEM+HEPES at 34°C at 7% CO₂. The pH of the medium during the experiment was 7.6 to 8.0.

The implants were added to the osteoblast culture and removed after 1, 12, 24h, 2, 4, and 10 days (n=6 each time point and each sample). Every second day the culture medium was changed. All cell cultures were incubated for in total 10 days.

Control: hFOB 1.19 cell culture without wires

Trypan blue stain was used to count live and dead cells (Proliferation/vitality assay).

Cell activity/metabolism was determined by the WST-test (Tetrazolium salt is converted by mitochondrial dehydrogenases to Formazan).

Collagen-1 synthesis was analyzed with the Procollagen-ELISA (Prolagen, Metra Biosystem, USA).

Immunological test: mice monocytes/macrophages (line J774 A.1) were incubated for 3 days with the cell culture medium from the degradation test (see above) and the IL-1 β production was measured with an ELISA test.

Statistics: one way ANOVA and Dunnett Post Hoc test

The vitality test showed no influence of the tested implants on the cells and ranged between 93 to 97% in all groups.

The cell count revealed a decrease in the amount of cells after treatment with growth factors (group 3). After incubation with growth factor for 4 days or longer the reduction was significant. The PDLLA coating alone (group 2) caused only a slight decrease in the proliferation activity compared to the control culture. The titanium implant stimulated slightly the proliferation activity in osteoblasts (Figure 1).

No differences were detectable in the activity of the osteoblasts after incubation with the titanium implant or the PDLLA implant compared to the control culture. The cells treated with growth factors showed a significantly reduced mitochondrial

activity. However, when the culture was incubated for 4 and 10 days the cell activity increased in this group. Compared to the decreased amount of cells in each well, the result led to the conclusion that the activity is enhanced in the growth factor treated cells.

A significant increase in the collagen-1 production was detectable in the osteoblast culture treated with growth factors. Even after a 1h incubation of the cells with the growth factor coated implants an enhanced collagen-1 production was measured. The PDLLA coating had no effect on the collagen-1 production (Figure 2).

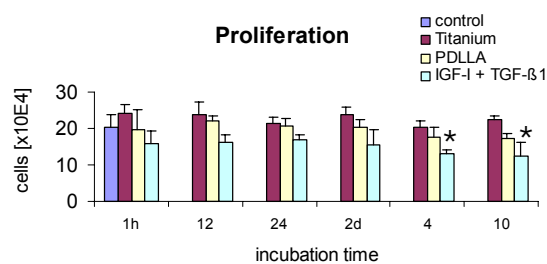


Fig. 1

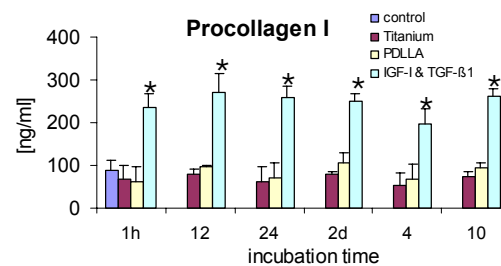


Fig. 2

Immunological test: No analyzed medium stimulated the production of IL-1 β .

The cell culture results clearly demonstrate that IGF-1 and TGF- β 1 incorporated into a polylactide coating influence osteoblast differentiation. The effect on the osteoblastic cell line was not the stimulation of cell proliferation but the stimulation of cell differentiation. No negative effect was seen in the vitality of the cells. Even an increase in cell activity was notable comparing the mitochondrial activity to the amount of cells in each well. In the growth factor group less cells were countable compared to the control culture, however the dehydrogenase activity increased at the later incubation time points (days 4 and 10). The effect of the PDLLA-coating on the osteoblasts was not very pronounced. No differences in proliferation activity, cell vitality and differentiation were detectable. Same results were found for the uncoated titanium implant. In conclusion no negative effect of the PDLLA on osteoblasts was found. The growth factors affect the osteoblasts more to differentiate than to proliferate. Neither the PDLLA-coating nor the incorporated growth factors evoked an immunological reaction in mice monocytes/macrophages.

Further experiments are planned to investigate the effect of the PDLLA and the incorporated growth factors on primary osteoblasts, chondrocytes and osteoclasts.

This study was partially supported by a grant of Synthes, U.S.A., Berliner Sparkassen Stiftung Medizin

Antibiotic coated intramedullary titanium implants in prophylaxis of acute implant related osteomyelitis in rats

Lucke M, Schmidmaier G, Wildemann B, Schiller R, Raschke M

Treatment of bone infections associated with foreign bodies like prostheses and other osteosynthetic devices still remains a challenge. Purpose of this study was to evaluate the efficacy of a new biodegradable gentamicin-bearing poly(D,L-lactide) (PDLLA) coating of metal implants for prophylaxis of implant related infections in rats.

40 female Sprague Dawley rats (5 months of age) were prepared and draped for surgery of the left tibia under sterile conditions. The medullary cavity was accessed by opening the proximal metaphysis with a 1mm titanium hand driven burr. 10 μ l of either phosphate buffered saline (PBS / controls) or 10 μ l PBS containing 10³ colony forming units (CFU) of Staph. aureus (ATCC 49230) were injected into the medullary cavity. Further a titanium K-wire (coated vs. uncoated) according to study groups was inserted.

Inoculum	K-wire	
Group I:	10 μ l PBS	uncoated
Group II:	10 ³ CFU / 10 μ l	uncoated
Group III:	10 ³ CFU / 10 μ l	coated with PDLLA
Group IV:	10 ³ CFU / 10 μ l	coated with PDLLA + gentamicin (10% w/w)

(CFU: colony forming units), n=10 each group

X-rays (p.a. & lateral) were performed at day of surgery and 14, 28 and 42 post op. X-rays were judged by 4 independent observers in a blinded manner according to a modified score by An (An YN, 1998 J Invest Surgery 11:139-146). After six weeks the animals were sacrificed. The tibiae were dissected under sterile conditions. K-wires were explanted, bones were weighed and five tibiae of every group were pulverized in a sterile bone mill. 150 mg of bone powder were suspended in 1.5 ml of sterile PBS, agitated for 2 minutes by vortex and then centrifuged for 10 sec. (10.000 rpm). 100 μ l of the supernatant were withdrawn for quantification of CFU Staph. aureus / g bone.

The remaining five tibiae of each group were analyzed histologically. Undecalcified longitudinal slices, stained with Masson Goldner were performed. Diaphysis, distal and proximal epi-/metaphysis were separately investigated and scored for osteolysis, periosteal reaction and for abscess and sequestrum formation. Score value ranged from 0 to 24 score points.

All animals of group II & III revealed radiographic signs of osseous destruction (Fig. 1), clearly detectable after two weeks. Destruction progressed during observation time. At all time points controls (I) and three animals of group IV showed no evidence of osteomyelitis. Radiographic score values of group IV were significantly lower at all time points compared to group II & III.

Histologically no signs of osteomyelitis were observed in group I and findings in group IV were significantly less obvious compared to group II & III. The microbiological analysis revealed, that two bones of group IV were completely sterile. Average CFU/g bone of groups II – IV was found significantly elevated compared to controls. All bones of group I remained completely sterile.

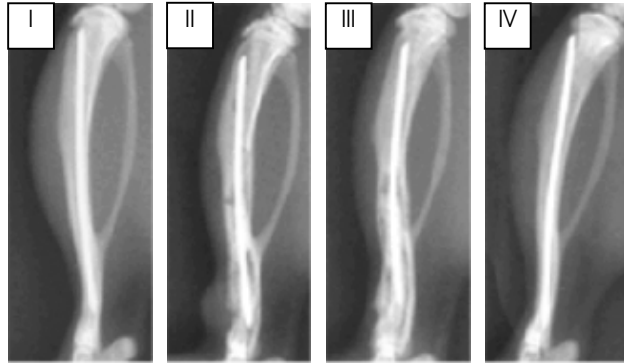


Fig. 1: X-rays 6 wks post. op. Osteolysis and periosteal reaction clearly detectable in groups II & III. No signs of osseous destruction in Group IV (PDLLA + Gentamicin) and control (group I)

A gentamicin bearing PDLLA coating of titanium implants is effective in preventing implant related osteomyelitis when inserted into the medullary cavity of rats with simultaneous inoculation of *Staph. aureus*. Radiological, histological and microbiological findings demonstrated significantly reduced manifestations of infection using gentamicin coated implants. This new technique could improve prophylaxis of infection related to orthopaedic devices.

This study was partially supported by a grant of Synthes, U.S.A.

Osteogenesis and vascularization of the fracture callus are affected by local application of growth factors IGF-1 and TGF-beta 1

Stange R, Wildemann B, Schmidmaier G, Raschke M

In the early phase of fracture healing cells proliferate, differentiate and blood vessels grow into the newly formed callus. These processes are influenced by different growth factors, cytokines and growth hormone. Several *in vitro* and *in vivo* studies have indicated a stimulatory effect of growth factors like Insulin like growth factor-I (IGF-I) and transforming growth factor- β (TGF- β 1) on cell proliferation and differentiation. Osteoinductive and angiogenesis promoting properties have been described for these growth factors *in vitro*. The mechanisms of these growth factors *in vivo*, however, remain unknown. Therefore, the influence of IGF-I and TGF- β 1 locally applied from poly(D,L-lactide) coated implants on proliferation, osteogenesis and vascularization during different phases of fracture healing was investigated in a rat model.

A standardized closed fracture of the right tibia of 5-month-old female Sprague Dawley rats (n= 45) was performed. The fractures were intramedullary stabilized with coated versus uncoated titanium-K-wires.

The following groups were investigated:

G I : implant uncoated, G II: coated with PDLLA, G III: coated with PDLLA + rhIGF-I (5%) + rhTGF- β 1 (1%)

After 5, 10, and 15 days animals were sacrificed. After dissection of the right tibia, the bones were fixed in formalin for 48 h, decalcified and paraffin-embedded. Serial paraffin sections (5 μ m) were performed in sagittal plane. Proliferating cells were stained with a monoclonal antibody against "proliferating cell nuclear antigen" (PCNA). Monoclonal mouse antibody against E11, a cell surface marker of mature osteoblasts, and Smooth Muscle Actin (SMA), a marker of the contractile filaments in smooth muscle cells of the vessels, pericytes and myofibroblasts, were used to detect osteoblastic cells and blood vessels. The ABC detection system was coupled with alkaline phosphatase to perform immunohistochemical staining. Slices were counterstained with methyl green to detect cell nuclei and cartilage. Proliferation, osteogenesis and vascularization of the callus was determined by localisation and distribution the immunoreactivity (IR) and judged by semiquantitative score.

Cell proliferation is a very fundamental and early event during fracture healing. To investigate this process antibody against PCNA was used to detect cells during the early G1 and S-phase of mitosis. We found a significantly higher proliferation of cartilage cells in the IGF-I and TGF- β 1 treated group at day 5 compared to the other groups. At day 10 a decrease of proliferating cells in the cartilage of group III was detected. At this time point the woven bone of group I showed significantly more immunoreactivity compared to the other groups. After 15 days a significant increase in the number of proliferating cells was detectable in the woven bone of the calluses of group III. In soft tissue group II and III showed more proliferating cells than group I.

At day 5 after surgery we found single osteoblasts in the periost at a distance to the fracture gap in the uncoated group I. Only few E11-positive cells could be detected

in group I at day 10 and 15. In group III with the growth factors coated implants several islands of osteoblastic cells could be detected at day 5, especially in the soft callus tissue close to the fracture. The IR increased until day 15. After 5 days a strong IR of E11-positive cells could also be seen in group II with a continuous decrease from day 5 to day 15.

Recruitment of a blood supply is critical for successful bone induction and fracture healing. Therefore we studied angiogenesis during the early phase of fracture healing by staining the actin filaments of smooth muscle cells in the vessels. Group II and III showed a high amount of SMA positive cells in soft tissue on day 5, and Group III also in woven bone. The signal decreased continuously in group II but not in group III until day 15. Group I showed an almost constant level of SMA-positive cells from day 5 to day 15 which is significantly lower at day 5 compared to group II and III.

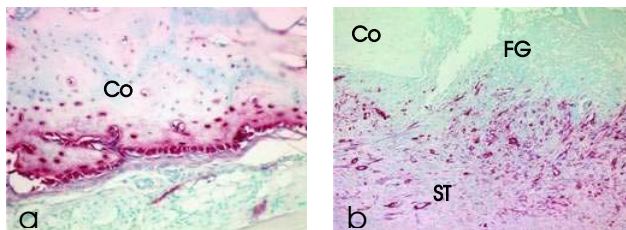


Fig. 1: a. E11-IR of osteoblastic cells, b. SMA-IR of vessels in the callus 5 days after fracture (group III). Co.: cortical bone; ST.: soft tissue; FG.: fracture gap

The morphology of the callus, the angiogenesis, and the proliferation of cells showed differences in the three groups during the early phase of fracture healing. An interesting difference in morphology displays the earlier appearance of cartilage at day 5 in group III (PDLLA + IGF-I + TGF- β 1) and the amount of vessels and osteoblasts compared to the other groups at this timepoint. This is accompanied by an early onset of cell proliferation in the cartilage in this group. The results lead to the conclusion that, in accordance with other investigations, locally applied growth factors stimulates the chondrogenesis. The callus of group II and III showed an accelerated and increased ingrowth of vessels compared to group I at the early phase of fracture healing. This effect could be explained by an unknown stimulatory effect of the PDLLA-coating and by the influence of the growth factors. The effect of the PDLLA decreases, whereas the effect of the growth factors remains up to 15 days. These results indicate that the local application of growth factors rhIGF-I and rhTGF- β 1 from a biodegradable PDLLA-coating accelerates early cellular processes during fracture healing. This assumption is supported by biomechanical and histomorphological data of recent investigations.

The influence of systemic GH- application on VEGF- expression and revascularisation during intramembraneous bone- healing

Lindner T, Hüning M, Kroeller A, Flyvbjerg A*, Raschke M, Bail H

Callus vascularisation is essential for successful bone- healing. Vascular Endothelial Growth factor (VEGF) is established as an angiogenic factor during enchondral ossification of the epiphysis. Furthermore, VEGF was shown to have an osteogenic effect during intramembraneous and enchondral ossification.

In several studies, systemic application of Growth Hormone (GH) stimulated bone- healing. Therefore, our research question was, whether systemic application of GH results in a stronger vascularisation of the callus and increases the expression of VEGF.

Left femora of 48 adult female Sprague- Dawley rats were osteotomized under standardized conditions after an external fixation device was applied. A 3 mm fracture gap was created. 24 animals received 3 mg GH /kg bw/day subcutaneously (divided into two doses), the others received sodium chloride as control. Femora were harvested on postoperative day 7, 14 and 21 (n=8), fixed, decalcified and embedded in paraffine. Callus formation and maturation were examined qualitatively. On 4 μ m serial slices VEGF [Santa Cruz Biotechnologies] and α -smooth-muscle-actin (α -sma) [Dako] were detected by immunohistochemistry. Using an image analysis system (Zeiss KS 400 Imaging Analysis System) the callus area was measured on decalcified slices and positive signals for α -sma were counted on 3 slices of each animal in defined regions of interest. For the evaluation of VEGF expression, a histological score was developed. The Mann- Whitney- U- Test was used for statistical testing.

7 days:

In both groups, the fracture gap was filled with mesenchymal tissue and islands of woven bone. VEGF was massively expressed in preosteoblasts and osteoblasts. In the GH- group, a higher number of vessels could be detected in the callus without any statistical significance. Neglecting the vessels in the periosteal layer and focusing on the callus, there was a significantly higher number of vessels in the callus of the GH- treated animals. This also resulted in a higher number of vessels in relation to the callus area in the GH- group.

14. days:

In comparison to animals receiving sodium- chloride, the gap of the GH- treated animals already showed bridges of woven bone in the intramedullary canal. Compared to the 7- days- animals, VEGF- expression was reduced in both groups, but still seen in the same cells at the ossification fronts. The number of α -sma positive cells was significantly lower in both groups. There was no significant difference between the groups.

21 days:

Parts of the intramedullary callus of the GH- treated animals were already resorbed, leaving a bony bridge inbetween the cortices on both sides.

Animals receiving sodium chloride showed incomplete bridging in the gap and still more callus in the intramedullary canal. In both groups there was weak expression of VEGF in the osteoblasts, the number of vessels did not significantly change in comparison to day 14.

Conclusions: Using a rigid external fixation device, the osteotomy gap is filled by intramembraneous callus formation originating in the endostal layer. Under systemic GH- application this process seems to be accelerated.

Strong expression of VEGF in preosteoblasts / osteoblasts in the gap after 7 days indicates that this growth factor plays a role especially in the early phase of the healing process. In both groups, the highest number of vessels is detected after 7 days, which then declines parallel to lower VEGF- expression levels after 14 and 21 days. Systemic application of GH does not lead to higher VEGF- expression at any time point examined in our model.

Nevertheless, in the GH- treated animals there is a stronger vascularisation of the callus after 7 days. This may contribute to the histologically accelerated callus maturation found in the GH- treated animals after 14 and 21 days.

*Aarhus Kommunehospital, Aarhus, Denmark

This study was supported by a grant of the German Research Foundation DFG Hu 867/1-1

Locally administered Growth Hormone and its mediator insulin-like growth factor exert similar effect on callus formation in a femur osteotomy model in rats

Bail H, Huening M, Lindner T, Krummrey G, Flyvbjerg A*, Raschke M

It has been demonstrated, that the systemical application of growth hormone (GH) results in enhancement of fracture healing. However, whether GH itself or its mainly liver-produced mediator insulin-like growth factor I (IGF-I) exerts the bone promotive effect at the fracture site remains unclear. In a model using small defects in rat mandibulae, it was demonstrated, that in combination with osteopromotive membranes locally as well as systemically administered GH accelerates defect healing. However, to our knowledge, there exist neither quantitative data about the effect of local administered GH in a fracture healing model, nor a comparison with the local administration of IGF-I *in-vivo*. Therefore, we performed a histomorphometrical analysis of the the callus in a femur osteotomy model in rats in order to determine, whether local administration of GH and its mediator IGF-I leads to different callus stimulation.

The left femurs of 24 female Sprague- Dawley rats were osteotomized (creating a gap of 3 mm) after a monolateral external fixation device was applied. All procedures were carried out with the ethical permission from the animal rights protection authorities. In each animal a mini-osmotic pump with a flexible tube at the fracture site was implanted. Using this pump, 8 animals received 100 $\mu\text{g}/\text{kg}$ bodyweight/day human GH (group III), 8 received 100 $\mu\text{g}/\text{kg}$ bodyweight/day IGF-I (group II) and 8 received phosphate buffer as placebo (group I) via the flexible tube. The femurs were harvested after 21 days and processed for histomorphometrical analysis (4 μm decalcified serial slices). The sections were stained with Safranin-O stain combined with light-green stain. The regions of interest were digitized and processed using the KS 400 image analysis workstation (Zeiss, Oberkochen, Germany). With specially developed algorithms, the following parameters were evaluated: callus area (Cl.B.Ar.), mineralized callus area (Cl.Md.B.Ar.), cartilage area (Cg.Ar.) and the callus diameter (Cl.Wd.). Based on this measurements the callus bone density (Cl.B.Dn.) and the cartilaginous share of the callus area (Cg.Ar./Cl.B.Ar.%) were calculated. The Cl.B.Ar. and the Cl.Md.B.Ar. was significantly higher in the GH - treated and the IGF-I - treated group compared to the placebo group (Tab. 1). The Cg.Ar. and the Cg.Ar./Cl.B.Ar.% was nearly doubled in the placebo group compared to group II and III. However, due to huge standard deviations, there was no significant difference. The structure of the callus, represented by the Cl.B.Dn. and the Cl.Wd., was not different between the three groups (Tab 1).

Table 1: Histomorphometrical parameters, the data are given \pm standard deviation

	Group I	Group II	Group III
Cl.B.Ar. (mm ²)	7.75 \pm 5.04	10.9 \pm 3.24*	10.97 \pm 2.03*
Cl.Md.B.Ar (mm ²)	5.04 \pm 2.11	8.31 \pm 2.38*	8.0 \pm 1.21*
Cl.B.Dn. (%)	64.6 \pm 9.93	76.47 \pm 7.27	73.59 \pm 6.43
Cl.Wd. (mm)	5.11 \pm 0.81	5.58 \pm 0.54	5.09 \pm 1.11
Cg.Ar. (mm ²)	0.41 \pm 0.37	0.24 \pm 0.23	0.25 \pm 0.28
Cg.Ar./Cl.B.Ar% (%)	4.4 \pm 3.4	2.11 \pm 2.21	1.87 \pm 1.65

* significant difference to placebo group (group I) $p < 0.05$

We sought to determine whether local administration of both GH or its mediator IGF-I lead to similar acceleration of fracture healing or whether these substances show a different effect on callus formation. Our results demonstrate, that after 21 days of fracture healing local application of both, GH and IGF-I increases hard callus formation nearly to an equal amount. Similarly, both substances change the callus composition in the same way towards a lower share of cartilage. The results propose, that GH may exert a direct, nonliver mediated effect on fracture healing. One weakness of the study is, that the data let not judge, whether the lower callus area in the control group results from advanced remodeling. However, the slightly lower callus bone density and the higher share of cartilage in the placebo group argue against that assumption. In conclusion, our findings in fracture healing may resemble the so called "dual effector theory", which hypothesised a direct effect of GH on longitudinal bone growth additionally to the sytemical effect mediated by IGF-I.

*Institute of Experimental Clinical Research, University of Aarhus, Denmark

This study was supported by a grant of the German Research Foundation DFG Hu 867/1-1

Poly(D,L-lactide) coating enhances osseous integration of mechanically loaded and unloaded Schanz' screws

Partale K, Klein P, Schell H, Schmidmaier G, Bail H, *Schiller R, **Bragulla H, Duda GN

Stable fracture fixation requires osseous integration, a process which is most often compromised by pintrack infections. Previous experimental studies have demonstrated that bony anchorage may be improved by means of various coatings. In addition, the mechanical loading of pins in external fixation is known to have an influence on the osseous integration. In a previous study that investigated fracture healing, a Poly(D,L-lactide) coating alone was shown to enhance bone healing. The goal of this study was to analyze the influence of a Poly(D,L-lactide) coating and mechanical loading on osseous integration of Schanz' screws and thereby reduce the risk of pin loosening in external fixation.

Standardized osteotomies (3mm fracture gap) of the right tibia were performed on twelve healthy female Merino sheep and stabilized by an AO mono-lateral fixator. The fixator consisted of three proximal and three distal Schanz' screws and two carbon fiber rods. Additional Schanz' screws were mounted on either side of the osteotomy gap. These additional screws were not connected to the fixator construct and therefore were mechanically unloaded. Each fixator involved two to three screws, coated by a 10 μ m thin biodegradable Poly(D,L-lactide) layer, that were randomly positioned. X-rays were taken at weekly intervals. The sheep were sacrificed after 9 weeks and all screws were removed. The screws were then rolled back and forth across the surface of agar plates for microbiological analyses. Bone sections through the pin tracks were taken for histological, histochemical and histomorphometrical analyses. Undecalcified sections, embedded in methylmethacrylate, were cut and stained with Masson-Goldner trichrome and Safranin-Orange/von Kossa. To visualize osteoclastic activity a staining method for TRAP (tartrate resistant acid phosphatase) was used. The histological sections were analyzed at the screw bone interface for the cortical bone reaction using a grading score that included histological, histochemical and histomorphometrical parameters. The score graded the extent of osseous intergration. Quantitative histomorphometry considered cortical bone density and periosteal and endosteal callus formation. Statistical methods consisted of a nonparametric analysis of longitudinal data.

During the first week animals unloaded the operated limb but returned to full weight bearing thereafter. Radiologically all animals showed regular callus formation and bone healing. Clinically, no signs of infections were visible. Microbiological analyses showed that coated screws amounted to 19% (4 out of 21) of severe pintrack infections by *Staphylococcus aureus*, whereas uncoated screws amounted to 32% (10 out of 31). Infected samples were excluded from further examination. Histological scoring of the residual samples demonstrated that significantly ($p < 0,05$) more osseous integration had occurred on coated screws. An intermediate tissue layer between screw and bone was observed more often in uncoated screws. In the Poly(D,L-lactide) coated screw group histomorphometrical analyses of the bone surrounding the Schanz' screws revealed a significantly ($p < 0,05$) higher bone density at the far cortex than in the uncoated screw group. Likewise there was significantly ($p < 0,05$) less osteoclastic activity seen near the screw-bone interface. Loaded

screws showed more extensive new bone formation around the screw entry and significantly ($p < 0,05$) more around the exit sites, with less dense cortical bone at the screw entry site.

Poly(D,L-lactide) coating alone was seen to enhance the process of fracture healing in rats. In the present study, Poly(D,L-lactide) coating of Schanz' screws was found to enhance their osseous integration in sheep by causing less cortical remodeling and less osteoclastic activity in the cortices compared to uncoated screws. Additionally, it appears to reduce the instances of pintrack infections. Mechanical conditions are essential for bone modeling and remodeling. In comparison to the unloaded screw group, loading increased the amount of callus formation seen at the screw entry and exit sites. Callus formation surrounding the pintracks allows a closer bone-implant contact which acts as a stabilizing factor. In addition to the positive effect of the coating, the mechanical conditions appear to be beneficial to the osseous integration of a screw. Furthermore this study demonstrates a superior anchorage of screws at the far cortices, documented by a higher cortex density and a lower osteoclastic activity compared to the near cortices. Higher drilling stress and higher loading conditions at the screw entry site may explain this observation. In summary, the Poly(D,L-lactide) coating of Schanz' screws demonstrated a superior osseous integration and reduced infection rates.

In the future torque measurements will be performed in addition to analyze the biomechanical properties of screw anchorage in bone. The results will be correlated with histological findings of the pin tracks. Furthermore different time points will be evaluated to observe the pathways that have been taken to get to these results. Analyses of other cellular reactions are in progress to further understand the remodeling process and the impact of Poly (D,L-lactide) on adjacent soft tissue reactions.

*Institute for Microbiology and Hygiene, Charité, Humboldt-University of Berlin, Germany

**Institute for Veterinary Anatomy, Free University of Berlin, Germany

This study was supported by a grant of the AO/ASIF Foundation, Switzerland

Tibio-femoral loading during human gait

Taylor WR, Heller MOW, Bergmann G*, Duda GN

Surgical intervention of the knee joint routinely endeavors to recreate a physiologically normal joint loading environment. The loading conditions resulting from osteotomies, fracture treatment and arthroplasties of the knee are considered to have an impact on the long term clinical outcome. Knowledge regarding the in vivo loading conditions in the knee is limited, however. The goal of this study was to determine validated human tibio-femoral contact loads that occur during typical daily activities.

A musculo-skeletal model of the human lower extremity was developed¹ based on CT-data from the Visible Human (NLM). Muscles were represented as straight lines spanning from origin to insertion, wrapped around the bones where necessary to approximate their real curved path. Muscles with large attachment areas were modelled by more than one line of action, totalling 95 modelled fibres. The tibio-femoral joint was modeled with three rotational degrees of freedom (DOF) while the patello-femoral joint had one rotational DOF around the medio-lateral axis, and two translational DOF in the sagittal plane.

An instrumented femoral prosthesis was used to measure the in vivo hip contact forces in four patients (mean 61 years) as described in a previous study¹. Clinical gait analysis was conducted for six trials of both walking and stair climbing and time dependent kinematics and kinetics data were gathered. The in vivo hip contact forces were measured during all activities. An optical system (Vicon, UK) consisting of six infrared cameras and 24 reflective markers attached to the patients' skin was used to determine movement of the lower limbs.

The musculo-skeletal model, including muscle origins, insertion sites and wrapping points, was then scaled to the individual patient anatomies using bony landmarks positions. Muscle force distribution was then computed using numerical optimization techniques. From the muscle and the resultant intersegmental forces, joint contact forces were calculated for the ankle, knee and hip joints for the tested activities in all patients. Measured and calculated hip contact forces revealed good agreement in both pattern and magnitude for all activities in all patients¹.

The average resultant peak tibio-femoral contact force during walking was 3.2 times body weight (BW) across all four patients (Figure 1). Compared to the variation of forces for each patient repeating the same task, inter-individual variation proved larger. During stair climbing, forces through the knee were considerably larger than during walking. The average maximum force for this activity was 5.4 BW although peaks of up to 6.2 BW were calculated for one particular patient. Average anterior-posterior peak shear forces of 0.6 BW were determined during walking and 1.3 BW during stair climbing.

For the first time, this study has established fundamental knowledge of the loading occurring in the human knee during the most common daily activities, calculated using a validated musculo-skeletal model and without physical intervention of the knee. The results demonstrate both intra-individual variation between repetitions of the same exercise but also inter-individual variations between different patients performing the same task. The calculated in vivo tibio-femoral contact loads were

comparable to those seen in the literature and larger than the corresponding loads in the hip joint which were reported as up to 3.1 BW during walking and 3.7 BW during stair climbing.

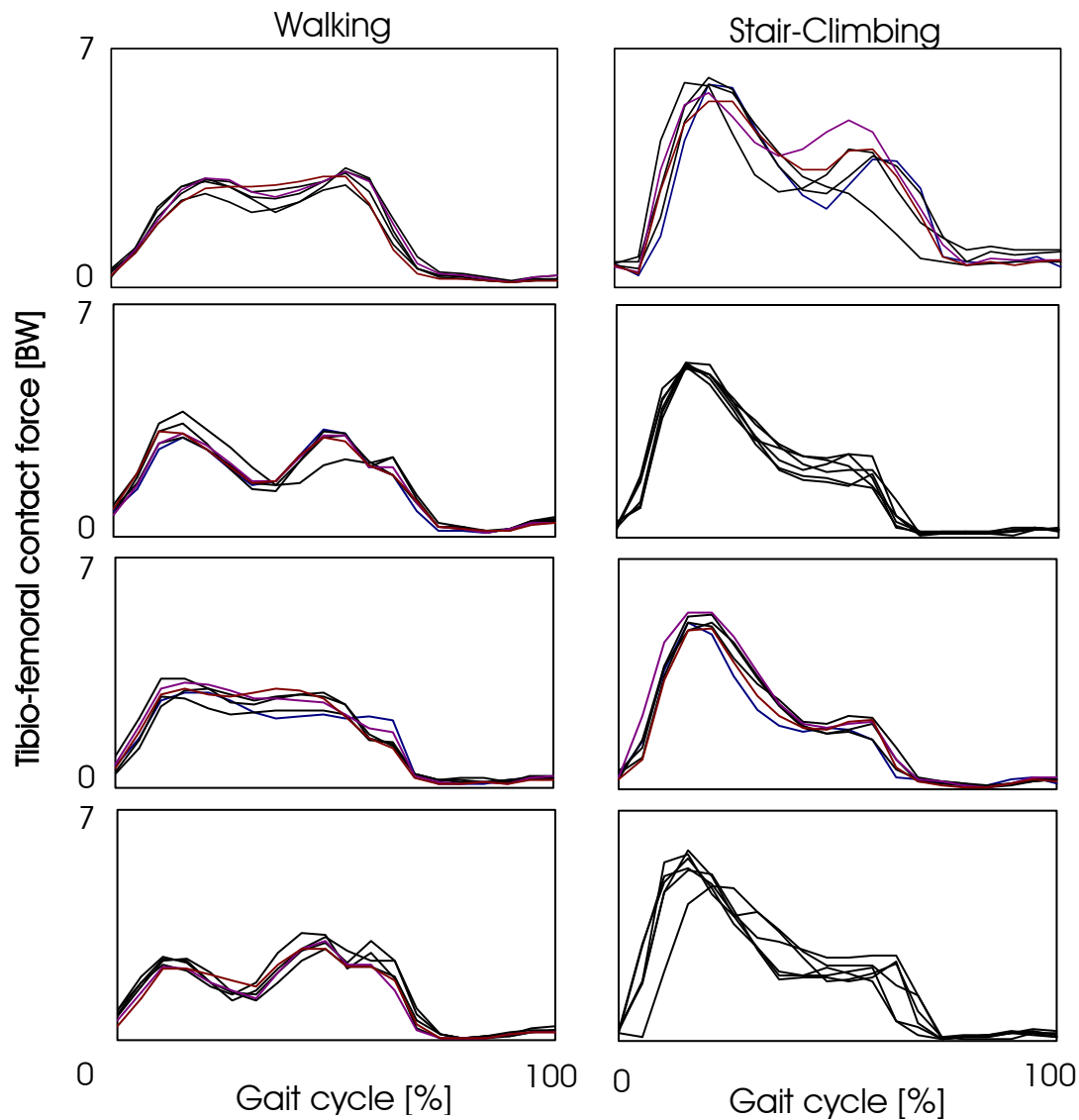


Figure 1: Tibio-femoral resultant contact forces of four different patients calculated throughout the gait cycle using the musculo-skeletal model. All forces in body weight.

*Biomechanics Lab, Orthopedic Clinic, Universital Hospital Benjamin Franklin, Free University of Berlin

This study was supported by a grant of the German Research Foundation DFG KFO 102/1 and the Sonnenfeld Foundation, Berlin

Kinematics of the in vivo sheep knee

Taylor WR, Schell H, Klein P, Heller MOW, Duda GN

Knowledge of knee kinematics forms the basis of analyses of the local loading environment, including bone remodelling and soft tissue straining. Complete determination of the physiological joint motion that occurs during the human gait cycle, however, is not possible due to the invasive nature of testing. Establishment of measurement techniques and an initial understanding of the tibio-femoral joint loading in the sheep knee, recognised as being a similar to the human knee, can lead to improvements in patient specific clinical analyses of musculo-skeletal loading. The aim of this study, was therefore to establish the movement of the sheep hindlimb throughout the gait cycle as the basis for establishing the loading conditions that occur throughout the hind limb. In addition, this process can then lead to an improvement in the current understanding of the interaction of the tibia and femur in an attempt to determine the kinematics of the knee, the loading in the soft tissue structures and the distribution of the loading across the femoral condyles.

Three marino-mix sheep were trained to walk over a gangway which included a pressure sensitive force platform (Emed, SF-4, novel, Germany). Gait analysis was performed pre-operatively: up to 15 reflective markers were attached to the skin of the rear right limb and the 3-dimensional position of each marker was recorded at a rate of 60Hz using an infra-red optical measurement system (PCReflex, Qualysis, Sweden; accuracy ± 0.1 mm) during repetitions of walking over the gangway.

Schanz' screws were then surgically inserted bicortically into the pelvis, femur, tibia, metatarsus (all \varnothing 4.5 mm) and the patella (\varnothing 2.5 mm) of the right hindlimb of all sheep. The soft tissue was preserved to exclude damage to the process of weight bearing and walking. The wounds were sutured and all sheep received an analgesic (Finadyne®, Germany) until further gait analysis tests, performed two or three days postoperatively.

During the postoperative gait analysis, light-weight aluminum frames, each holding four reflective markers (3 for the patella due to weight minimisation), were attached to each of the Schanz screws. Gait analysis was performed both with and without the additional skin markers from the pre-operative analysis. All animals were then sacrificed and the complete hindlimb was CT scanned (Siemens Somatom PLUS4 VolumeZoom, Erlangen, Germany); 1mm scan spacing, 1mm slice thickness, 0.742 x 0.742mm in plane resolution). Surfaces of each bone (Figure 1) were reconstructed from the CT scan data (Amira v2.3, ZIB, Berlin). Local coordinate systems were defined and the relative position of each reflective marker was reconstructed in the global CT coordinate system. Using a least squared best fit process, the transformation matrix for each set of markers was determined between the CT and the gait analysis coordinate systems for each bone and time frame of the test data. The surface of each bone was then transformed using the same matrix, thus creating the complete gait cycle (Figure 1). Through the creation of local coordinate systems, parallel to the long axis of each bone and at the centre of the joint, (e.g. on the tibial plateau at the the intercondylar tubercles in the case of the knee), it was possible to generate the relative movement and translation of each joint.

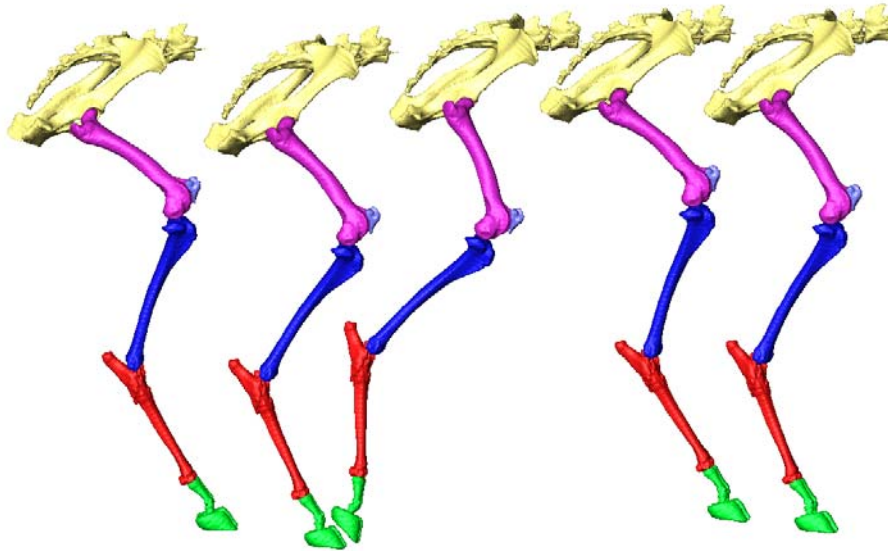


Figure 1: Reconstruction of a sheep right hind limb, shown at stages throughout one gait cycle.

Results of the pre- and post-operative gait analyses show a significant reduction in the ground reaction forces after surgery, implying an alteration to the gait patterns as a result of the insertion of the Schanz' screws. In order to both be able to account for this unloading and to be able to transform the experience ascertained from this sheep study into the clinic for knowledge of movement and loading in the human knee, several additional sections of this project are being concurrently undertaken. These include the development of new techniques to accurately establish the underlying movement of bones from reflective markers placed on the skin and the determination of transcondylar loading in the knee.

This study was supported by a grant of the German Research Foundation DFG KFO 102/1 and the Sonnenfeld Foundation, Berlin

Surgical approach in THA causes long term differences in periprosthetic femoral bone densities

Heller MO, Perka C*, Wilke K*, Haas NP, Zippel H*, Duda GN

Periprosthetic bone loss is one of the greatest problems in total hip arthroplasty (THA). Until recently, however, little attention has been given to the influence of the surgical approach and the extent of soft tissue trauma on the periprosthetic bone mineral density (BMD). The muscles surrounding the hip are altered as a result of preoperative pain and morphology, but especially by the selected surgical approach. The goal of the present study was to compare the change in musculo-skeletal loading and periprosthetic BMD in relation to the alteration of the musculature after the anterolateral and transgluteal surgical approaches in THA.

150 patients with primary coxarthrosis received a cementless primary arthroplasty (Alloclassic, Sulzer Medica, Switzerland). 52 patients with 67 artificial hip joints were available at a 5 year follow up period. Group A comprised 30 hips in 25 patients who had received a prosthesis via the anterolateral approach. Group B included 37 hips (27 patients) in which the transgluteal approach had been used. No significant differences were detected between groups in respect to age and gender distribution as well as in respect to average stem size or the ratio of prosthesis stem/femoral canal filling in a Wilcoxon test (confidence interval: 95%, $p > 0.05$). The clinical assessment was performed by a single investigator using the Harris Hip Score. Quantitative measurements of BMD using DEXA on a DPX-L densitometer (Lunar, Germany) were taken of the proximal femur until 2 cm distally of the tip of the prosthesis with the patient in a fixed supine position. The BMD values were averaged within each of the seven Gruen zones. The t-test and Mann-Whitney U test were used to evaluate differences between groups. The significance level was set to 95% ($p < 0.05$).

The loading conditions of the lower limb were evaluated using a previously reported, validated numerical model: A computer model of the bones and muscles of the human lower extremities was scaled to match the anatomies of 4 THA patients with telemetric prostheses. Gait data for walking and stair climbing was determined simultaneously with *in vivo* hip contact forces. Muscle and joint contact forces were calculated throughout the gait cycle for both activities and validated against the *in vivo* hip contact forces. To simulate the estimated damage caused during the transgluteal approach, the physiological cross sectional areas of the major abductor muscles were reduced by 30%, thus limiting the maximum transmittable force in the tissue. The resulting muscle force distribution and hip contact forces were then calculated for the 4 patients during both activities.

There were no significant differences in the functional outcomes between both groups postoperatively. The Harris Hip Score improved from a mean of 38 (range 3 to 65) points to 82 (range 36 to 100) in group A versus an improvement from a mean of 38 (range 13 to 63) to 86 (range 41 to 100) in group B. The osteodensitometric measurements showed a significant reduction in bone density (Tab. 1) in Gruen zones I, II, VI and VII after the transgluteal approach (group B) compared with the anterolateral approach (group A). In zones II, VI and VII, the reduction of BMD was highly significant ($p < 0.01$). Remarkably, the reduction

affected not only the lateral but also the medial proximal Gruen zones. A reduction of the capacity of the gluteus medius by 30% after a simulated transgluteal approach led to a considerable redistribution of the musculo-skeletal loading across the hip joint: While the forces in the muscles attaching directly at the proximal femur (single joint muscles) were generally lower (max. 21%), the forces in the muscles spanning the hip and the knee (two joint muscles) increased by up to 57%. Overall, the weakening of the major abductors increased the hip contact forces by 10% (min: 8, max: 12%) during walking and by 8% (min: 4, max: 12%) during stair climbing.

Gruen zone	median		min		max	
	group A	group B	group A	group B	group A	group B
I*	0.862	0.699	0.464	0.357	1.352	1.472
II**	1.591	1.112	0.903	0.333	2.903	2.033
III	1.839	1.724	1.155	0.968	2.499	2.578
IV	1.784	1.892	1.328	1.278	2.353	3.562
V	1.848	1.803	1.371	1.331	2.752	2.272
VI**	1.369	0.945	0.922	0.424	2.577	1.908
VII**	0.933	0.661	0.616	0.280	1.506	1.305

* $p < 0.05$; ** $p < 0.01$ (follow up at 5.8 (group A) and 5.5 years (B) post op)

Table 1: Comparison of periprosthetic BMD (g/cm^2) in all Gruen zones after the anterolateral (group A) and transgluteal approach (group B)

Periprosthetic bone loss poses a major challenge to the long term performance of hip endoprostheses. The findings of the present study demonstrate the influence of two different surgical approaches on musculo-skeletal loading and long term periprosthetic bone loss. The redistribution of muscle forces at the proximal femur, as shown by the computer model, corresponded with the reduced BMD in the proximal Gruen zones. Although the damaged soft tissues surrounding the hip would recover in a relatively short period of time, this redistribution of muscle forces might cause a long term adaptation of the loading conditions at the hip and therefore alter the bone remodeling as seen in the clinical study. Based on the data presented in this study, future research and development on hip endoprostheses should focus on a muscle-sparing implantation. However, long-term and randomized, prospective studies are necessary to further elucidate this question.

*Dept. of Orthopaedics, Charité, Humboldt-University of Berlin

This study was supported by a grant of the German Research Foundation DFG Du 298/4-1

THA loading arising from increased anteversion and offset may lead to critical cement stresses

Heller MO, Kleemann RU, Stöckle U, Taylor WR, Duda GN

Total hip arthroplasty (THA) is one of the most successful procedures in orthopaedic surgery. However, the long term survival of the reconstructed joint is influenced by factors like the prosthesis design and surgical aspects such as the orientation of the implant. The predominant failure mode for cemented hip reconstruction is aseptic loosening caused by cement crack initiation and osteolysis. Clinical and experimental studies have discussed the influence of femoral offset and anteversion on the function of the intact hip joint and its possible relationship to joint degeneration. However, the role of these variations in artificial hip joints is unknown. The goal of the present study was therefore to quantify the influence of both femoral anteversion and prosthesis offset on bone and cement loading.

Based on a validated musculo-skeletal model, muscle and joint contact forces were determined for a full cycle of walking and stair climbing in a THA patient. Employing the model, muscle and joint contact forces were also determined for different implant designs (standard vs. +5mm increased offset) and orientations (4° vs. 24° anteversion). Corresponding finite element models of a femur with a prosthesis were generated for a clinically successful cemented stem design (MS-30, SulzerMedica, Swiss). The gap between the prosthesis and bone (3 mm) was filled with cement elements. The boundary between the stem and cement was modelled as a fully debonded interface using coulomb friction ($\mu=0.25$). A Young's modulus of 17 GPa was assigned to the cortical bone together with a Poisson's ratio of 0.33. The properties of the trabecular bone were graded from proximal to distal in 4 steps (2.0 to 0.25 GPa) with a Poisson's ratio of 0.33. The cement modulus was 2.6 GPa, whilst the Protasul S30 stem was assigned a Young's modulus of 200 GPa. A Poisson's ratio of 0.3 was used for all artificial materials. All materials were assumed isotropic and linear elastic in behaviour. The models were analysed using the MARC/Mentat software (MSC, USA). Straining of the bone at the peaks of the gait cycle loading was analysed to establish the worst case loading scenarios. These cases were then used for the comparative analyses. Minimum principle (tensile) stresses were analysed throughout the complete cement layer. Additionally, cement stresses in specific regions of clinical interest (e.g. calcar and tip regions) were evaluated as these regions are considered important for the longevity of artificial joints.

Increasing the prosthesis anteversion from 4° to 24° caused higher muscle and joint contact forces, resulting in an increase in bone strains of up to 16%. At the same time, the average cement stresses were increased by up to 52% (walking). Despite lower muscle and joint contact forces, the FE models with an increased prosthesis offset showed a minor increase in strains at the bone surface (up to +5%). Only small changes were found in cement stresses (up to +9%). Combining increased anteversion and larger prosthesis offset during walking had a similar effect as increased anteversion alone: The stress magnitudes in the cement mantle were almost doubled compared to the case with increased offset alone. During stair climbing, however, the increased loads caused substantial rises in cement stresses (up to +67%, Fig. 1).

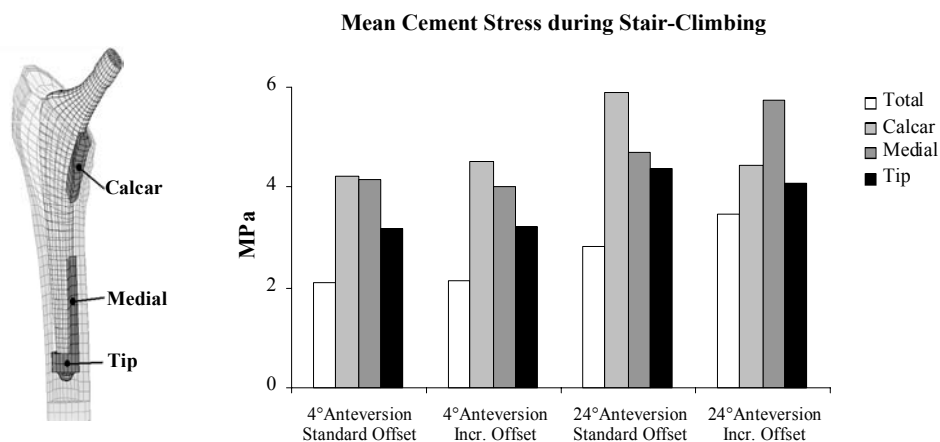


Fig. 1: Distribution of cement elements in the specific regions of interest into discrete stress ranges for different loading scenarios during stair-climbing.

A long prosthesis offset together with increased anteversion raised the percentage of elements with cement stresses in the range responsible for damage accumulation (3-10MPa) from 19% to 51%. Examination of cement stresses in the specific regions showed mean stresses of almost 50% greater than in the complete cement mantle: When analysing the combined effects of large anteversion and increased offset, nearly 80% of the elements in these regions were found to be within the 3-10MPa range. Cement stresses in the calcar and regions medial and lateral of the implant tip locally exceeded the assumed cement fatigue strength of 8MPa under the reference THA conditions, but did not change after modifications in anteversion and offset were made.

This analysis has demonstrated that changes in implant orientation and design are capable of causing substantial rises in cement stresses, most importantly in the critical regions, e.g. the calcar. The results indicate that anteversion plays a more important role in determining cement mantle loading than prosthesis offset. Femoral anteversion may therefore be considered a more influential parameter than offset in the long-term clinical outcome of THA, but their combination, especially during stair climbing, can produce critical cement stresses. In the clinical situation, these undesirable effects should be considered, and when an implant with a large offset is to be used, the surgeon should be careful to avoid large angles of anteversion.

Influence of muscle force simulation *in vitro* on the pre-clinical evaluation of the initial stem stability in THA

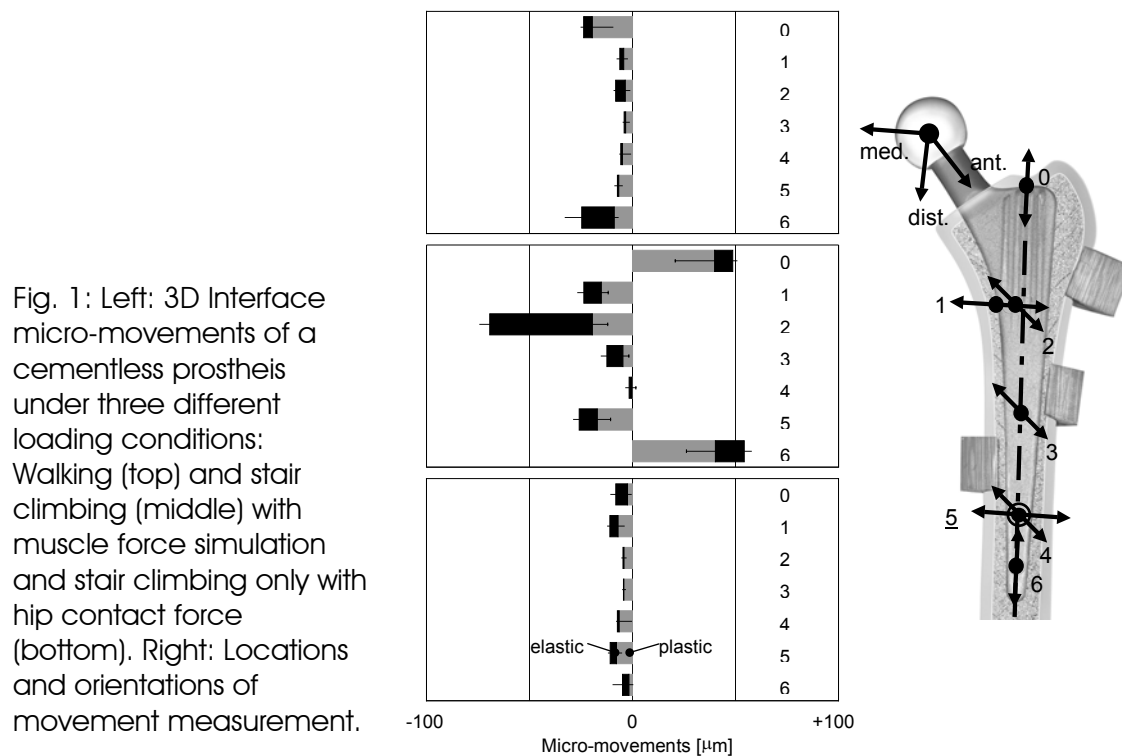
Kassi J-P, Heller MOW, Stoeckle U, Perka C*, Duda GN

Primary stability is long established as a determinant of the long-term performance of total hip prostheses. Initial mechanical stability is the prerequisite for an extensive biological integration of the implant (osteointegration). Pre-clinical *in vitro* tests ought to evaluate the implant behavior and thus, to predict their long term clinical outcome. These tests often reduce the loading of the hip region to the resultant joint contact force, producing implant micromotions of the order of 10-20 μm . However, the complex *in vivo* loading of the hip region (due to muscle activity) gives rise to initial implant movements of up to 100 μm .

This study investigated the influence of muscle forces on the primary stability of cementless hip endoprotheses *in vitro*.

Based on *in vivo* hip contact force measurements and gait data of 4 patients with THA, a validated musculo-skeletal computer model was employed to determine the distribution of muscle and joint forces of the lower limb. From this model, simplified load cases of the proximal femur region including both muscles (max. 5) and weight bearing were extracted. A mechanical loading set-up, consisting of a servo-hydraulic testing machine (Instron) to apply the bodyweight and four servo-electrical actuators to simulate muscle forces, was realized. 18 composite femora (Sawbones), were randomly divided into three groups and implanted with a clinically successful cementless prosthesis (CLS, Spotorno). The femora were transcortically instrumented at six locations (1-6, Fig.1) with Linear Variable Displacement Transducers (LVDT) to measure the 3D interface movements. In addition, the longitudinal displacement of the prosthesis shoulder (0, Fig.1) was recorded. The femur was first distally mounted on a ball bearing and simultaneously loaded by muscle forces (tensor fascia lata, abductor, vastus lat. and med.) and partial bodyweight simulating walking and stair climbing. For comparison with conventional primary stability tests, the femur was proximally unconstrained and distally fixed with polymethylmethacrylate (PMMA) in the stair climbing position and loaded only by the equivalent hip contact force. In all cases, the applied dynamic load (1000 cycles, 0.25 Hz) represented 50% of the peak resultant force (walking: 1062 N, stair climbing: 1174 N).

The total movements after 1000 cycles walking was always lower than 10 μm . The implant principally moved in the lateral direction and no significant distal migration occurred (Fig.1, top). In comparison, stair climbing showed substantially higher movements of up to 50 μm with a clear distally oriented component and a pronounced posterior-anterior (rotational) elastic movement (LVDT 2, Fig.1, middle). The micro-movements without muscle force simulation (Fig.1, bottom) were lower than those with muscle force simulation (Fig.1, middle). In addition, the rotational component was comparatively low (LVDT 2, Fig.1, bottom).



Even though the load level and number of cycles were relatively low compared to the *in vivo* situation, the study demonstrates a clear difference between the load cases. Pre-clinical *in vitro* testing which employs hip contact force only, tends to cant the implant into the femur and subsequently leads to lower interface micromotions. These tests underestimate the relative movements of hip endoprostheses compared to the clinical situation. Loading that considers the muscle forces, albeit at a less critical level, leads to considerably higher movements. Stair climbing, in producing the highest implant movements, confirmed its status as the most critical activity for THA patients. Therefore, pre-clinical tests should consider stair climbing and the active role of muscles in the assessment of initial implant stability, otherwise micromovements may be underestimated. The physiologic-like loading *in vitro* produced micromotions comparable with those seen radiographically in patients following THA. The analyses suggest an influence of muscle activity on the initial stability of total hip endoprostheses. However, *in vivo* clinical data is required to further confirm the interaction between activity and implant stability.

*Dept. of Orthopaedics, Charité, Humboldt-University of Berlin

This study was supported by a grant of the Federal Institute for Drugs and Medical Devices, BfArM

Influence of anchorage principle on the primary stability in cementless THA under physiologic-like loading conditions

Kassi J-P, Heller MOW, Stoeckle U, Duda GN

Aseptic loosening is one of the most frequent failure scenarios of femoral stems in THA¹. Cementless fixation is considered an alternative to cement fixation techniques, particularly in young and active patients. Sufficient initial stability is a prerequisite for osseointegration and thus, for long-term fixation. Primary stability of the stem in the host bone is commonly achieved by proximal or distal fixation, which may lead to stress shielding and osteolysis. Pre-clinical analyses of stem stability aim to determine the magnitude and pattern of interface movements of different stem designs in vitro and to link these to the bone ongrowth expected clinically. However, in vitro applied loads rarely simulate the musculo-skeletal loading conditions in vivo adequately.

Therefore, the aim of this study was to analyze the influence of different anchorage principles on the primary stability of cementless stems under physiologic-like loading conditions in vitro.

Two clinically successful, cementless stems were selected for mechanical evaluation: a proximal, metaphyseal (CLS, Spotorno) and a mainly distal (Alloclassic-SL, Zweymueller) anchoring femoral stem. Six stems of each design were implanted in medium-sized composite femora (Sawbones), which were chosen to minimize the inter-specimen variability associated with the use of cadaveric femora. The femoral canal was machined using standard broaches and implantation was performed according to the manufacturer's recommended procedure. The femora were transcortically instrumented at six locations (1-6, *Fig. 1*) with Linear Variable Displacement Transducers (LVDT) to measure the relative interface movements. In addition, the distal movement at the prosthesis shoulder (0, *Fig. 1*) was recorded. Mechanical loading was performed on the previously described physiologic-like loading set-up. Stair climbing was simulated because of the high forces and moments generated during this activity. The elastic and plastic movements were measured during the sinusoidal loading (1000 cycles, 0.25 Hz) and evaluated at a load level corresponding to 50% of the peak forces.

Both stem designs exhibited similar movement patterns (*Fig. 1*). The stems principally moved distally (0 & 6, *Fig. 1*) with a characteristic retroversion movement (2, *Fig. 1*). The proximal, metaphyseal anchoring stem experienced a more considerable initial migration and showed higher plastic movements than the distal anchoring stem. Latter was subjected to larger elastic and comparatively smaller plastic movements. The elastic movement components at the interface were comparable for the two stems.

This study aimed to analyze the influence of different anchorage principles on the primary stability in cementless THA under physiologic-like loading conditions.

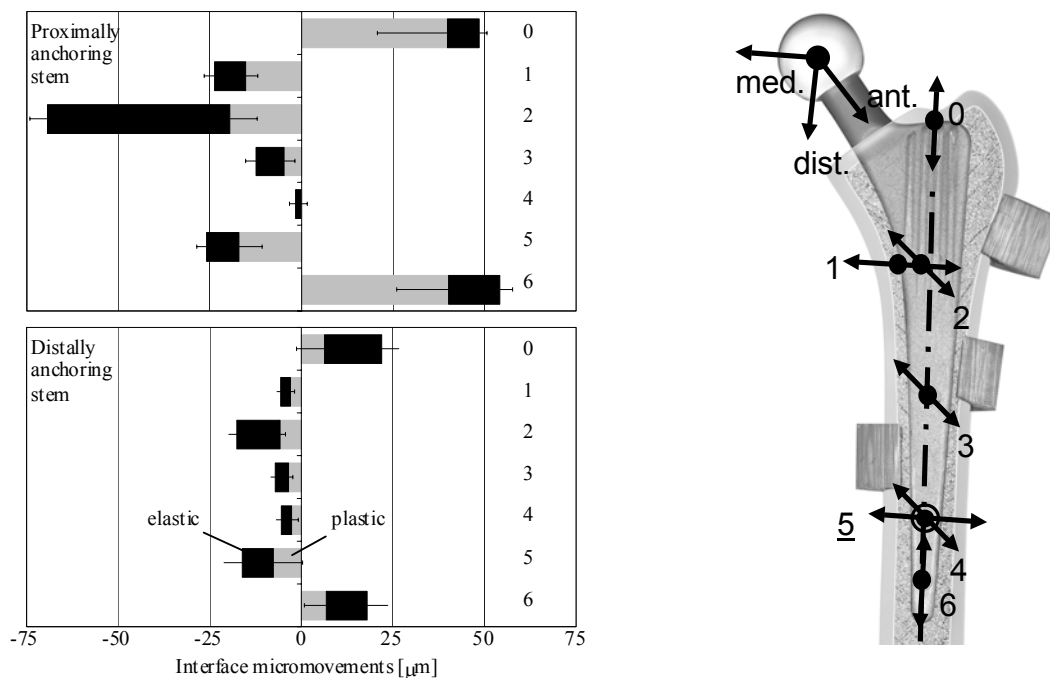


Fig. 1: Left: Interface micromovements of a proximal (top) and a distal (bottom) anchoring cementless stem under physiologic-like loading conditions. Right: Sensor locations (0-6) and orientations

A proximal, metaphyseal and a distal, meta-diaphyseal anchoring stem were investigated. The implanted femora were subjected to a cyclical loading regime corresponding to the activity of stair climbing. Under this loading regime, the stems experienced high axial forces coupled with considerable retroversion torque forces. Both stems showed similar movement patterns, which reflect the aforementioned load distribution. The stems principally migrate distally and were twisted backwards. Even though both anchorage principles exhibited comparable and relatively small elastic movements, the distal anchoring stem provided a more stable initial fixation with lower plastic interface movements. In contrast, the metaphyseal anchoring stem underwent more considerable initial plastic migration and retroversion. This gradual stabilization may adversely affect the osteointegration process of the implant in the metaphyseal region, particularly in THA patients with poor bone quality or with osteoporotic bones.

This study was supported by a grant of the Federal Institute for Drugs and Medical Devices, BfArM

The initial phase of Fracture healing is specifically sensitive to mechanical conditions

Klein P, Schell H, Streitparth F, Bail H, Kandziora F, Bragulla H, Duda GN

It is generally accepted that movements of the fracture fragments stimulate and determine quality and quantity of callus formation. The amplitude and direction of initial movement is determined by the implant's stiffness. The mounting plane of external fixators is usually determined by surgical needs and the appropriateness of the surgical approach. Recent analyses suggest a considerable influence of the mounting plane on osteotomy fragment movement. The aim of this study was to investigate the influence of mounting plane on the healing mechanisms associated with monolateral external fixators. In doing so the following mechanical and histological parameters were evaluated: Osteotomy fragment movement, biomechanical stability of the fractured tibia, quality and quantity of callus formation and its orientation.

Two groups each consisting of six female merino sheep, two years of age, underwent a standardized midshaft osteotomy of the right tibia (gap=3 mm). The osteotomy was stabilized with a monolateral external fixator, mounted medially and anteromedially in groups I and II respectively. The fixator consisted of 6 Schanz` screws (\varnothing 5mm, 3 inserted proximally, 3 inserted distally of the osteotomy gap) and 2 carbon fiber rods (\varnothing 10mm). The distance between inner rod and skin was 5 mm. Biomechanically the different mounting planes were tested for torsional strength and torsional stiffness and found to be equal. Both groups received one additional Schanz` screw proximally and distally of the osteotomy gap that served for measurement.

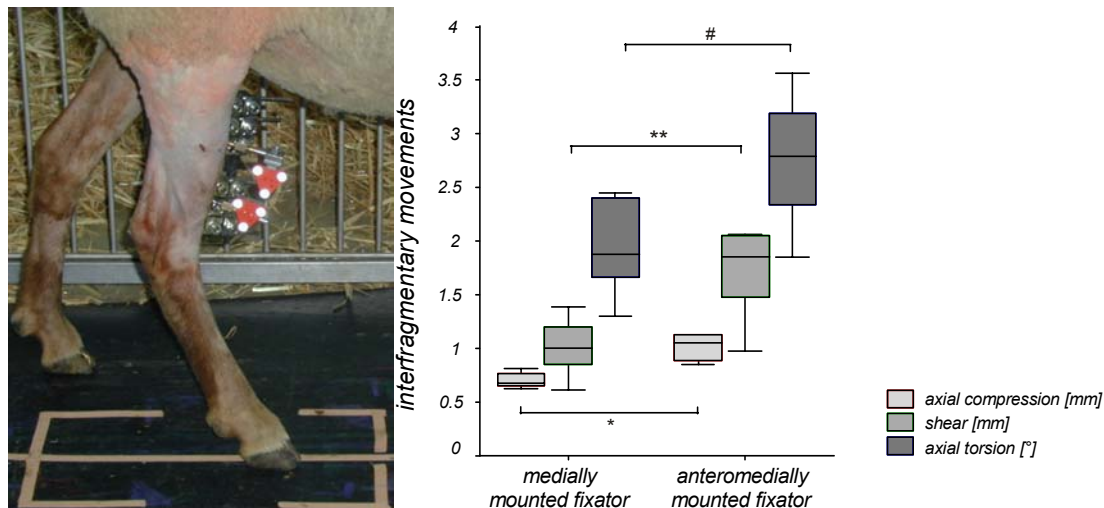


Fig 1: Measurement and results of initial interfragmentary movement

Measurements of fragment movements (Fig 1) were taken up to three times a week using an infrared camera system (PCReflex, Qualisys). Limb loading was recorded pre- and postoperatively using a force platform (Emed, novel). X-rays were taken once a week throughout the nine-week healing period until the animals were sacrificed. The fractured tibiae were explanted and tested in torsion until failure and compared with the contralateral tibiae. The callus region was sectioned into 3mm slices in the frontal plane. After dehydration with alcohol, the sections were

embedded in methylmethacrylate. 4 μm histology sections, using modified Safranin-Orange/von Kossa and Safranin-Orange/Lightgreen stains, were prepared to determine the characteristics of the callus tissue. The callus tissue's quality and quantity were examined using an image analysis system. Tissue differentiation was quantified for bone, cartilage and fibrous tissue according to location.

Initially, i.e. two days postoperatively, significant differences for interfragmentary movements between both groups could be monitored (Fig 1): Axial as well as shear movements were significantly higher in the AM group ($p^* = 0.041$, $p^{**} = 0.041$, Mann-Whitney-U-Test). In addition, the axial torsion showed a strong but not significant difference for the initial measurement session between both groups ($p\# = 0.065$, Mann-Whitney-U-Test). However, within one week, the movements in both groups reached similar levels. In addition, a decrease of interfragmentary movements over healing time could be observed. At 9 weeks there was a significant increase in callus strength in the AM mounted group.

Safranin-Orange/von Kossa stains of both groups show uniform, mostly osseous callus tissue formation. The osteotomy was bridged periosteally as well as endosteally. The intercortical osteotomy gap was filled with mineralized bone tissue. Periosteally, both groups showed more extensive callus tissue formation on the medial side. The periosteal callus on the medial side in group I, was significantly different in terms of greater total area, osseous area and callus perimeter than in group II.

In this study, the initial interfragmentary movements were higher when the fixator was mounted anteromedially. The overall higher movement of the anteromedially mounted fixator must be attributed to a difference between the initial stiffness of both bone-fixator complexes caused by the different mounting planes. Shifting the external fixator from the medial to the anteromedial position caused no difference in callus orientation (the principal axes of the callus were nearly identically orientated in all animals) but rather in the rate of tissue formation and maturation. Interestingly, the anteromedial fixator, which affords more initial movement, seemed to stimulate more callus formation and maturation, as revealed by biomechanical testing as well as histomorphometrical evaluation: The callus of the anteromedial fixator group was stiffer than the callus generated in the medially mounted fixator group. This increase in biomechanical quality may be due to a faster callus remodelling in this group as demonstrated by the histomorphometric results.

Capability of bone turnover markers to predict the course of bone consolidation during fracture healing

Klein P, Bail HJ, Schell H, *Michel R, *Amthauer H, Duda GN

Bone turnover markers (BTM) have been reported to predict the course of fracture healing. PICP (carboxyterminal propeptide of procollagen type I), and skeletal alkaline phosphatase (sALP) represent the course of bone consolidation as their systemic levels increase with callus mineralization. PIIINP (aminoterminal propeptide of procollagen type III) predicts delayed fracture healing. Interfragmentary movements (IFM) at the fracture site decrease with increasing callus stiffness and therefore predict the course of fracture healing. The aim of this study was to determine the capability of BTM to predict the course of bone healing. Possible correlations between BTM and IFM in vivo were investigated by comparing two different types of osteosyntheses in a standardized experimental animal model.

An osteotomy of the right tibial diaphysis was performed in two groups of female merino mix sheep (n=14). The osteotomy was distracted to 3 mm and stabilized either with a monolateral external fixator (EF) or a commercially available unreamed tibial nail (UTN9, Synthes).

Blood samples were taken preoperatively and postoperatively in weekly intervals over a healing period of nine weeks. At the same intervals, IFM were measured in all sheep using an infrared camera system (Qualisys, Sweden) and reflective markers. After sacrifice, both tibiae were evaluated biomechanically radiologically, and histologically. Commercially available radioimmunoassays (RIA) for human PICP, sALP and PIIINP were used to quantify BTM (PICP & PIIINP: Orion Diagnostica, Finland; sALP: Beckman Coulter Inc.).

A large inter-individual variability was observed for all BTM. Therefore, all parameters were expressed as a percentage of their preoperative values. In contrast to previous studies, bone healing did not increase the systemic PICP level (Fig 2, top). The systemic levels of sALP and PIIINP were clearly influenced by bone healing (Fig 2, middle & bottom) but no general correlation between BTM and IFM could be detected. IFM generally decreased over time (Fig. 1). For the first four weeks the UTN group showed significantly more IFM ($p^* = 0.035$, $p^{**} = 0.004$, $p^{***} = 0.005$, $p^{****} = 0.002$). Biomechanically, radiologically and histologically, the UTN group showed inferior healing results. No statistical differences were detected between groups

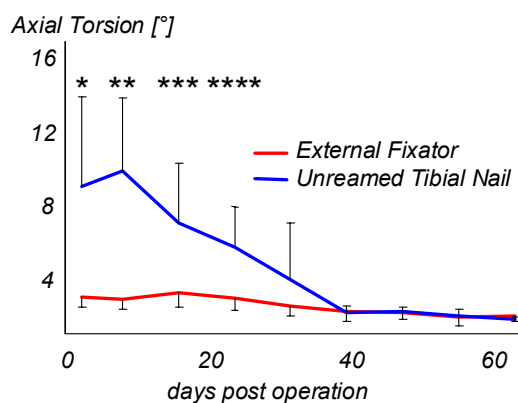


Fig. 1: Course of IFM during bone healing

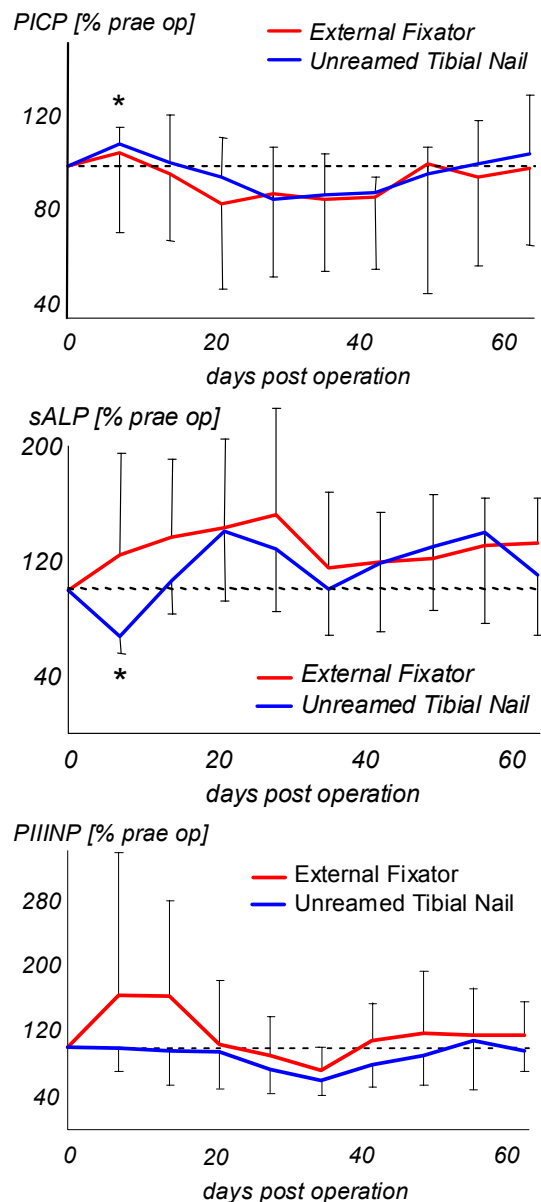


Fig. 2: Systemic levels of PICP (top; $p = 0.028$), sALP (middle; $p = 0.018$) and PIIINP (bottom) during bone healing

Within the EF group, no statistical differences compared to the preoperative values were observed at any time point (Fig. 2) Within the UTN group, the initial increase in PICP (Fig. 2, top) as well as the initial decrease in sALP (Fig. 2, middle) were significant. At all other time points, no significant differences compared to the preoperative values were observed. The pre-operative systemic level of the BTM appeared to be highly individual. Therefore, the use of individual reference values seemed to be mandatory to serve as controls.

The experimental bone healing model seemed to influence the systemic level of the BTM. However, the analysed markers failed as general predictors for the course of bone consolidation. Furthermore, none of the markers appeared to be sensitive to the individual progress of healing due to different osteosyntheses: In contrast to the IFM and biomechanical and histological outcomes, it was not possible to detect differences between the courses of bone healing from the analysed BTM.

*Radiology of the Charité , Humboldt-University of Berlin

This study was supported by a grant of the German Research Foundation DFG KFO 102/1

Influence of unreamed nailing and external fixation on the mechanical conditions during fracture healing

Schell H, Klein P, Opitz M, Kandziora F, *Bragulla H, Bail H, Duda GN

It is widely accepted that the mechanical stability of osteosynthetic devices has an effect on the healing process and clinical outcome. Rigid fixation and immobilization of fracture fragments leads to direct cortical union; interfragmentary movement leads to callus formation. Locked intramedullary nailing is currently one of the most frequently used osteosynthetic procedures for the stabilization of tibial shaft fractures. Clinically, use of an intramedullary nail is preferred to external fixators.

The goal of this study was to determine the mechanical stability at a comminuted diaphyseal fracture and establish its influence on the long term biological outcome after unreamed tibial nailing in an *in vivo* sheep model. In particular, this study aims to quantify the influence of external fixation versus unreamed nailing on the initial mechanical stability and the long term biological outcome at the osteotomy site.

Two groups each consisting of six female merino sheep (2 years, f), underwent a standardized midshaft osteotomy of the right tibia (gap = 3 mm). The osteotomy was stabilized with a monolateral external fixator in group I and an unreamed tibial nail in group II. The fixator was mounted medially and consisted of 6 Schanz' screws (\varnothing 5mm, 3 inserted proximally, 3 inserted distally of the osteotomy) and 2 carbon fiber rods (\varnothing 10mm). The fixator of group I was constructed to have an axial stiffness similar to that of the unreamed nail. A statically locked unreamed nail (UTN, \varnothing 9mm) was shortened to 21cm in order to fit to the length of a sheep tibia. To measure the fragment movements, both groups received additional screws proximal and distal to the osteotomy. Measurement of fragment movements were taken two times a week using an infrared camera system (PCReflex, Qualysis). Ground reactions were determined by means of a force platform (emed, novel). X-rays were taken once a week throughout the healing period of nine weeks.

The fractured tibiae were explanted and tested for torsional stability and until failure. The biomechanical data of the fractured tibia was reported as a percentage of the intact contralateral side. The callus region was sectioned into 3mm slices in the sagittal plane. After dehydration with alcohol the sections were embedded in methylmethacrylate. 4 μ m histology sections were stained with modified Safranin-Orange/von Kossa and Safranin-Orange/Lightgreen to analyze the characteristics of callus tissue. The callus tissue's quality and quantity in regard to bone, cartilage and fibrous tissue formation was examined. Tissue differentiation was analyzed for various locations within the callus (endosteal vs. periosteal; lateral vs. medial) using an image analysis system. Mann-Whitney-U tests were used for statistical analysis (SPSS8).

The amount of axial compression was similar in both osteosynthetic systems. However, the unreamed nail shows initially a significantly higher mediolateral shear movement and twisting angulation. After six weeks, the gap movement of the unreamed nail group (II) approaches that of the external fixator group (I). The *in vitro* testing of the explanted tibiae showed a significantly higher torsional strength ($p=0,014$) of the external fixator group compared to the unreamed nail group.

The unreamed nail occupies the entire medullary cavity, largely inhibiting endosteal callus formation. Safranin-Orange/von Kossa stains of the external fixator group show uniform, mostly osseous callus tissue periosteally and endosteally. The periosteal callus is more pronounced on the medial side. The osteotomy gap is filled with calcified bone. Stains of group II show a completely different situation: The callus tissue appears to be non-uniform with osseous areas surrounded predominantly by fibrous tissue. Periosteal osseous bridging can only be seen laterally, while bridging on the medial side was incomplete or non-existent. Osseous filling of the intercortical gap did not occur. Bone area and area of mineralized bone were significantly lower in group II ($p=0,002$) as well as cortical and cortical bone area ($p=0,002$). Medial periosteal bone area ($p=0,0026$) and bone density ($p=0,041$) were significantly higher in group I, as well as callus bone area ($p=0,026$) and bone density ($p=0,015$) in the medial and lateral endosteal callus areas.

In both groups, the midshaft surgical trauma, the bone defect situation and the axial rigidity of the osteosynthetic devices were identical. From the results of the histomorphometrical analysis and the relative loading of the limbs postoperatively, it appears that the fixator produces better healing results. The lower stiffness of the nail osteosynthesis allows the larger interfragmentary movements and can therefore hinder healing in situations without cortical contact. Having compared two similar fracture situations, this study has shown larger interfragmentary movements and massive unloading of the operated limb, combined with poor histomorphometrical callus healing in the UTN group. The mechanical difference between the two situations is the significantly less stiff osteosynthesis and the massive unloading of the operated joint after treatment with unreamed tibial nails. From this, we conclude that the aetiology of joint unloading should be diligently examined and that UTN could be further optimised by increasing the *in vivo* stability, particularly the axial torsional stiffness of the osteosynthesis. This could help to avoid excessive interfragmentary movements which can delay fracture healing.

*Institute for Veterinary Anatomy, Free University of Berlin, Germany

This study was supported by a grant of the German Research Foundation DFG KFO 102/1

Mechanical Conditions in the Early Phase of Fracture Healing

Epari D, Schell H, Klein P, Duda GN

The influence of mechanical stability on fracture healing is well documented. Mechanical stability is reflected in the interfragmentary movements. In vivo interfragmentary movements are observed to consist of shear movements and rotations in addition to axial movements. Shear movements may be of the same order or greater than those occurring in the axial direction.

To reduce incidences of delayed healing or non-union and accelerate fracture healing, researchers have sought to determine optimum mechanical stability. Optimal axial interfragmentary movements of 0.2 – 1mm have been determined. However the influence of shear movements on fracture healing remain unclear and statements from the literature are contradictory. Clinically, shear interfragmentary movements continue to be regarded as detrimental to the healing process.

Experimental evidence suggests that the early phase of fracture healing may be especially sensitive to the mechanical stability and may determine the healing pathway.

Our aim was to characterise the mechanical conditions in a healing fracture under the influence of different modes of interfragmentary movement. The finite element method was used to investigate various mechanical parameters in an early phase fracture callus subjected to axial, shear and combined axial and shear interfragmentary movements.

The finite element method was used to calculate the straining in an early phase fracture callus. The biological tissues were modeled using a biphasic poroelastic formulation. Callus geometry, based on histology sections, was simplified and idealized. The interfragmentary space was assumed to be composed entirely of granulation tissue. The size of the fracture gap was modeled as 3mm. The model, constructed in 3D in order to model shear movements, consisted of 3168 hexagonal elements.

Interfragmentary movements were applied to the elements representing cortical bone. Axial, shear and combined axial and shear movements were applied to the model and various mechanical parameters investigated. Strains were analysed in light of proposed theories of mechano-transduction.

Axial interfragmentary movements (0.5mm) resulted in high intra-cortical strains (30%) which extended into the periosteal interfragmentary space and diminished with distance from the fracture gap along the bone cortex. Additionally a relatively high endosteal pressure was developed leading to higher strains along the endosteal cortex. Conversely shear movements (0.5mm) resulted in relatively uniform straining (<10%) in and isolated to the fracture gap. The unsymmetrical movement produced proximal-distal asymmetries in the strain pattern.

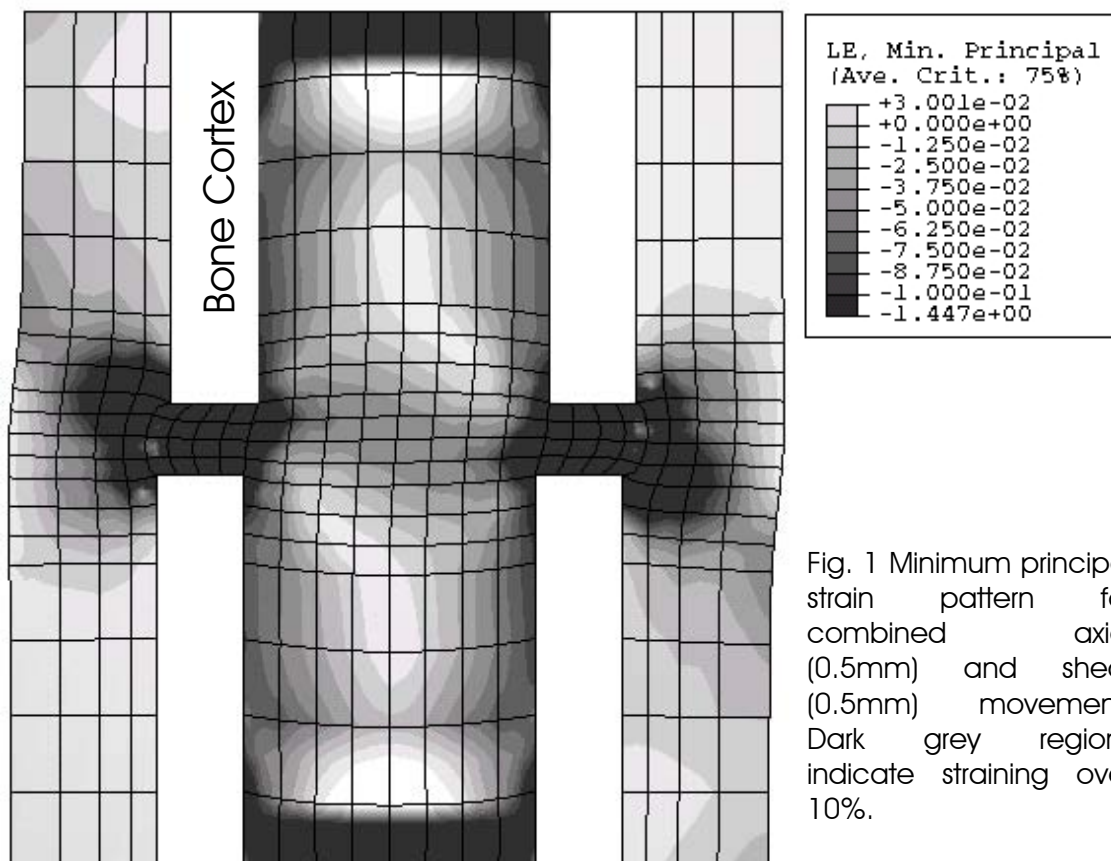
Combining the axial and shear movements resulted in a strain pattern that resembled that produced from axial movements alone (Figure 1). The combination of axial and shear movements led to a reduction of strains in some areas. The magnitude of the reductions was greater than the increases in strain in the opposing areas.

A comparison of strain patterns from axial and shear movements of the same order of magnitude clearly demonstrated that the axial movement is the dominant component, producing a significantly larger straining. Axial movements become increasingly dominant as the magnitude of the movement increases.

It was seen that the magnitude of strains produced from shear loading alone was relatively low. Too little strain stimulus in the periosteal regions may explain the delayed healing results when shear movements alone are applied to a fracture.

The loading produced from combined movements was found to be not a direct superposition of the individual movements. The strain reductions that were observed with the addition of shear movements point towards the existence of a window of shear in combination with axial movements that produces a strain environment that may not be detrimental to healing.

Further analyses are required to characterise the full range of combined axial and shear movements and also to assess the influence of rotations on callus straining.



This study was supported by a grant of the AO/ASIF Foundation, Switzerland

Bone graft straining in Box and Cylinder Cervical Spine Interbody Fusion Cages

Epari D, Mladek M, Kandziora F, Duda GN

Cervical spondylosis, a degeneration of the intervertebral disc, is often treated with anterior decompression and interbody fusion. Complications associated with iliac crest bone grafts have led to the use of cervical spine interbody fusion cages. Interbody fusion cages are required to provide interspace structural stability during bony fusion.

A comparative *in vivo* animal study demonstrated that both box and cylinder cage designs incorporating bone grafts perform better than traditional tricortical bone grafts. The Harms cylinder cage is a clinically successful cage design. Despite its poor initial stability, as determined by *in vitro* biomechanical testing, the Harms cage achieves good *in vivo* stability (Sheep model, 12 weeks postoperative). On the other hand, the Syncage (box design) has a high initial *in vitro* stability, but does not attain the same *in vivo* stability as exhibited by the Harms cage. Histological analysis of the Syncage revealed a high osteoclastic activity that led to a resorption of the bone graft tissue. The differences in bone matrix formation between the cages were attributed to stress shielding of the bone graft within the Syncage.



Fig. 1: Left: Harms (cylinder) cage. Right: Syncage (box) cage.

The aim of this study is to investigate how cage design, box or cylinder, influences the straining in the bone graft tissue. Bone graft strain patterns will be correlated with histology specimens to determine possible stress-shielding conditions. The effects of design parameters such as stiffness, hole size and endplate surface area will be investigated with respect to the bone graft straining.

To investigate the straining in the bone graft tissue the finite element method is being used. A biphasic poroelastic approach has been chosen to model the biological tissues.

Preliminary results show reduced straining in the bone graft material in the box design due to the higher stiffness of the construct. Further the straining is concentrated under the endplates. Conversely, a uniform strain pattern is seen in

the case of the cylinder cage (Figure 2). The unloading in the centre of the box cage is consistent with observed patterns of resorption in the bone graft material.

The combination of the higher rigidity of the Syncage (box design) and the unloading of the graft material in the cage center provide a mechanical explanation for the bone resorption observed *in vivo* through stress shielding phenomena. Further analyses will be performed to determine the influence of the design parameters: hole size and endplate surface area. Additionally, the effect of subsidence on bone graft tissue straining will be investigated.

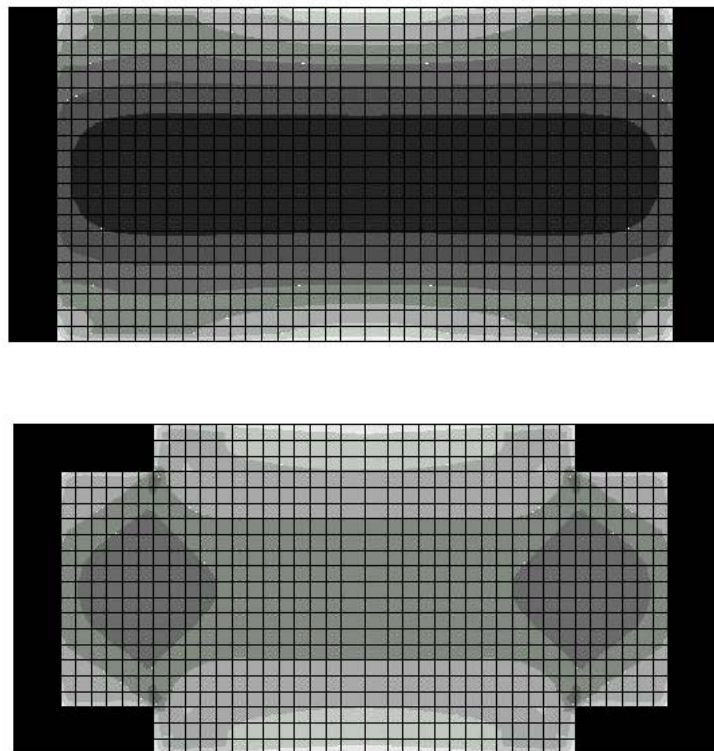


Fig. 2: Preliminary graft tissue strain pattern for Harms cylinder cage: larger uniformly distributed strain (above) and Syncage box cage: lower and concentrated strain under endplates. (below). *Black shaded region indicates 2D profile of modelled cage design.*

Biomechanical analysis of biodegradable interbody fusion cages augmented with Poly(propylene glycol-co-fumaric acid)

Kandziora F, Pflugmacher R, Kleemann R, Duda G, Wise DL, Trantolo DJ, Lewandrowski KU

Three different types of biodegradable poly(L-lactide-co-D,L-lactide; PDLLA) cages with and without augmentation of a biodegradable poly(propylene glycol-co-fumaric acid) scaffold were compared to autograft and metallic cages of the same design and size by determining the stiffness and failure load of the L4/L5 motion segment of cadaveric human spines.

To determine the *in vitro* biomechanical properties of the PDLLA cages in the human lumbar spine and to compare the limitation of lumbar spine motion to a metallic cage. If biomechanically equivalent, biodegradable spinal fusion systems ultimately could reduce local stress shielding and diminish the incidence of clinical complications including device-related osteopenia, implant loosening and breakage. Previous studies in dogs and humans have demonstrated vertebral body osteopenia as a result of instrumented spine fusions. To the authors knowledge, neither an *in vitro*, nor an *in vivo* biomechanical analysis of a biodegradable interbody fusion system has been performed.

Forty-eight L4/L5 motion segment were isolated from 22 male and 26 female human donors with an average age of 49.6 +/-2.7 (36 - 55) years. Cages of similar dimensions and design including a threaded, hollow, porous titanium BAK cage and three different BIO-cages (BIO-cage 1 – pure polymer, BIO-cage 2 - polymer plus hydroxyapatite buffer, BIO-cage 3 – polymer plus nano-sized hydroxyapatite) produced from the same (poly(L-lactide-co-D,L-lactide) polymer were tested in a comparative analysis to intact motion segment, interbody implantation of autograft, and a BIO-cage augmented with an expandable biodegradable foam-scaffold fashioned from poly(propylene glycol-co-fumaric acid).

All cages were able to increase stiffness and failure load of the unstable motion segment significantly ($p < 0.01$). In comparison with the bone graft, the BAK-cage ($p < 0.01$), BIO-cage 1 and 3 ($p < 0.05$) were able to increase stiffness and failure load. There was no significant difference between BIO-cage 2 and the bone graft. Augmentation of Bio-cage 1 with the foaming PPF-scaffold resulted in higher stiffness and similar failure load as seen with the BAK cage.

By comparison, the *in vitro* lumbar spinal motion segment stiffness and failure load produced by implantation of a biodegradable interbody fusion cage augmented with an expandable PPF-scaffold is similar to that of the titanium BAK cage. This suggests that biodegradable anterior interbody fusion systems could be further developed for clinical applications.

Biomechanical comparison of bioabsorbable cervical spine interbody fusion cages

Pflugmacher R, Schleicher P, Gumnior S, Schaefer J, Turan O, Scholz M, Ludwig K, Duda G, Haas NP, Kandziara F

In vitro biomechanical study of bioabsorbable cervical spine interbody fusion cages (CSIFC) using a sheep model.

The purpose of this study was to evaluate the segmental stability provided by two new developed bioabsorbable CSIFC and to compare it with a tricortical iliac crest bone graft and a titanium meshed interbody fusion cage. Further the biomechanical effect of an additional anterior plate instrumentation was determined. Despite the initial favourable results, the long-term effects of metallic cage devices on spinal motion segments are still unknown. Furthermore, shortcomings of metallic cages like migration, adjacent level degeneration, stenotic myelopathy and artefacts in postoperative radiological assessment have already been reported. Bioabsorbable cages have been designed to avoid these complications. Currently, no information is available about the biomechanical properties of bioabsorbable cervical interbody fusion cages.

40 sheep cervical spines (C2 to C5) were tested in flexion, extension, axial rotation, and lateral bending with a non-destructive stiffness method using a nonconstrained testing apparatus. Complete discectomy C3/C4 was performed. CSIFC were implanted according to producers information. The following groups were tested: (1) intact (2) autologous iliac crest bone graft (3) titanium mesh cylinder (Harms, DePuy Acromed) (4) PDLLA-cage (experimental) (5) Resorbon cage (Biomet Merck). Additionally all implants were tested with an additional anterior plate instrumentation. The mean apparent stiffness, ROM (range of motion), NZ (neutral zone) and EZ (elastic zone) were calculated from the corresponding load-displacement curves.

No significant difference in ROM and segmental stiffness between the tricortical iliac crest bone graft, meshed titanium Harms cage and PDLLA-cage could be determined. The Resorbon cage significantly ($p < 0.05$) decreased ROM and increased stiffness in rotation and flexion in comparison to all tested implants and the intact motion segment. An additional anterior plate significantly ($p < 0.05$) decreased ROM and increased stiffness in flexion and extension.

In this study bioabsorbable cages demonstrated biomechanical *in vitro* properties equal or superior to metallic cages. From the biomechanical point of view bioabsorbable cages, especially the Resorbon-cage, may be a viable alternative to current metallic interbody cage devices. However, animal experimental *in vivo* evaluation of bioabsorbable CSIFC still has to be performed.

Biomechanical comparison of cervical spine interbody fusion cages

Kandziora F, Pflugmacher R, Schäfer J, Born C2, Duda G, Haas NP, Mittlmeier Th

In vitro biomechanical study of cervical spine interbody fusion cages (CSIFC) using a sheep model.

Purpose of this study was to evaluate the biomechanical effects of CSIFC and to compare three different CSIFC design-groups. Recently, there has been a rapid increase in the use of CSIFC as an adjunct to spondylodesis. CSIFC can be classified into 3 groups: screw, box or cylinder designs. Although several comparative biomechanical studies of lumbar interbody fusion cages are available, biomechanical data for cervical spine constructs are lacking. Additionally, only limited data are available concerning comparative evaluation of different cage designs.

80 sheep cervical spines (C2 to C5) were tested in flexion, extension, axial rotation, and lateral bending with a non-destructive stiffness method using a nonconstrained testing apparatus. Three-dimensional displacement was measured using an optical measurement system (Qualysis). Complete discectomy C3/C4 was performed. CSIFC were implanted according to producers information. The following groups (n=8/group) were tested: (1) intact (2) autologous iliac bone graft (3) two titanium screws (Novus CTTi, Sofamor Danek) (4) two titanium screws (BAK-C 8 mm, Sulzer Orthopedics) (5) one titanium screw (BAK-C 12 mm, Sulzer Orthopedics) (6) carbon box (Novus CSRC, Sofamor Danek) (7) titanium box (Syncage, Synthes) (8) titanium mesh cylinder (Harms, DePuy Acromed) (9) titanium cylinder (MSD, Ulrich) (10) titanium cylinder (Kaden, BiometMerck). The mean apparent stiffness values were calculated from the corresponding load-displacement curves. Additionally, cage volume and volume related-stiffness was determined.

After CSIFC implantation, flexional stiffness increased compared to the intact motion segment. On the contrary, rotational stiffness decreased after implantation of a CSIFC, except for the Novus CSRC, Syncage and Kaden-Cage. If two screws were inserted (Novus CTTi and BAK-C 8mm) there was no significant difference in flexional stiffness between screw and cylinder design groups. If one screw was inserted (BAK-C 12mm) flexional stiffness was higher for cylinder designs ($p < 0.05$). Extensional and bending stiffness were always higher with cylinder designs ($p < 0.05$). Volume-related-stiffness for flexion extension and bending was highest for the Harms-cage ($p < 0.05$). There was no difference for rotational volume-related-stiffness between Harms- and Syncage.

Biomechanical results indicate that design variations in screw and cylinder design-groups are of little importance. However, cages with cylinder design were able to control extension and bending more effectively than cages with screw design.

Cage design significantly influences interbody fusion in a sheep cervical spine model

Kandziora F, Schollmeier G, Scholz M, Schaefer J, Scholz A, Schmidmaier G, Schröder R, Bail H, Duda G, Mittlmeier Th, Haas NP

The purpose of this study was to compare interbody fusion of an autologous tricortical iliac crest bone graft with a cylinder- and a box-design cage in a sheep cervical spine model. This study was designed to determine whether there are differences between the three interbody fusion techniques in (1) the ability to preserve postoperative distraction, (2) the biomechanical stability, and (3) the histological characteristics of intervertebral bone matrix formation

24 sheep underwent C3/4 discectomy and fusion: Group 1: autologous tricortical iliac crest bone graft (n = 8); Group 2: titanium cylinder-design cage filled with autologous iliac crest bone graft (n = 8); Group 3: titanium box-design cage filled with autologous iliac crest bone graft (n = 8). Radiographic scans were performed pre- and postoperatively and after 1, 2, 4, 8, 12 weeks, respectively. At the same time points, disc space height (DSH), intervertebral angle (IVA) and lordosis angle (LA) were measured. After 12 weeks animals were killed and fusion sites were evaluated using functional radiographic views in flexion and extension. Quantitative computed tomographic scans (QCT) were performed to assess bone mineral density (BMD), bone mineral content (BMC) and bony callus volume (BCV). Biomechanical testing was performed in flexion, extension, axial rotation and lateral bending. Stiffness, range of motion (ROM), neutral (NZ) and elastic zone (EZ) were determined. Histomorphological and histomorphometrical analysis were performed and polychrome sequential labeling was used to determine the time frame of new bone formation.

Over a 12 weeks-period the cage groups showed significantly higher values for DSH and IVA compared to the bone graft. Functional radiographic assessment revealed significantly lower residual flexion/extension movement in the cylinder design cage group than in the bone graft group. The cylinder-design cages showed significantly higher values for BMC, BCV and stiffness in axial rotation and lateral bending than in any other group. Histomorphometrical evaluation and polychrome sequential labeling showed a more progressed bone matrix formation in the cylinder design cage group than in both other groups.

In comparison to the tricortical bone graft both cage designs showed significantly better distractive properties. The cylinder design cage demonstrated a significantly higher biomechanical stiffness and an accelerated interbody fusion in comparison to the box design cage and the tricortical bone graft. The differences in bone matrix formation inside both cages were a result of the significantly lower stress shielding on the bone graft by the cylinder design cage.

This study was supported by a grant of Max-Biedermann Institut Berlin

Biomechanical comparison of expandable cages for vertebral body replacement in the thoraco-lumbar spine

Pflugmacher R, Schleicher P, Schaefer J, Scholz M, Ludwig K, Khodadadyan-Klostermann C, Haas NP, Kandziara F

An *in vitro* biomechanical study of expandable cages for vertebral body replacement in the human thoraco-lumbar spine. Purpose of this study was to compare the *in vitro* biomechanical properties of three different expandable cages with a non-expandable cage. Recently, there has been a rapid increase in the use and the commercial availability of expandable cages for vertebral body replacement in the thoraco-lumbar spine. Although all three expandable cages, evaluated in this study, are approved for the clinical use in Europe, only little information is available concerning the biomechanical properties of these implants.

32 human thoraco-lumbar spines (Th11 to L3) were tested in flexion, extension, axial rotation, and lateral bending with a non-destructive stiffness method using a nonconstrained testing apparatus. Three-dimensional displacement was measured using an optical measurement system. First all motion segments were tested intact. After complete corporectomy of L1, cages were implanted according to producers information. The following implants (n=8/group) were tested: (1) meshed titanium cage (non expandable cage, DePuy Acromed); (2) X-tenz (expandable cage, DePuy Acromed); (3) Synex (expandable Cage; Synthes) and (4) VBR (expandable cage, Ulrich). Finally, posterior stabilisation using USS (Synthes) and posterior-anterior stabilisation using USS (Synthes) and anterior plating (LCP, Synthes) was applied. The mean apparent stiffness values, range of motion, neutral and elastic zone were calculated from the corresponding load-displacement curves.

No significant differences could be determined between the *in vitro* biomechanical properties of expandable and non-expandable cages. In comparison to the intact motion segment, isolated anterior stabilisation using cages and anterior plating significantly decreased stiffness and increased range of motion in all directions. In contrast, additional posterior stabilization significantly increased stiffness and decreased range of motion in all directions compared to the intact motion segment. The combined anterior-posterior stabilization demonstrated greatest stiffness results.

Biomechanical results indicate that design variations of expandable cages for vertebral body replacement are of little importance. Additionally, no significant difference could be determined between the biomechanical properties of expandable and non-expandable cages. After corporectomy isolated implantation of expandable cages plus anterior plating was not able to restore normal stability of the motion segment. Therefore, isolated anterior stabilisation using cages plus LCP should not be used for vertebral body replacement in the thoraco-lumbar spine.

Biomechanical comparison of expandable cages for vertebral body replacement in the cervical spine

Kandziora F, Pflugmacher R, Schäfer J, Scholz M, Ludwig K, Schleicher P, Haas NP

Recently, expandable cages for vertebral body replacement in the cervical spine have been developed. In comparison to non-expandable cages these implants offer several surgical advantages. However, until today the biomechanical properties of expandable cages have not been described. Therefore, purpose of this study was to compare the biomechanical properties of expandable cages with a tricortical iliac crest graft and a non-expandable cage in the human cervical spine.

40 human cervical spines (C3 to C5) were tested in flexion, extension, axial rotation, and lateral bending with a non-destructive stiffness method using a nonconstrained testing apparatus. Three-dimensional displacement was measured using an optical measurement system. First all motion segments were tested intact. After complete corpectomy of C4 the following stabilisation techniques were used (n=8 / group): (1) autologous iliac crest bone graft (2) meshed titanium cage (Harms, DePuy Acromed) (3) anterior distraction device (ADD, Ulrich) (4) Synex-C titanium (Synthes) (5) Synex-C PEEK (Synthes). Additionally, anterior plating (CSLP, Synthes) and anterior plating plus posterior screw-rod fixation (Cervifix, Synthes) were applied. Range of motion, neutral and elastic zones were determined. The mean apparent stiffness values were calculated from the corresponding load-displacement curves.

In comparison to the intact motion segment all implants significantly increased stiffness in flexion and bending, but decreased stiffness in extension. No difference could be determined between the intact motion segments and all implants in rotation. There were no biomechanical differences between the non-expandable cage and the expandable cages. Further there were no biomechanical differences between the tricortical iliac crest graft and the cages, except for Synex-C in rotation. Additional anterior plating significantly increased biomechanical stiffness in all test modes. Anterior plating plus posterior screw-rod fixation showed the highest biomechanical stability. Especially in rotation combined anterior-posterior stabilisation increased stiffness up to 102% compared to anterior plating alone.

In comparison to a tricortical iliac crest bone graft and a non-expandable cage, expandable cages have no significant biomechanical advantages. Due to the low extension and rotational stiffness none of the implants tested should be used as a "stand alone" devices for vertebral body replacement in the cervical spine. Although additional anterior plating significantly increased biomechanical results, a further posterior stabilisation should be considered in severe rotational instability of the cervical spine.

BMP-2 application by a Poly-(D,L-lactide) coated interbody cage In vivo results of a new carrier for growth factors

Kandziora F, Bail H, Schmidmaier G, Schollmeier G, Scholz M, Knispel C, Hiller T, Pflugmacher R, Mittlmeier Th, Raschke M, Haas NP

Growth factors such as BMP-2 have proven to promote spine fusion and to overcome the disadvantages of an autologous bone graft. The optimum method to deliver such growth factors is still a matter of discussion. The purpose of this study was to determine the safety and efficacy of a new Poly- (D,L-lactide) carrier system and to compare this PDLLA carrier system with an collagen sponge carrier in a sheep cervical spine interbody fusion model using BMP-2.

32 sheeps underwent C3/4 discectomy and fusion: Group 1: titanium cage (n = 8); Group 2: titanium cage coated with a PDLLA carrier (n = 8); Group 3: titanium cage coated with a PDLLA carrier including BMP-2 (150 µg) (n = 8). Group 4: titanium cage plus a collagen sponge carrier including BMP-2 (150 µg) (n = 8). Blood samples, body weight and temperature were analysed. Radiographic scans were performed pre- and postoperatively and after 1, 2, 4, 8, 12 weeks, respectively. At the same time points, disc space height (DSH), intervertebral angle (IVA) and lordosis angle (LA) were measured. After euthanasia 12 weeks postoperatively fusion sites were evaluated using flexion/extension views. Quantitative computed tomographic scans (QCT) were performed to assess bone mineral density (BMD), bone mineral content (BMC) and bony callus volume (BCV). Biomechanical testing was performed in flexion, extension, axial rotation and lateral bending. Stiffness, range of motion (ROM), neutral (NZ) and elastic zone (EZ) were determined. Histomorphological and histomorphometrical analysis were performed and polychrome sequential labelling was used to determine the time frame of new bone formation.

There were no differences between the groups concerning blood counts, body weight and temperature. In comparison to the non-coated cages all PDLLA-coated cages showed significantly higher values for BMD of the callus, and slightly higher values for BMC, BCV and bone volume/total volume ratio. In comparison to the cage alone group, the BMP-2 groups showed significantly higher values for BMD and biomechanical stiffness. Histomorphological, histomorphometrical and polychrome sequential labelling analysis showed a more progressed callus formation in the BMP-2 groups than in any other group. In comparison to BMP-2 application with a collagen sponge carrier, BMP-2 application with a PDLLA carrier resulted in a higher BCV and a progressed interbody callus formation in histomorphometrical analysis.

PDLLA-coating of cervical spine interbody fusion cages as a delivery system for growth factors was effective. In this 12 week-follow-up study the PDLLA coating showed no adverse effects. The slight but not significant positive effect of the PDLLA carrier on interbody fusion might be a result of degradation process of the biodegradable carrier. In comparison to the collagen sponge BMP-2 application by a PDLLA coated interbody cage significantly increased results of interbody bone matrix formation. In this new combination (implant + PDLLA + growth factor) the cage represents a "real fusion" cage, because it does not only serve as a mechanical device for spinal fixation but also as a local drug delivery system.

IGF-I and TGF- β 1 application by a Poly-(D,L-lactide) coated cage promotes intervertebral bone matrix formation in the sheep cervical spine

Kandziora F, Schmidmaier G, Schollmeier G, Bail H, Pflugmacher R, Görke Th, Wagner M, Raschke M, Mittlmeier Th, Haas NP

The purpose of this study was to determine the effect of a new PDLLA carrier system and to evaluate the effect of combined IGF-I and TGF- β 1 application in a sheep cervical spine model. Growth factors have proven to promote spine fusion and to overcome the disadvantages of an autologous bone graft. The optimum growth factor to promote spinal fusion as well as the optimum method to deliver such growth factors is still a matter of discussion.

32 sheep underwent C3/4 discectomy and fusion: Group 1: autologous tricortical iliac crest bone graft (n=8); Group 2: titanium cage (n=8); Group 3: titanium cage coated with a PDLLA carrier (n=8); Group 4: titanium cage coated with a PDLLA carrier including IGF-I (5% w/w) and TGF- β 1 (1% w/w) (n=8). Blood samples, body weight and temperature were analysed. Radiographic scans were performed pre- and postoperatively and after 1, 2, 4, 8, 12 weeks. At the same time points, disc space height (DSH), intervertebral angle (IVA) and lordosis angle (LA) were measured. After 12 weeks animals were killed and fusion sites were evaluated using functional radiographic views in flexion and extension. QCT scans were performed to assess bone mineral density (BMD), bone mineral content (BMC) and bony callus volume (BCV). Biomechanical testing was performed in flexion, extension, axial rotation and lateral bending. Stiffness, range of motion (ROM), neutral (NZ) and elastic zone (EZ) were determined. Histomorphological and histomorphometrical analysis was performed and polychrome sequential labelling was used to determine the time frame of new bone formation.

There were no differences between the groups concerning blood counts, body weight and temperature. Over a 12 weeks-period the cage groups 2-4 showed significantly higher values for IVA compared to the bone graft. Functional radiographic assessment revealed significantly lower residual flexion/extension movement in group 4 than in any other group. The PDLLA coated cages with IGF-I and TGF- β 1 showed significantly highest values for BMD, BMC and BCV. Average stiffness in rotation and bending was significantly higher and ROM, NZ and EZ in rotation were significantly lower in group 4 than in any other group. Although, only one animal in group 4 demonstrated solid bony fusion after 12 weeks, histomorphometrical evaluation showed a more progressed bone matrix formation in PDLLA coated cages with IGF-I and TGF- β 1 than in any other group. Polychrome sequential labelling showed accelerated intervertebral bone matrix formation in group 4.

PDLLA-coating of cervical spine interbody fusion cages as a delivery system for growth factors was effective. Although, IGF-I and TGF- β 1 application by a PDLLA coated interbody cage was not able to achieve solid bony fusion during the follow-up period, these growth factors significantly increased interbody bone matrix formation. Further longer term studies are required to determine whether combined IGF-I and TGF- β 1 application leads to a successful spinal fusion.

Comparison of BMP-2 and combined IGF-I/TGF- β 1 application in a sheep cervical spine fusion model

Kandziora F, Pflugmacher R, Scholz M, Knispel C, Hiller T, Schollmeier G, Bail H, Schmidmaier G, Duda G, Raschke M, Haas NP

Growth factors have proven to promote spine fusion. However, no comparative evaluation of growth factors in spinal fusion has been performed up till now. Purpose of this study was to compare the efficacy and safety of combined IGF-I and TGF- β 1 application, with BMP-2 application and autologous cancellous bone graft at an early time point in a sheep cervical spine fusion model.

32 sheep underwent C3/4 discectomy and fusion: Group 1: titanium cage (n = 8) ; Group 2: titanium cage filled with autologous cancellous iliac crest bone grafts (n = 8); Group 3: titanium cage coated with a PDLLA carrier including BMP-2 (5% w/w) (n = 8); Group 4: titanium cage coated with a PDLLA carrier including IGF-I (5% w/w) and TGF- β 1 (1% w/w) (n = 8). Blood samples, body weight and temperature were analysed. Radiographic scans were performed pre- and postoperatively and after 1, 2, 4, 8, 12 weeks, respectively. At the same time points, disc space height and intervertebral angle were measured. After 12 weeks animals were killed and fusion sites were evaluated using functional radiographic views in flexion and extension. Quantitative computed tomographic scans were performed to assess bone mineral density, bone mineral content and bony callus volume. Biomechanical testing has been carried out and range of motion, neutral and elastic zone were determined. Histomorphological and histomorphometrical analysis were performed and polychrome sequential labelling was used to determine the time frame of new bone formation.

In comparison to the cage alone group (group 1) the cage plus BMP-2 (group 3) and the cage plus IGF-I and TGF- β 1 group (group 4) demonstrated a significantly higher fusion rate in radiographic findings, a higher biomechanical stability, an advanced interbody fusion in histomorphometric analysis, and an accelerated interbody fusion on fluorochrome sequence labelling. In comparison to the bone graft group (group 2) the BMP-2 (group 3) and IGF-I/TGF- β 1 group (group 4) showed significantly lower residual motion on functional radiographic evaluation, higher bone mineral density of the callus and higher biomechanical stability in extension, rotation and bending. The BMP-2 group showed significantly lower residual motion on functional radiographic evaluation and higher intervertebral bone matrix formation on fluorochrome sequence labelling at 9 weeks in comparison to the IGF-I/TGF- β 1 group. In contrast, the IGF-I/TGF- β 1 group showed a significantly higher bone mineral density of the callus than the BMP-2 group.

In comparison to the autologous cancellous bone graft group both growth factors (BMP-2 and combined IGF-I and TGF- β 1) significantly improved biomechanical results of interbody fusion. No systemic side effects were observed for both growth factors. Due to this preliminary results, the combined IGF-I/TGF- β 1 application yields equivalent results to BMP-2 application at an early time table in anterior sheep cervical spine fusion.

Dose-dependent effects of combined IGF-I and TGF- β 1 application in a sheep cervical spine fusion model

Kandziora F, Pflugmacher R, Scholz M, Schäfer J, Schollmeier G, Schmidmaier G, Duda G, Raschke M, Haas NP

Combined IGF-I and TGF- β 1 application by a Poly-(D,L-lactide)(PDLLA) coated interbody cage has proven to promote spine fusion. Purpose of this study was to determine, whether there is a dose-dependent effect of combined IGF- I and TGF- β 1 application on intervertebral bone matrix formation in a sheep cervical spine fusion model.

32 sheep underwent C3/4 discectomy and fusion. Stabilisation was performed using a titanium cage coated with a PDLLA carrier including no growth factors in group 1 (n = 8), 75 μ g IGF-I plus 15 μ g TGF- β 1 in group 2 (n = 8), 150 μ g IGF-I plus 30 μ g TGF- β 1 in group 3 (n = 8) and 300 μ g IGF-I plus 60 μ g TGF- β 1 in group 4 (n = 8). Blood samples, body weight and temperature were analysed. Radiographic scans were performed pre- and postoperatively and after 1, 2, 4, 8, 12 weeks, respectively. At the same time points, disc space height and intervertebral angle were measured. After 12 weeks animals were killed and fusion sites were evaluated using quantitative computed tomographic scans to assess bone mineral density, bone mineral content and bony callus volume. Biomechanical testing was performed and range of motion, neutral and elastic zone were determined. Histomorphological and histomorphometrical analysis were carried out and polychrome sequential labelling was used to determine the time frame of new bone formation.

In comparison to the group without growth factors (group 1) the medium and high dose growth factor groups (group 3 and 4) demonstrated a significant higher bony callus volume on CT-scans, a higher biomechanical stability, an advanced interbody bone matrix formation in histomorphometric analysis, and an earlier bone matrix formation on fluorochrome sequence labelling. Additionally, the medium and high dose growth factor groups (group 3 and 4) demonstrated a significant higher bony callus volume, a higher biomechanical stability in rotation, and an advanced interbody bone matrix formation in comparison to the low dose growth factor group (group 2). No significant difference could be determined between the medium (group 3) and high dose growth factor group (group 4).

The local application of IGF-I and TGF- β 1 by a PDLLA coated cage significantly improved results of interbody bone matrix formation in a dose dependent manner. The best dose-response-relationship was achieved with the medium growth factor dose (150 μ g IGF-I and 30 μ g TGF- β 1). With an increasing dose of these growth factors no further stimulation of bone matrix formation was observed. Although these results are encouraging, safety issues of combined IGF-I and TGF- β 1 application for spinal fusion still have to be addressed.

Detection of alpha-smooth muscle actin (ASMA) containing contractile fibroblastic cells in knee arthrofibrosis tissue

Unterhauser FN, Weiler A, Zeichen J*, Höher J, Bosch U*

The occurrence of arthrofibrosis as a response to trauma or operation to the joint is a severe complication with consecutive limitation for range of motion. While the secondary arthrofibrosis is caused by a distinct mechanical problem e.g. as the result of malpositioning of the graft or interference screw after ACL reconstruction, the etiology of the primary form of arthrofibrosis is still unclear. Primary arthrofibrosis is characterized by an activation and proliferation of fibroblastic cells and an excessive increase in the deposition of extracellular matrix proteins due to an exaggerated synovial inflammatory response.

Similar mechanisms are detectable during wound healing and wound contraction. Since specific α -smooth muscle actin containing fibroblastic cells have been detected to play a key role in tissue contraction during wound healing, these cells have also been identified in various pathological settings such as Dupuytren's palmar fibromatosis and organ fibrosis.

We hypothesize that ASMA expressing fibroblasts are also responsible for the contraction of joint capsules and scar tissue in primary arthrofibrosis.

Therefore, samples of the infrapatellar fatpad and intercondylar region of 9 patients with arthrofibrosis of the knee were harvested. Samples from 5 asymptomatic patients who underwent primary ACL reconstruction were taken as control tissues. To detect ASMA containing myofibroblasts, sections were immunostained with a monoclonal antibody (anti-human rabbit IgG). Vascular smooth muscle cells were used as internal positive controls. Pericytes and myofibroblasts were morphologically differentiated by means of cell shape, proximity to vessels, and distribution between matrix fibers. The total cell amount, ASMA containing myofibroblasts and vessel cross sections were analysed, using a digital image analysing system.

The arthrofibrosis tissue showed a dense distribution of collagen fibres with only little fatty tissue. In contrast, the control group consisted of broad fat tissue with sporadic collagen fibres. There was a significantly higher total cell density in the arthrofibrosis tissue in comparison to the control tissue.

The arthrofibrosis group showed a significantly higher expression of ASMA containing cells ($p < 0.001$) and a lower density of vessel cross sections per 1 mm^2 ($p < 0.001$) comparing to the control tissue

A generalized and overwhelmed inflammatory and fibrotic response to trauma or surgery, the so called primary arthrofibrosis, represents a disease of severely impaired knee function. Myofibroblasts have been shown to be responsible for scar tissue contraction during wound healing.

In arthrofibrosis, fibroblast contraction may be involved in capsule fibrosis with consecutive loss of motion. We have found that myofibroblasts are markedly upregulated in arthrofibrosis tissue.

Myofibroblast expression may present a target for future therapeutical interventions, such as the use of specific antifibrosis agents.

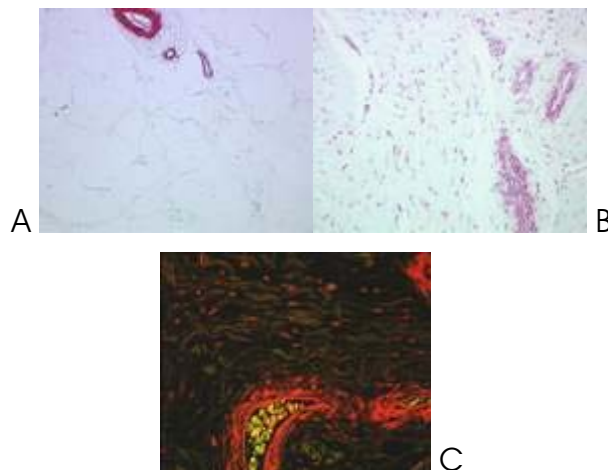


Fig. 1: A: AF-tissue showing a high expression of ASMA containing fibroblasts and a dense collagen fibre distribution (x200). B: Control-tissue showing fatty tissue with only sporadic collagen fibres and missing myofibroblasts (x200) C: ASMA expressing fibroblasts in arthrofibrosis tissue, fluorescence microscopy (x400)

*Department of Trauma Surgery, Hannover Medical School, Hannover, Germany

Histologic comparisons of the ACL in humans, dogs, cows and sheep

Murray M*, Weiler A, Juliao S*, Spindler K*

The future of treatment of the ruptured anterior cruciate ligament (ACL) is likely to involve cell-based therapies, such as tissue engineering with cell-seeded scaffolds or genetically altered cells. Both the development and evaluation of such therapies will be dependent on the cellular distributions and phenotypes in the intact and ruptured ligament. This study investigated histologic differences between intact ACLs obtained from young humans with no known history of joint disease and intact ACLs obtained from patients with osteoarthritis (OA), as well as ACLs from cows, sheep and canines. The "OA human" and bovine ACLs are frequently used as sources of ACL cells for in vitro work, while dogs and sheep represent two commonly used in vivo models of ACL injury and reconstruction. The cellular distribution, nuclear morphology, myo-fibroblast density and vascularity of the ligaments were compared in an effort to determine which ACL model is closest histologically to the young human population who sustain ACL rupture.

Intact ACLs were retrieved from 5 human trauma victims with no known joint disease, average age 23 years (young human ACLs). ACLs were also obtained from 12 patients undergoing total knee arthroplasty, average age 68 years (OA ACLs). Non-human ACLs were obtained from 12 canine, 5 ovine and 5 bovine knees with no evidence of joint disease on gross examination. The ligaments were fixed, sectioned and stained routinely. Immunohistochemistry for α -smooth muscle actin (ASMA) was performed using a monoclonal antibody for the actin isoform. Histomorphometry to quantify cell number density, nuclear morphology, vascularity and ASMA expression was performed at 2 mm increments for all ligaments, beginning at the proximal ligament and moving distally. One and two factor ANOVA was used to determine statistical significance of parameters and Fisher's PLSD testing used to evaluate differences among groups.

The cell number density of the young human ACLs was similar to that of the canine, but lower than that for all other groups (Fig 1; ANOVA, $p < 0.0003$; Dunnett's $p < 0.05$). In the ligaments from patients with OA, the cell density was higher in the first 2 mm of the ligament, then decreased to a value similar to that in the young human ACLs more distally.

The wide variability within each group precluded determination of similarities or differences between the groups for percentage of cells staining positive for ASMA; however, the canine ($3.1 \pm 1.1\%$) and OA ACLs ($10.2 \pm 1.3\%$) were most similar to that of the young human ACLs ($6.9 \pm 3.1\%$; $p < 0.09$). The percentage of ASMA positive cells was lower in the bovine ($0.9 \pm 0.3\%$) and ovine ($0.5 \pm 0.2\%$) ligaments. Although the percentage of non-vascular cells was lower in the bovine and ovine ligaments, the vasculature in both species stained positively, suggesting that interspecies differences in SMA isoform did not prohibit staining in these species.

The blood vessel density was similar in the canine, OA human, ovine and young human ACLs. The bovine ACLs had a significantly higher vessel density than the young human ACLs (ANOVA, $p < 0.0001$; Dunnett's $p < 0.05$). The cell nuclear aspect ratio of the young human ACLs was most similar to the canine and OA ACL tissue (Fig 2). The bovine and ovine ligaments all had cells with more elongated

nuclei than the young human ACLs (ANOVA, $p < 0.0001$; Dunnetts, $p < 0.05$); however, the OA ACLs, canine ACLs and the normal human ACL tissue had a similar distribution in cell nuclear aspect ratio, with more elongated nuclei in the proximal ligament and more spheroid nuclei found distally (Fig 2).

The young human ACL is most similar to the canine ACL with respect to the histologic features of blood vessel density, percentage of SMA positive cells, and cell nuclear morphology. The osteoarthritic human ACL and the young human ACL share a similar distribution in blood vessel density and cell nuclear morphology; however, the OA ACLs had a lower cell density. The bovine and ovine ACLs have higher vascularity and cells with more elongated nuclei than the young human ACLs. As previous investigators have suggested that variations in the light microscopic appearance of cells may correlate with alterations in phenotype, future studies may wish to select an ACL model with the most relevant histologic characteristics. Whether the histologic similarities between the young human and canine ACLs are responsible for the relatively high rate of ACL injury in these two populations requires further study.

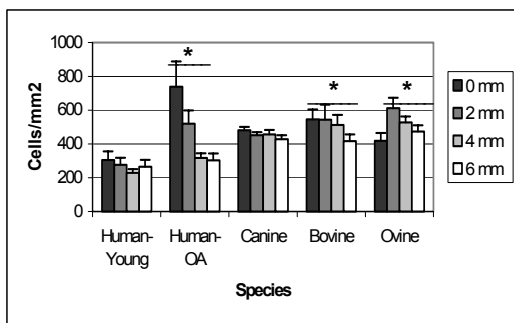


Fig 1: Cell number density as a function of location in the ligament for all five groups. (Bars represent mean \pm SEM; significant differences with $p < 0.05$ between groups denoted by *).

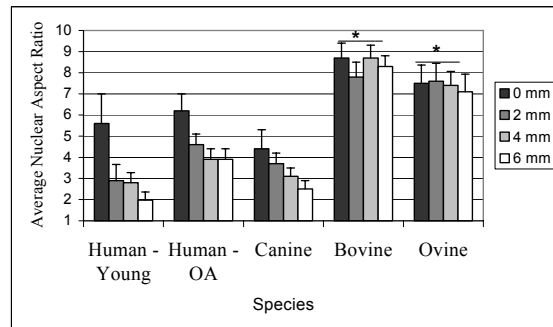


Fig 2: Cell nuclear aspect ratio as a function of location in the ligament for all five groups. (Bars represent the mean \pm SEM; significant differences with $p < 0.05$ between groups denoted by *).

*Brigham and Women's Hospital Boston, USA

Effect of Locally applied PDGF on cellularity, revascularisation and ultrastructural changes during ACL graft remodelling

Unterhauser FN, Hunt P, Jung T, Bergmann H*, Weiler A

After anterior cruciate ligament (ACL) reconstruction the grafted tissue undergoes a process of remodeling to adapt to its intraarticular environment. During that time there is a drop of mechanical properties which determines postoperative rehabilitation and return to strenuous activities. The use of growth factors may be able to accelerate graft tissue remodeling by means of increasing fibroblast proliferation and the synthesis of extracellular matrix proteins. Recently, it has been shown that the local application of platelet derived growth factor (PDGF) ameliorates the mechanical properties of the graft tissue during remodeling after ACL reconstruction in a sheep model. To further study this positive effect on tissue remodeling we investigated cellularity, vascularization, and ultrastructural changes of the grafted tissue over time.

48 sheep underwent ACL replacement surgery using a flexor tendon autograft. In each graft 4 polyglactin sutures (2/0) were longitudinally inserted. Prior to insertion sutures were coated with poly-(D,L-lactide) as a drug delivery vehicle (300 µg/suture). In 6 animals at each time point recombinant human PDGF-BB (R&D Systems) was incorporated into the coating (approx. 5 % total coating mass). Animals were sacrificed in groups of 12 after 3, 6, 12, and 24 weeks. Midsubstance tissue samples were taken for conventional (cell density) and polarized light (crimp) microscopy. Cell density and crimp length was measured at 5 representative sites along the section using a calibrated scale with a digital image analysis system. For capillary detection endothelial cells were immunostained in transverse sections using anti - v. Willebrand factor (rabbit anti human polyclonal antibody, Dako, DK). Vessel cross sections were counted separately in 5 regions in the subsynovial and central zone of the graft cross section. To study collagen fibril characteristics and composition 12 and 24 weeks tissue samples were prepared for transmission electron microscopy (TEM). From each specimen 12 regions (2 µm² each) were measured at x 80.000. The total amount of fibrils, fibril diameter distribution, and total fibril area was calculated. Data were analysed using Mann-Whitney U Wilcoxon rank sum testing and Kruskal-Wallis analysis of variance.

Cell density measurements showed no significant differences between the study and control groups at all time points. Crimp length in the PDGF treated grafts was significantly higher at 3 and 6 weeks. Vascular density in the study group was significantly higher in the central and subsynovial area at 6 weeks as compared to the control, whereas there was no significant difference at all other time points (Fig. 1). TEM data showed a significantly higher total collagen fibril amount in the study group at 12 weeks. There was no difference for fibril area at 12 and 24 weeks.

With respect to the collagenous part of the free tendon graft tissue, we found that the local application of PDGF-BB increases crimp length at 3 and 6 weeks. We further found, that at 12 weeks the total collagen fibril amount was significantly higher with PDGF treatment. Thus, we can conclude, that PDGF treatment of a free tendon graft changes mechanical properties of the tissue by influencing collagen

fibril structure. If this may be due to a better nutrition of the tissue by an increased vascularity, as we found it after 6 weeks, needs to be further clarified.

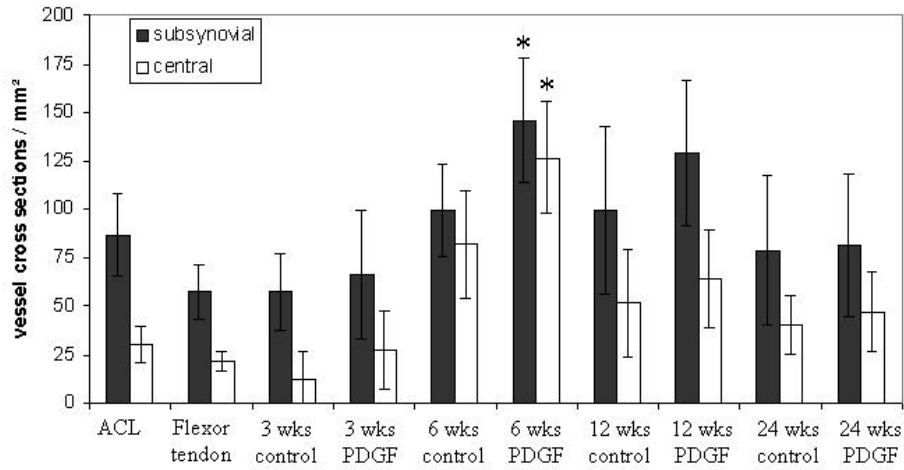


Fig. 1: Results for vascular density (* p < 0.05 study vs. control)

*Veterinary Pathology, Free University of Berlin, Germany

Locally applied platelet derived growth factor-BB ameliorates structural properties of a free tendon graft after anterior cruciate ligament reconstruction

Weiler A, Förster C, Falk R, Schmidmaier G, Südkamp NP

Growth factors such as platelet derived growth factor (PDGF), transforming growth factor beta and epidermal growth factor have a known positive effect on fibroblast proliferation and the synthesis of extracellular matrix proteins. The local application of PDGF has been shown to successfully improve mechanical properties of the medial collateral ligament (MCL) after injury. Although a positive effect of PDGF on anterior cruciate ligament (ACL) fibroblasts has also been demonstrated, no data on its potency for improving ACL healing or free tendon graft remodeling after ACL reconstruction are available. Furthermore, after ACL reconstruction the graft undergoes a process of remodeling leading to a reduction of tensile strength. During the remodeling process an overconstraintment may lead to a persistent graft elongation or rerupture. This potential risk ultimately influences the rehabilitation protocol. Thus, there is a strong need to accelerate or suppress tendon graft remodeling after ACL reconstruction to speed up rehabilitation. Therefore, our research question was whether the local long term application of PDGF-BB using a new biodegradable drug delivery tool accelerates biomechanically free tendon graft remodeling after ACL reconstruction in a sheep model.

48 sheep (mean 32 kg bodyweight) underwent ACL replacement in an open fashion using an ipsilateral Achilles tendon split-graft. Animals were sacrificed in groups of 12 after 3, 6, 12, and 24 weeks. In each graft 4 polyglactin sutures (2/0) were longitudinally inserted. Prior to insertion sutures were coated with poly-(D,L-lactide) as a drug delivery vehicle (300 μg /suture). In 6 animals at each time point recombinant human PDGF-BB (R&D Systems) was incorporated into the coating (5 % total coating mass). Animals were allowed to bear full weight without any restriction of motion.

Knee joints were tested for anterior-posterior drawer displacement (apD) at ± 50 N in 90° of flexion. Graft cross-sectional area (CSA) was measured using an area micrometer and a force transducer. Finally, the femur-ACL graft-tibia complex was tested until failure in 60° of flexion with the graft aligned to the axis of the applied load. Stiffness (St), yield load (F_{yield}), maximum load to failure (F_{max}), and energy (E) to failure were determined from the load/displacement data and tensile strength (TS) was calculated. Data were tested for equal distribution using the Kolmogorov-Smirnov test. Since non-parametric distribution was found data were compared using the Mann-Whitney U Wilcoxon test ($p < 0.05$).

For apD and F_{yield} there was no significant difference between the study and the control groups. CSA in the study groups was significantly lower at 3 ($p = 0.002$) and 12 weeks ($p = 0.002$). Stiffness in the study group was significantly higher at 24 weeks ($p = 0.038$). F_{max} was significantly higher in the study group at 6 weeks ($p = 0.026$). Energy to failure was significantly higher in the study group at 12 weeks ($p = 0.014$). Tensile strength in the study groups was significantly higher at 3 ($p = 0.004$) and 12 weeks ($p = 0.025$) (Fig. 1).

We could demonstrate that the local long term application of PDGF-BB via a biodegradable drug delivery system improves structural properties during free tendon graft remodeling after ACL reconstruction. To our knowledge this is the first study using a growth factor to accelerate graft remodeling in an intraarticular setting using a large animal model. In the present study the effect of PDGF-BB on the tissue's biomechanical properties was mainly presented by a reduced CSA combined with an unchanged F_{yield} . This finding indicates an improvement of the structural properties of the graft tissue which undergoes no compensative hypertrophy. However, other biomechanical parameters such as stiffness and F_{yield} remained unchanged in the early phase. Although we found a significantly higher F_{max} in the study group at 6 weeks our findings are in contrast to those of other studies investigating MCL healing. This may be due to the different intrinsic properties of ACL fibroblasts, the intraarticular environment and the fact that graft tissue was used instead of investigating the healing capabilities of the native ligament tissue. There was no further increase of TS in the study group between 12 and 24 weeks, whereas the control specimen showed still a significant improvement. This finding indicates that the PDGF treatment in the present study may lead to an early termination of remodeling.

In the past, all studies investigating ligament healing or graft remodeling described inferior structural properties such as a reduced tensile strength or an increased CSA compared to the uninjured native tissue. This observation has a tremendous clinical consequence for the functional restitution of injured knee joints. Therefore, there is a strong need to improve structural properties of healing or remodeling ligament tissue. The use of growth factors solely or in combination may thus present a promising tool towards the complete structural restitution of healing soft tissue.

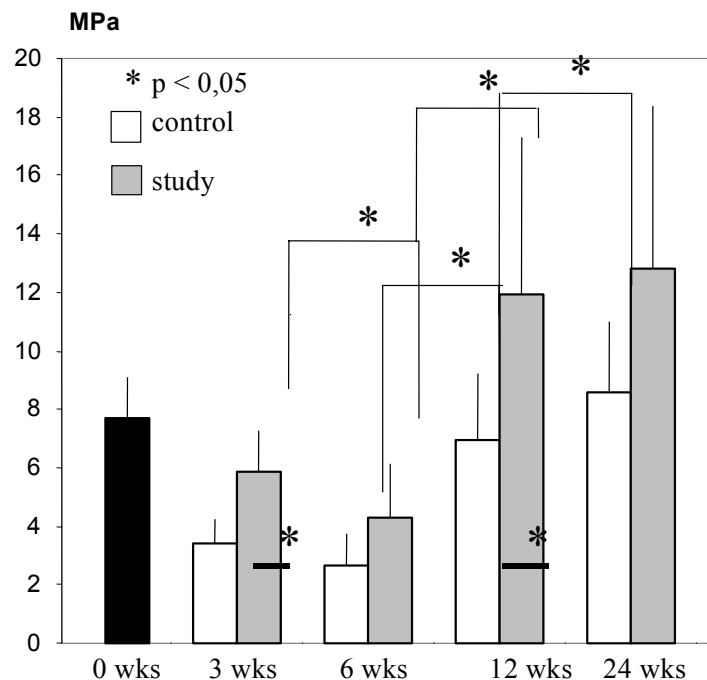


Fig. 1: Changes of tensile strength (TS) over time

Comparison of tendon-to-bone healing using extracortical and anatomic interference fit fixation of soft tissue grafts in a sheep model of acl reconstruction

Weiler A, Unterhauser FN, Faensen B, Hunt P, Bail HJ, Haas NP

The short and long term fate of soft tissue graft ACL reconstruction relies on a proper osseous graft incorporation. Using conventional extracortical fixation techniques, the tendon-to-bone healing progresses via the development of a fibrous interzone (FIZ) which results in an indirect, periosteal-like insertion site. The original ACL insertion, however, is characterized as a direct ligament insertion with a transition zone consisting of mineralized and fibrocartilage. A direct insertion may be more appropriate to transmit tensile forces between the ligament tissue and the underlying bone. In contrast, an anatomic interference fit fixation of soft tissue grafts may reduce graft-tunnel motion, thus eliminating a tunnel enlargement. Therefore, it has been suggested that anatomic interference fit fixation promotes tendon-to-bone healing, resulting in the development of a direct type of ligament insertion. To test the hypothesis that different healing patterns apply for different soft tissue graft fixation techniques we studied the tendon-to-bone healing histologically in an intraarticular model of soft tissue graft ACL reconstruction using extracortical and anatomic graft fixation.

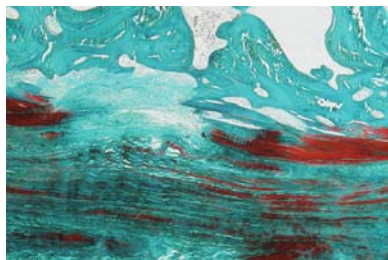
36 mature sheep underwent open ACL replacement surgery using an ipsilateral flexor tendon graft. Animals were followed for 6, 12, and 24 weeks. ACL reconstructions were either performed with anatomic interference fit (IF) fixation using biodegradable interference screws or extracortical with Endobutton/polyester suture (ES) fixation. After sacrifice proximal tibiae and distal femora were harvested and embedded into PMMA for an undecalcified histology. 6 μ m sections were stained using Masson Goldner's Trichrome, Safranin-O v. Kossa, and Alcian Blue techniques. Sharpey-like fibers were visualized using polarized light. To determine osseous ingrowth over time all animals underwent a polychrome sequential labeling (tetracycline, xylenol orange, calcein green). Precision grinds were created and analysed using fluorescent light microscopy.

With IF fixation the development of a FIZ was only partial or already blended at 6 weeks as determined by fluorescence microscopy. At the intratunnel site Sharpey-like fibers were only present in areas where a FIZ developed (Fig. 1). At the tunnel aperture site there was a first blending of graft tissue and mineralized cartilage at 12 weeks (Fig. 2). At 24 weeks a broad direct ligament insertion consisting of mineralized and fibrocartilage was found to be developed in all tibial and femoral specimens (Fig. 3). In contrast, with ES fixation there was a broad FIZ present at all time points and an obvious tunnel enlargement was found. The tunnel enlargement was maximally pronounced on the femur reaching an increase of + 106 % at 6 weeks and a subsequent narrowing (+ 60 %) at 24 weeks (Fig. 4). At 24 weeks a direct ligament insertion with a mineralized cartilage tidemark was developed in none of the specimens at the femur and partially in 4 out of 6 at the tibia.

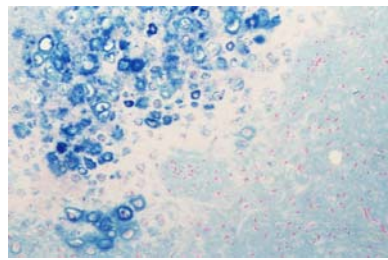
To our knowledge, this is the first report describing the occurrence of a direct type of ligament insertion after soft tissue graft ACL reconstruction consisting of 4 distinct zones: bone, mineralized cartilage, fibrocartilage, and ligament. In contrast to

previous studies and the ES fixation specimens of the present one, the intratunnel healing progresses only partially via the development of a FIZ. Furthermore, the development of Sharpey-like fibers, which has been viewed as an integral part of osseous graft incorporation, was only present at sites where a FIZ has developed. Thus, we conclude, that two different healing patterns may be found during tendon-to-bone healing. The early intratunnel healing and the later surface healing which results in a direct ligament insertion at the articular aperture site. We further found that in extracortical soft tissue graft fixation a direct ligament insertion on the femur did not develop and only partially at the tibia. This may be due to extensive graft-tunnel motions which has been described to occur with extracortical linkage fixation. In contrast to ES fixation, there was no tunnel enlargement with IF fixation. It may be reasonable to suggest, that anatomic interference fit fixation reduces graft-tunnel motion and may additionally seal the tunnel aperture site against a synovial inflow, thus preventing tunnel enlargement.

There is evidence that anatomic interference fit fixation promotes tendon-to-bone healing by leading to the development of a direct ligament insertion at the joint line, such as it is found with the intact ACL. In contrast to extracortical graft fixation the development of a tunnel enlargement can be prevented as it has recently been demonstrated clinically.



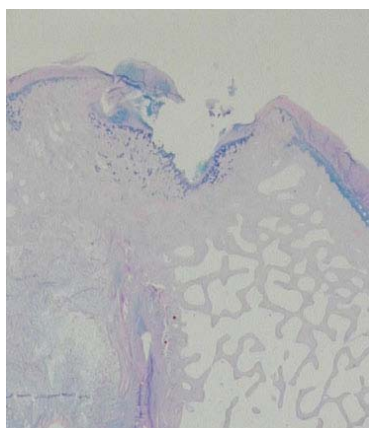
1



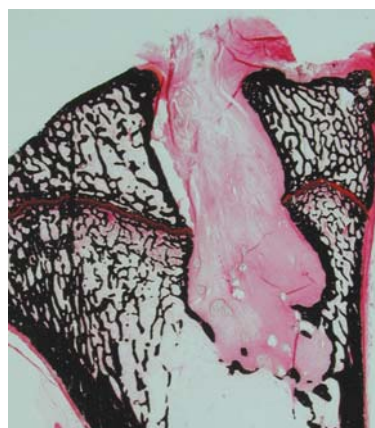
2

Fig. 1: IF specimen at 6 wks. The graft is in direct contact to the bone. A FIZ is only partially developed. Sharpey-like fibers are present where a FIZ is present.

Fig. 2: IF specimen at 12 wks showing a blending between graft tissue and mineralized cartilage at the articular tibial tunnel site.



3



4

Fig. 3: Tibial IF specimen at 24 wks. There is a broad band of mineralized cartilage at the tunnel aperture site indicating the development of a direct ligament insertion at the joint surface.

Fig. 4: Tibial ES specimen at 24 wks showing a severe tunnel enlargement with sclerosis. At the articular aperture site there are first signs of narrowing

Crimp frequency is strongly correlated to myofibroblast density in human tendon tissue

Unterhauser FN, Weiss M, Weiler A

The actin isoform α -smooth muscle actin (ASMA) has been identified in fibroblastic cells of normal tendon and ligament tissue. These highly differentiated cells, so called myofibroblasts may transmit tensile forces to the extracellular matrix, thus it has been suggested that these cells play a role during tissue contraction, such as in wound healing. Since these cells are up regulated during tendon and ligament healing, it was thought that the contractile potency of these cells might also be responsible for the wrinkling of the extracellular matrix and the formation of crimp. Therefore, it was the objective of the present study to determine the relationship between myofibroblast density and crimp frequency in fresh human tendon tissue.

Semitendinosus, gracilis, quadriceps and tibialis anterior tendons were harvested from a human multi organ donor (44 years) immediately after death. The tendons were sectioned into segments of 1 cm. A different number of segments were analyzed per tendon specimen (range 11 to 24). Specimens were fixed in formalin, dehydrated, embedded in paraffin, and cut into 4 μ m thick longitudinal section. For the detection of ASMA containing fibroblastic cells, samples were immunostained with a monoclonal antibody (anti human rabbit IgG, Dako AS, Glostrup, DK). Vascular smooth muscle cells were used as internal positive controls. Ten randomly chosen regions (0.44 x 0.44 mm each) were evaluated per section and the mean density of ASMA positive cells was determined using a digital imaging system. The same regions were used to measure crimp length under polarized light. For statistical calculations Pearson's correlation analysis with a power of 80% was used.

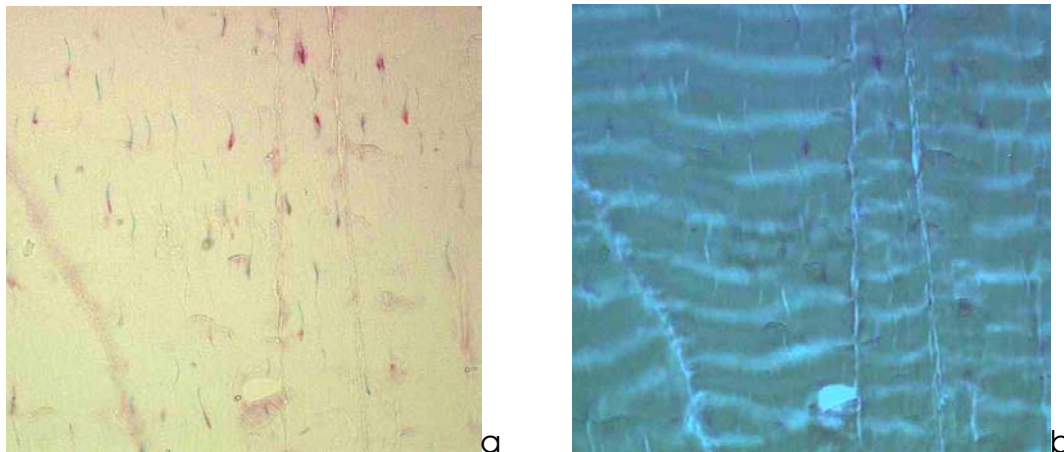


Fig. 1.: Immunohistochemical myofibroblast detection of a patellar tendon (a). Same section under polarized light showing the crimp pattern (b).

All examined tendons showed a significant correlation of myofibroblast density and crimp frequency (Table 1). The strongest correlations were found for the semitendinosus and patellar tendon and the poorest for the gracilis tendon.

We found that crimp frequency is strongly correlated to myofibroblast density in human tendon tissue. It has been hypothesized that myofibroblasts are involved in crimp formation. This hypothesis evolved out of the finding that ligament zones with the shortest crimp contained the highest amount of myofibroblasts. Furthermore,

myofibroblasts were found to be present at the edges of crimped fascicles. With the present investigation we found that myofibroblast are involved in crimp formation and should be viewed as an integral part of normal tendon tissue. The mechanism of the proposed contraction of the extracellular matrix will need further investigations to explain the specific crimp formation.

Table: Results for myofibroblasts density and crimp length.

	Semi-T Tendon	Gracilis Tendon	Patella Tendon	Quads Tendon	Tib.Ant. Tendon
ASMA +/mm²	23.9 ± 6.9	30 ± 5.5	39.7 ± 8.9	51.4 ± 14.9	25.2 ± 9.2
Crimp length/μm	72.1 ± 19.1	57.2 ± 9.8	41 ± 10.8	36 ± 7.5	77.7 ± 29.1
R²	0.7	0.42	0.81	0.61	0.62
R	-0.83	-0.68	-0.9	-0.78	-0.78
p	< 0.01	< 0.04	< 0.01	< 0.02	< 0.01
Power	99%	80%	95%	80%	99%

Biocompatibility and osseous replacement of composite interference screws

Dahne M, Scheffler S, Unterhauser FN, Hunt P, Weiler A

Satisfactory results have been reported using biodegradable interference screws for graft fixation in anterior cruciate ligament reconstruction (ACL). However data of in vivo biocompatibility and osseous replacement comparing different biodegradable materials do not yet exist.

The aim of the present study is to compare Poly-L-Lactide (PLLA), PLLA-Tricalciumphosphate composite and Hydroxyapatite-co-PLLA composite interference screws in a long term follow up sheep model using a loaded vs. unloaded and intraarticular vs. extraarticular setting.

42 sheep received an open ACL replacement of the left hind limb through a medial parapatellar arthrotomy. According to the study protocol a PLLA screw or a HA/TCP/PLLA screw was used for graft fixation in a randomised order. 3 different biodegradable screws were implantated at the right knee to simulated an unloaded setting.

Animals were followed in 6 groups with 7 specimen each 6, 24, 52 and 104 weeks.

After sacrifice the left knees underwent biomechanical testing at 60° of flexion. First anterior-posterior drawer tests are performed of the entire knee followed by tests without secondary restraints and soft tissue. Finally the isolated anterior crutiate ligament is tested with cycle loads followed by a pullout test. The right knee served as control.

Histological analyses of the left hind limb using synovial tissue biopsy and inguinal lymph nodes are performed to detect crystalline screw remnants. The graft-bone-surface and graft ingrowth as well as the degradation of the different screws will be followed by conventional histology and immunofluorescence microscopy.

The same histological analysis are used to describe the kinetic in degradation of the different biodegradable composite interference screws and osseus replacement in the unloaded setting of the right knee.

Goal of this study is to find differences and specific degradation patterns of composite interference screws with different amounts of HA and TCP to show their biomechanical behaviour their biocompatibility. This will be of importance for development of biodegradable implants and application of biodegradable interference screws for ACL replacement in the future.

Remodeling of the flexor tendon vs. bone patellar tendon bone graft after anterior cruciate ligament (ACL) reconstruction in a sheep model

Dahne M, Scheffler S, Unterhauser FN, Hunt P, Weiler A

Graft selection in ACL replacement depends on biomechanical properties, fixation and possible complications, like donor site morbidity, arthrofibrosis, secondary arthritis or anterior knee pain. However, there is a lack of in vivo data about the influence of graft choice on graft remodelling and possible joint degradation.

Therefore an animal study is performed to investigate the short and long term remodelling of bone-patellar-tendon-bone and soft tissue graft after ACL reconstruction by means of cellularity, revascularization, collagen type distribution and graft influence in joint degradation.

42 sheep received an open ACL replacement of the left hind limb through a medial parapatellar arthrotomy. According to the study protocol either a bone-patellar-tendon-bone graft or a flexor tendon graft was used for ACL reconstruction. The graft was fixed by biodegradable interference screws. For bone patellar tendon bone graft fixation graft preparation required a flipping technique tibial to handle graft-tunnel mismatch.

The animals were followed in 6 groups with 7 specimen each 6, 24, 52 and 104 weeks. Polychrome sequential labelling is performed during follow up.

Cell apoptosis, cell proliferation and differentiation are measured to describe cellular changes during graft remodelling. The tendon revascularisation is evaluated by immunohistochemical staining of the endothelial cells with anti-v. Willebrandt factor VIII antibody.

Differences in osseous graft incorporation is shown by immunofluorescence microscopy.

Furthermore, an immunohistochemical staining with monoclonal anti-alpha-smooth muscle actin antibodies is performed to detect activation and proliferation of myofibroblasts, which are characteristic for primary arthrofibrosis.

Purpose of this study is to show the influence of graft choice for ACL reconstruction on graft remodelling and joint degeneration.

Assessment and comparison of the tendon remodeling and the tendon-to-bone healing of a free allogenic and autologous graft for the reconstruction of the anterior cruciate ligament (ACL) in a sheep model

Scheffler S, Unterhauser F, Dahne M, Hunt P, Weiler A

For reconstruction of the ACL autologous transplants are the primary graft choices. However, in cases of multiple ligament injuries or revision surgery autologous tissue might not be available. Allogenic grafts from human donors are an attractive alternative. In several clinical and basic science studies it was shown that allografts showed a comparable outcome to autografts. However, there have been an increasing number of studies that found a delay in graft remodelling, ligamentization and restoration of mechanical properties of allogenic graft tissue. Additionally, almost all scientific data are available from studies on the allogenic bone-patellar-tendon-bone graft (BPTB). There are no scientific data available on the comparison of free autologous and allogenic graft tissue.

Therefore, the purpose of this study was the assessment and comparison of a free allogenic and autologous tendon graft for the reconstruction of the anterior cruciate ligament (ACL) with with biomechanical and histological analyses in an in-vivo sheep model.

In separate projects a thorough analysis of the tendon-bone healing processes is conducted until the completion of graft incorporation. The cellular and extracellular changes of the intraarticular tendon part are assessed for investigation of differences in the remodelling behaviour between both graft types.

ACLs of 54 mature female merino sheep were reconstructed in an open fashion using the long flexor tendon either as an auto- or an allograft.

For description of the time dependent changes, 9 specimens in each auto- and allograft group are tested at 6, 12 and 52 weeks. Histological analyses are performed on all 9 specimens, while biomechanical tests are performed on 7 out of 9 specimens.

For analysis of tendon-to-bone healing, revascularisation of the tendon-bone interface and markers for local immune reaction (CD68, 4, 6) are identified immunohistochemically. The kinetics of bony ingrowth are analysed with polychrome sequential labelling with 3 different fluorochromes. The newly developing tendon insertion is also visualised by conventional histology.

For description of the cellular changes during graft remodelling, apoptosis, cell proliferation and differentiation are measured. The kinetics and distribution of tendon revascularisation are evaluated by immunohistochemical staining of the endothelial cells with anti-v. Willebrandt factor VIII. Local immune response and inflammatory reactions are also analysed.

The extracellular changes during the remodelling phases of the intraarticular tendon part are explored by conventional histology and immunohistochemistry. Under polarised light microscopy the restoration of the typical collagen crimp pattern is analysed. The appearance of myofibroblasts, which are believed to be responsible for the development of the crimp pattern, are visualised by immunohistochemical

staining with alpha-smooth muscle actin antibodies. A quantitative and qualitative collagen analysis is also performed.

Goal of this study is to find differences in quality and quantity of the specific processes and their time-dependency comparing free allogenic and autologous tendons for ACL reconstruction. This will be of importance for the development of adequate rehabilitation protocols and will aide in the clarification of the controversial data that exist about the use of allografts as an important alternative to autologous tendon grafts.

The impact of thermal radio-frequency shrinkage on the mechanical and histological properties of the chronically elongated ACL

Scheffler S, Unterhauser F, Schönfelder V, Hunt P, Südkamp P, Weiler A

Since introduction of thermal radio-frequency (RF) treatment for shrinkage of elongated soft-tissue structures in the shoulder, this technique is becoming increasingly popular to treat other joints. The shrinkage of the chronically elongated anterior cruciate ligament (ACL) is a well accepted and a widely performed procedure. However, there are only limited data available on the impact of such thermal shrinkage on the mechanical properties and the histological appearance of treated soft-tissue structures, such as the ACL. In particular, the long-term effect of radio-frequency application on the stability of the RF treated ACL has not been well documented. Therefore, the objective of this study was to examine the effect of RF shrinkage of the chronically relaxed ACL on its biomechanical and histological properties after 6 months in the sheep model

In 16 Marino sheep the tibial insertion of the ACL was surgically elevated simulating ACL elongation. For this purpose a rectangular osteotomy was carried out to lift the eminentia intercondylaris, which was then fixed with a bicortical screw. In 8 sheep the chronically relaxed ACL's were treated with monopolar radio-frequency shrinkage (Karl Storz Endoscopy, Tuttlingen, Germany). The treatment was continued until manual anterior posterior (A P) drawer testing revealed restoration of knee laxity to the intact side. For reduction of early load bearing and simulation of careful rehabilitation an achillotomomy was performed. At 24 weeks all animals were sacrificed and each knee underwent mechanical testing at 60° of flexion. First, A P displacement under a ± 50 N load was measured, followed by a load to failure test with measurements of stiffness and failure load. At time zero, mechanical properties were compared between the intact (ACL), chronically relaxed (CR) and the RF treated ACL's (RF). For histological analysis cell numbers and vascular density in the subsynovial, intermediate and central region of the ACL were also examined.

Statistical analysis was performed using the Mann Whitney U Test. Level of statistical significance was set at $p < 0.05$

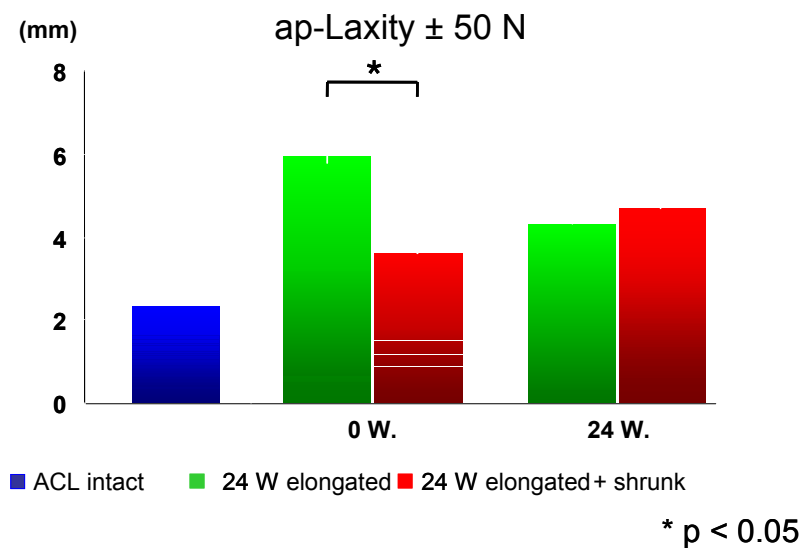
A significant increase was found for A-P displacement (+ 202%) comparing the chronically relaxed untreated group with the ACL intact group ($p < 0.001$). Following thermal shrinkage, A-P displacement of the RF treated group (2.94 ± 0.69 mm) was reduced to nearly the level of the intact ACL specimens (2.31 ± 0.52 mm). At 24 weeks, the A-P displacement of the RF treated group had increased to 4.68 ± 1.99 mm, which was not significantly different from the ACL relaxed untreated group (4.19 ± 0.86 mm). There was even a significantly lower stiffness and failure load in the RF treated when comparing it to the ACL relaxed untreated group (105 ± 51 vs. 143 ± 31 N/mm and 445 ± 203 N vs. 788 ± 305 N) ($p < 0.05$). The mechanical properties of both groups were significantly lower than in the intact ACL.

At 24 weeks, cell numbers were significantly reduced in the midportion of the ACL's in the RF treated group compared to the relaxed untreated ACL's. The same relationship between these two groups was found for vascularity with significantly lower vessel density in the RF treated group, especially in the central region of the

ligament. Subsynovial hypervascularity was found in each group, with no differences between the RF treated and relaxed untreated ACL's.

Even though thermal RF shrinkage of the chronically relaxed ACL allowed for initial restoration of AP laxity to the intact state, this stability could not be maintained after 24 weeks. In addition to the significant increase in A-P laxity, a significant deterioration of the mechanical properties, even in comparison to the ACL relaxed untreated group was found at 24 weeks after RF shrinkage. The histological analysis of the RF treated groups supports the mechanical findings. While there was a significant increase in vascular density in the central region of the untreated chronically relaxed group suggesting ongoing remodeling activity, no such difference was found in the RF treated group. Considering the decreased cell numbers in the midportion and decreased mechanical properties in this group, this might indicate necrosis of the ligament caused by the initial RF shrinkage application.

Our data demonstrated that a clinical advantage through general thermal shrinkage of the chronically relaxed ACL is questionable and that precise indications for the application of RF shrinkage will have to be established. Moreover, this study suggests that appropriate rehabilitation protocols should be designed for patients, which underwent RF treatment.



This study was partially supported by Storz, Storz Endoscopy, Sports Medicine, Inc.

Impact of tendon graft suturing on the interference fixation strength of quadrupled hamstring tendon grafts

Scheffler S, Steenlage E, Weiler A, Caborn D, Höher J

Interference fixation of soft tissue cruciate ligament grafts has become increasingly popular. The impact of the graft suturing technique on both graft fixation strength and graft motion in the bone tunnel is not well defined. The goal of this study was to determine whether uniform suturing of the tendon graft affects 1) ultimate fixation strength; 2) tendon graft motion during cyclic loading.

Ten pairs of matched mature porcine tibias (age < 2 years) and ten pairs of human quadrupled Semi-tendinosus and Gracilis (QSTG) hamstring tendons were used, divided into two groups. In group one, single cerclage sutures were placed 3 and 6 cm from the doubled graft end (Fig.1). In group two, additional heavy suture was used in a baseball/ whip stitch fashion between the cerclage sutures to join the four tendon strands (Fig.2). The sutured portions of the grafts were fixed in individually sized bone tunnels with matching diameter 28 mm bioresorbable screws. After preconditioning, the grafts were cycled 100 times at 20-250 N, followed by pullout to failure. Infrared cameras (Qualisys Inc.) were used for 2-D measurement of graft motion and tendon graft stretch Fig.2).



Fig.1: Graft preparation

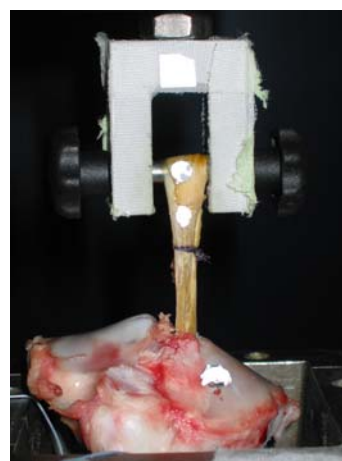


Fig.2: Test setup

Ultimate fixation strength for the grafts without sutures averaged 623 N (range 342 – 818); grafts with the sutures averaged 809 N (range 578 – 1176). stiffness averaged 270 N/mm without sutures, 325 N/mm with sutures. Total graft motion (graft/tunnel motion + tendon stretch) during cycling averaged 4.0 mm (+/- 1.3) without sutures, and 3.1 mm (+/- 0.7) with sutures. Isolated graft motion in the tunnel during cycling averaged 2.9 mm (+/- 2.0) without sutures, and 2.1 mm (+/- 0.8) with sutures.

Uniform tendon graft suturing significantly improved the ultimate graft fixation strength ($p < 0.05$), increased stiffness ($p = 0.05$), and decreased motion ($p = 0.26$). Uniform suture preparation of the tendon graft increased the reconstructed graft fixation strength and may contribute to a successful clinical outcome.

Analysis of the tendon remodeling of a free allogenic and autologous graft for the reconstruction of the anterior cruciate ligament (ACL) in a sheep model

Scheffler S, Unterhauser F, Dahne M, Hunt P, Weiler A

For reconstruction of the ACL autologous transplants are the primary graft choices. However, in cases of multiple ligament injuries or revision surgery autologous tissue might not be available. Allogenic grafts from human donors are an attractive alternative. In several clinical and basic science studies it was shown that allografts showed a comparable outcome to autografts. However, there have been an increasing number of studies that found a delay in graft remodelling, ligamentization, revascularisation and restoration of mechanical properties of allogenic graft tissue.

Therefore, the purpose of this study was the assessment and comparison of the intra- and extracellular changes in a free allogenic and autologous tendon graft for the reconstruction of the anterior cruciate ligament (ACL) during the first postoperative year.

ACLs of 54 mature female merino sheep were reconstructed in an open fashion using the long flexor tendon either as an auto- or an allograft.

For description of the time dependent changes, 9 specimens in each auto- and allograft group are tested at 6, 12 and 52 weeks. Histological analyses are performed on all 9 specimens, while biomechanical tests are performed on 7 out of 9 specimens.

For description of the cellular changes during graft remodelling, apoptosis, cell proliferation and differentiation are measured. The kinetics and distribution of tendon revascularisation are evaluated by immunohistochemical staining of the endothelial cells with anti-v. Willebrandt factor VIII. Local immune response and inflammatory reactions are also analysed.

The extracellular changes during the remodelling phases of the intraarticular tendon part are explored by conventional histology and immunohistochemistry. Under polarised light microscopy the restoration of the typical collagen crimp pattern is analysed. The appearance of myofibroblasts, which are believed to be responsible for the development of the crimp pattern, are visualised by immunohistochemical staining with alpha-smooth muscle actin antibodies. A quantitative and qualitative collagen analysis is also performed.

Goal of this study is to find differences in quality and quantity of the specific processes and their time-dependency comparing free allogenic and autologous tendons for ACL reconstruction. This will be of importance for the development of adequate rehabilitation protocols and will aid in the clarification of the controversial data that exist about the use of allografts as an important alternative to autologous tendon grafts.

Comparison of the tendon-to-bone healing of free allogenic and autologous grafts for the reconstruction of the anterior cruciate ligament (ACL) in a sheep model

Scheffler S, Unterhauser F, Dahne M, Hunt P, Weiler A

Tendon-to-bone healing of autologous ACL grafts has been intensively studied during the last decade. The development of a new tendon-to-bone anchorage and the distinction between different types of insertions has been described in different animal models. With the increasing popularity of allogenic grafts for ACL reconstruction, it is important to identify any possible differences in the tendon-to-bone healing from autologous grafts. In the existing literature almost all scientific data are limited to studies on the allogenic bone-patellar-tendon-bone graft (BPTB). There are no scientific data available on the comparison of free autologous and allogenic graft tissue. Additionally, little is known about the impact of the revascularisation on the development of a new tendon-to-bone interface and type of the newly formed tendon insertion.

Therefore, the purpose of this study was the assessment and comparison of the underlying processes during tendon-to-bone healing of a free allogenic and autologous tendon graft for the reconstruction of the anterior cruciate ligament (ACL). For this purpose different histological and biomechanical analyses were performed in an in-vivo sheep model.

ACLs of 54 mature female merino sheep were reconstructed in an open fashion using the long flexor tendon either as an auto- or an allograft.

For description of the time dependent changes, 9 specimens in each auto- and allograft group are tested at 6, 12 and 52 weeks. Histological analyses are performed on all 9 specimens, while biomechanical tests are performed on 7 out of 9 specimens.

For analysis of tendon-to-bone healing, revascularisation of the tendon-bone interface and markers for local immune reaction (CD68, 4, 6) are identified immunohistochemically. The kinetics and distribution of the revascularisation in the tendon-to-bone interface are evaluated by immunohistochemical staining of the endothelial cells with anti-v. Willebrandt factor VIII. The kinetics of bony ingrowth are analysed with polychrome sequential labelling with 3 different fluorochromes. The newly developing tendon insertion is visualised by conventional histology.

Goal of this study is to find differences in quality and quantity of the specific processes and their time-dependency comparing free allogenic and autologous tendons for ACL reconstruction. This will be of importance for the development of adequate rehabilitation protocols and will aide in the clarification of the controversial data that exist about the use of allografts as an important alternative to autologous tendon grafts.

Immediate microcirculatory derangements in skeletal muscle and periosteum following closed tibial fracture

Zhang L, Bail H, Mittlmeier T*, Haas NP, Schaser KD

Severe musculoskeletal soft tissue injury sustained after a closed fracture to the extremities significantly influences bone healing and determines patient's prognosis. The present study was aimed to quantitatively assess immediate microcirculatory changes in skeletal muscle and periosteum following standardized closed fracture.

Standardized closed fracture of left tibia in isoflurane-anesthetized Sprague-Dawley rats (n=14) was induced using a modified weight-drop-technique. The left extensor digitorum longus (EDL) muscle (n=7) and tibial periosteum (n=7) were surgically exposed for in vivo fluorescence microscopy 15 minutes following fracture. Non-fractured rats (n=14) served as controls. EDL-muscle edema was determined by the ratio of wet-to-dry-weight (EDL-water-content).

Closed tibial fracture resulted in a significant reduction of functional capillary density, red blood cell velocity and volumetric blood flow in both EDL-muscle and periosteum. Microvascular diameter, leukocyte adherence and macromolecular leakage were markedly increased, indicating trauma-induced inflammation and endothelial disintegration. EDL-muscle edema was found increased significantly following fracture.

This model permits for the first time direct in vivo visualization and quantification of fracture-induced microhemodynamic changes and cellular interactions within the surrounding soft tissue. It demonstrates that even simple fractures lead to profound microcirculatory disturbances in skeletal muscle and periosteum, also remote from the diaphyseal fracture site. It provides an useful approach for the development of therapeutic strategies to counteract fracture-induced microvascular dysfunction.

*Department of Trauma & Reconstructive Surgery, Universität Rostock, Germany

This was supported by a grant from the German Research Foundation DFG Scha 930/ 1-1

Fracture-induced periosteal microvascular injury: Characterizing the time course of changes in periosteum microcirculation.

Schaser KD, Bail H, Zhang L, Mittlmeier T*

Impaired periosteal perfusion following fracture has been proposed to contribute to delayed bone healing. This is illustrated by the clinical experience that severity and extent of injury to the periosteum ultimately influences the fracture healing response and determines return of limb function. Despite several microcirculatory studies of cortical bone blood flow following fracture have been performed a detailed study characterizing the time course of fracture-induced microcirculatory impairment and inflammatory reaction in periosteum is missing at present. The aim of the present study was to investigate the temporal profile of periosteum microcirculation and leukocyte-endothelial cell interaction during the first 6 weeks following a closed tibial fracture in rats in vivo.

Standardized closed fracture of left tibia (AO type A₂ & A₃; no significant closed soft tissue damage) in isoflurane-anesthetized (isoflurane 1.5 vol%, N₂O 0.5 l/min and O₂ 0.3 l/min) SD-rats (n=14) was induced using a modified weight-drop-technique and intramedullary stabilized by manual insertion of a 1.0 mm k-wire. All procedures were performed with the ethical and according to the NIH guidelines. For hemodynamic monitoring of mean arterial blood pressure (MABP); heart rate (HR) and fluid administration the left carotid artery and right jugular vein were cannulated with PE-catheters. Following fracture the left extensor digitorum longus (EDL) muscle (n=7) and the meta-/ diaphyseal tibial periosteum (n=7) were surgically exposed for in vivo fluorescence microscopy (IVM). Non-fractured rats (sham; n=14) served as controls, i.e. periosteum (n=7) and EDL-muscle (n=7). For IVM of either EDL-muscle or periosteum (15 minutes after preparation, i.e. 1 hour after fracture) each tissue was scanned (2mm steps, 8 observation areas. For contrast enhancement of the vascular network and for in vivo staining of leukocytes FITC-dextran and rhodamine 6G was injected intravenously prior to each observation. Microhemodynamic analysis included the determination of microvessel diameters (D in μm), functional capillary density (FCD: length of perfused capillaries per observation area, cm^{-1}), leukocyte-endothelial cell interactions (leukocyte rolling fraction: number of rolling leukocytes as % of the total leukocyte flux; number of sticking leukocytes per mm^2 of endothelial surface), microvascular permeability (macromolecular leakage) and red blood cell velocity (V_{RBC}). Volumetric capillary and venular blood flow (VBF, picoliter/sec) was calculated from V_{RBC} and D for each vessel as: $\text{VBF} = \pi/4 \times D^2 \times V_{\text{RBC}}$. After sacrificing the rats, the left and right EDL-muscles were harvested for measurement of the wet to dry weight ratio and calculation of the EDL-muscle water content and edema index (EI = exp./contralat. limb).

MABP/ HR remained stable with no significant difference between groups. EDL-Muscle: In non-fractured rats, capillaries were arranged in parallel and straightened in the longitudinal axis of the muscle fibers with no significant microvascular thrombosis, macromolecular leakage or leukocyte adherence. Following closed tibial fracture, a heterogeneous perfusion pattern with severe microvascular dysfunction, including stasis and collapse of capillaries, increase in intercapillary distance, microvascular thrombosis and direct disruption of microvessels with subsequent hemorrhage was found. FCD and V_{RBC} of EDL-muscle following fracture

were found to be significantly reduced compared to controls. Fracture-induced microvascular deteriorations were further characterized by a significant hypoperfusion as demonstrated by a marked decrease in capillary VBF. Fracture-induced changes in microvascular diameters displayed a simultaneous vasodilation of capillaries and postcapillary venules. In addition, a significant increase in microvascular leakage) was found, reflecting substantial endothelial disintegration in response to fracture. Analysis of leukocyte-endothelial cell interaction revealed a two-fold increased leukocyte rolling and adherence, mostly restricted to the endothelium of postcapillary venules when compared to non-fractured animals.

Periosteum: In non-fractured rats, a homogeneous periosteal microcirculation with no capillary dysfunction or leukocyte adhesion was found. Whereas at the metaphysis a densely meshed capillary network with many intercapillary connections was observed, the arrangements of diaphyseal capillaries, showed a parallel alignment to the tibia axis. Microvascular response of periosteum to fracture demonstrated a total microvascular perfusion failure and significantly increased microvascular permeability at the diaphyseal fracture site. Metaphyseal areas remote from the fracture site displayed heterogeneous and severely impaired perfusion with decreased V_{RBC} and scattered capillary thrombosis, increased microvascular leakage and leukocyte activation. Again, endothelial rolling and adherence of leukocytes were increased by two-fold when compared to controls, most pronounced in post-capillary periosteal venules. Closed tibial fracture caused a significant increase in EDL-muscle water content and EI, demonstrating fracture-induced skeletal muscle edema formation.

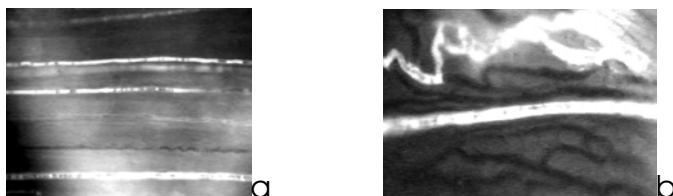


Fig.1: Intravital microscopy of rat (a) EDL-muscle and (b) periosteum following closed tibial fracture demonstrating severe microvascular injury, including capillary thrombosis, increased microvascular permeability and edema formation. Magn.: x405.

The present model permits for the first time direct in vivo visualization and quantification of fracture-induced microhemodynamic changes within the surrounding periosteum and skeletal muscle. It could be demonstrated that a simple fracture leads to profound microvascular injury, endothelial dysfunction, leukocyte-endothelial cell interaction and tissue edema in skeletal muscle and periosteum, also remote from the diaphyseal fracture site. Therefore, we conclude that these findings provide an useful approach for the pathophysiological analysis of tissue-confined microcirculatory disturbances and their local interaction. In conclusion, the present study may have therapeutic consequences in view of developing novel treatment strategies to improve fracture healing by counteracting fracture-induced microvascular dysfunction.

*Department of Trauma & Reconstructive Surgery, Universität Rostock, Germany

This was supported by a grant from the German Research Foundation DFG Scha 930/ 1-1

Temporal profile of microvascular dysfunction in tibial periosteum following closed soft tissue trauma in rats

Schaser KD, Bail H, Zhang L, Mittlmeier T*

Complex injuries to the extremities typically involve severe closed trauma to the soft tissue and periosteum. Based on the clinical observation that extensive soft tissue injury or periosteal stripping frequently precede delayed fracture repair possibly resulting in a non-union, points to the pathogenetic influence of trauma-induced cellular and microvascular changes within the periosteum. Despite a critical decrease in extraosseous and nutritional blood flow to the bone appears to be a pathogenetic factor the precise extent and the temporal relationship of microcirculatory deteriorations and posttraumatic inflammation in periosteum caused by isolated and severe closed soft tissue injury (CSTI) is not known. Therefore, we hypothesized that periosteal microcirculation, known for its nutritive and blood-supplying functions for the cortical bone is adversely affected by a severe CSTI. Consistent with the delayed healing response of fractures with severe soft tissue damage we further hypothesized that the manifestation of trauma-initiated microvascular impairment is substantially prolonged, possibly caused by persistently enhanced capillary and endothelial dysfunction, increased microvascular permeability and leukocyte activity in periosteum.

Standardized closed soft tissue injury was induced in the anterolateral tibial compartment of 24 isoflurane-anesthetized SD-rats using the computer-assisted Controlled Impact Injury (CII) device. Following trauma the rats were assigned to 4 groups (n=6) differing as to time point of analysis (2h, 24h, 48h and 1 week after the trauma). Non-injured, sham-operated rat served as controls. All experiments were ethically approved and according to NIH-guidelines. Before the meta-/ diaphyseal periosteum was surgically exposed intramuscular pressure (P_{im} in mmHg) within the anterior and posterior tibial compartment was measured percutaneously using a microsensors catheter. The right carotid artery and jugular vein were cannulated with PE-catheters for monitoring of MABP and HR and administration of fluorescence dyes. By use of intravital fluorescence microscopy (IVM) the tibial periosteum was scanned in 2 mm increments. Contrast enhancement of the plasma and in vivo labeling of leukocytes was achieved by intravenous injection of rhodamine 6G and FITC-dextran, respectively. Quantitative microcirculatory analysis included the determination of microvessel diameters (D in μm), functional capillary density (FCD: length of perfused capillaries per observation area, cm^{-1}), leukocyte-endothelial cell interactions (leukocyte rolling fraction: number of rolling leukocytes as % of the total leukocyte flux; number of sticking leukocytes per mm^2 of endothelial surface), microvascular permeability (macromolecular leakage) and red blood cell velocity (V_{RBC}). Volumetric capillary and venular blood flow (VBF, picoliter/sec) were calculated from V_{RBC} and D for each vessel as: $VBF = \pi/4 \times D^2 \times V_{RBC}$. At completion of IVM, rats were sacrificed and the left and right skeletal muscles (M. extensor digitorum longus; EDL) were taken for measurement of the wet to dry weight ratio as well as calculation of the EDL-muscle water content and edema index (EI = exp./contralat. EDL).

MABP/ HR remained stable with no significant difference between groups. Periosteum: Microcirculation of meta- and diaphyseal tibial periosteum in non-

injured rats demonstrated a homogeneous perfusion with no significant capillary or endothelial dysfunction. Microvascular deteriorations of periosteal microhemodynamics caused by isolated CSTI were reflected by persistent decrease in nutritive perfusion, markedly prolonged increase in transendothelial leakage (microvasc. permeability) associated with increasingly sustained leukocyte rolling and adherence throughout the entire study period, mostly pronounced 48 hours following the trauma. Peak level in capillary extravasation of macromolecules coincided with the maximum leukocyte adherence, tissue pressure and edema, supporting the concept of leukocyte-dependent endothelial dysfunction and subsequent tissue injury.

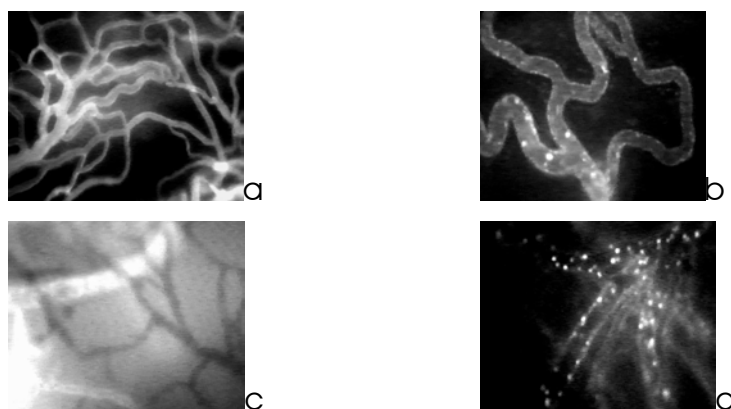


Fig.1: Capillary perfusion (a) and leukocyte adherence (b) in periosteum of control rats visualized by IVM. Note the marked capillary dysfunction (c), i.e. microvascular thrombosis and accumulation of leukocytes (d) following CSTI. Magn.: x405.

These results show that isolated skeletal muscle injury exerts adverse effects on periosteal microcirculation. The time course of developing deteriorations in periosteal microhemodynamics following CSTI suggests a prolonged and delayed temporal profile in manifestation of soft tissue trauma-induced microvascular dysfunction and inflammation. Since periosteal integrity is a key determinant for maintaining cortical blood flow and mediating initial steps of fracture healing the prolonged propagation of microcirculatory disturbances may be of causative importance for delayed healing following fractures with severe soft tissue trauma. Our findings could allow a temporal interrelation of soft tissue trauma-induced microvascular derangements and leukocyte-initiated endothelial dysfunction in periosteum to the healing response of fractures with associated soft tissue damage. Thus, our observations may have therapeutic implications for preserving periosteal integrity and considering the interaction of soft tissue injury and periosteal microvascular injury during management of musculoskeletal trauma.

*Department of Trauma & Reconstructive Surgery, Universität Rostock, Germany

Peer Reviewed Publications

2001

- Bail H.J., Kolbeck S., Lindner T., Dahne M., Weiler A., Windhagen H.J., Raun K., Skjaerbaek C., Flyvbjerg A., Orskov H., Haas N.P. & Raschke M.J.:
The effect of growth hormone on insulin-like growth factor I and bone metabolism in distraction osteogenesis.
Growth Horm Igf Res: 11(5) 314-23. 2001
- Bail H.J., Kolbeck S., Lindner T., Dahne M., Weiler A., Windhagen H.J., Raun K., Skjaerbaek C., Flyvbjerg A., Orskov H., Haas N.P. & Raschke M.J.:
The effect of growth hormone on insulin-like growth factor I and bone metabolism in distraction osteogenesis.
Growth Horm Igf Res: 11(5) 314-323. 2001
- Bergmann G., Deuretzbacher G., Heller M., Graichen F., Rohlmann A., Strauss J. & Duda G.N.:
Hip contact forces and gait patterns from routine activities.
J Biomech: 34(7) 859-71. 2001
- Duda G.N., Eilers M., Loh L., Hoffman J.E., Kaab M. & Schaser K.:
Chondrocyte death precedes structural damage in blunt impact trauma.
Clin Orthop Relat R: (393) 302-9. 2001
- Duda G.N., Haas N.P. & Bergmann G.:
Musculoskeletal loading and its implication for clinical practice:February 2000, Charite, Berlin.
J Biomech: 34(7) 837. 2001
- Duda G.N., Mandruzzato F., Heller M., Goldhahn J., Moser R., Hehli M., Claes L. & Haas N.P.:
Mechanical boundary conditions of fracture healing: borderline indications in the treatment of unreamed tibial nailing.
J Biomech: 34(5) 639-50. 2001
- Fernandez Dell'Oca A.A., Tepic S., Frigg R., Meisser A., Haas N. & Perren S.M.:
Treating forearm fractures using an internal fixator: a prospective study.
Clin Orthop Relat R: (389) 196-205. 2001
- Gerber A. & Masquelet A.C.:
The pronator quadratus compartment. Anatomical description and basis for intracompartmental pressure measurement.
J Hand Surg: 26A 1129-1134. 2001
- Gerber A., Ghalambor N. & Warner J.J.P.:
Shoulder arthroplasty: The problem of instability: Balancing mobility and stability.
Orthop Clin North Am: 32(4) 661-70. 2001

- Gerber A. & Warner J.J.P.:
Management of glenoid bone loss in total shoulder replacement.
Techniques in Shoulder and Elbow Surgery: 2(4) 255-266. 2001
- Gerlach J.C., Zeilinger K., Spatkowski G., Hentschel F., Schnoy N., Kolbeck S., Schindler R.K. & Neuhaus P.:
Large-scale isolation of sinusoidal endothelial cells from pig and human liver.
J Surg Res: 100(1) 39-45. 2001
- Haas N., Hauke C., Schütz M., Käab M. & Perren S.M.:
Treatment of diaphyseal fractures of the forearm using the Point Contact Fixator (PC-Fix): Results of 387 fractures of a prospective multicentric study (PC-Fix II).
Injury: 32 Suppl 2 51-62. 2001
- Haas N.P., Schütz M. & Kaisers U.:
Clinical Management of Chest Injuries in the Polytraumatized Patient
Kongressbd Dtsch Ges Chir Kongr: 118 421-3. 2001
- Heller M.O., Bergmann G., Deuretzbacher G., Claes L., Haas N.P. & Duda G.N.:
Influence of femoral anteversion on proximal femoral loading: measurement and simulation in four patients.
Clin Biomech: 16(8) 644-9. 2001
- Heller M.O., Bergmann G., Deuretzbacher G., Dürselen L., Pohl M., Claes L., Haas N.P. & Duda G.N.:
Musculo-skeletal loading conditions at the hip during walking and stair climbing.
J Biomech: 34(7) 883-93. 2001
- Hünerbein M., Raschke M., Khodadadyan C., Hohenberger P., Haas N.P. & Schlag P.M.:
Three-dimensional ultrasonography of bone and soft tissue lesions.
Eur J Ultrasound.: 13(1) 17-23. 2001
- Käab M.J., Schütz M. & Haas N.P.:
Minimal-invasive Stabilisierung von proximalen Tibiafrakturen mit dem LIS-System
Osteosynthese Intern.: 9 117-119, 2001
- Kaisers U., Schütz M. & Falke K.J.:
Management of ARDS
Kongressbd Dtsch Ges Chir Kongr: 118 336-8. 2001
- Kandziora F., Ludwig K., Pflugmacher R., Haas N.P. & Mittlmeier T.:
Biomechanical study of angle-stable anterior atlanto-axial spondylodesis plate
Orthopade: 30(3) 182-8. 2001

- Kandziora F., Pflugmacher R., Schafer J., Born C., Duda G., Haas N.P. & Mittlmeier T.:
Biomechanical comparison of cervical spine interbody fusion cages.
Spine: 26(17) 1850-7. 2001
- Kandziora F., Pflugmacher R., Scholz M., Schnake K., Lucke M., Schröder R. & Mittlmeier T.:
Comparison between sheep and human cervical spines: an anatomic, radiographic, bone mineral density, and biomechanical study.
Spine: 26(9) 1028-37. 2001
- Kandziora F., Schulze-Stahl N., Khodadadyan-Klostermann C., Schroder R. & Mittlmeier T.:
Screw placement in transoral atlantoaxial plate systems: an anatomical study.
J Neurosurg: 95(1 Suppl) 80-7. 2001
- Kandziora F., Stöckle U., König B., Khodadadyan-Klostermann C., Mittlmeier T. & Haas N.P.:
C-arch navigation for transoral atlanto-axial screw placement
Chirurg: 72(5) 593-9. 2001
- Kassi J.P., Hoffmann J.E., Heller M., Raschke M. & Duda G.N.:
Evaluating the stability of fracture fixation systems: mechanical device for evaluation of 3-D stiffness in vitro
Biomed Tech: 46(9) 247-52. 2001
- Kerschbaumer F., Rittmeister M., Ewald W. & Kandziora F.:
Atlantoaxial kyphosis
Orthopade: 30(12) 919-24. 2001
- Khodadadyan-Klostermann C., Raschke M., Dahne M., Kandziora F., Schule S. & Haas N. P.:
Treatment of Septic Nonunion Following Intramedullary Nailing of a Multisegmental Humerus Fracture with Ilizarov Ring Fixation
European Journal of Trauma: 6 327-332. 2001
- Khodadadyan-Klostermann C., Kandziora F., Schnake K.J., Lewandrowski K.U., Wise D., Weiler A. & Haas N.P.:
Biomechanical comparison of biodegradable lumbar interbody fusion cages
Chirurg: 72(12) 1431-8. 2001
- Khodadadyan-Klostermann C., Kandziora F., Schnake K.J., Haas N.P. & Harms J.:
[Transoral atlanto-axial plate fixation in the treatment of a malunited dens fracture and secondary atlanto-axial instability]
Chirurg: 72(11) 1298-302. 2001

- Khodadadyan-Klostermann C., Raschke M., Mittlmeier T., Melcher I. & Haas N.P.:
Ankle and pan-talar arthrodesis with Ilizarov composite hybrid fixation: operative technique and review of 21 cases
Foot Ankle.: 7 149-156. 2001
- Klein P., Mittlmeier T., Schmidt D., Kolbeck S., Bail H., Schmidmaier G., Raschke M. & Duda G.:
Functional recovery during osteochondral and bone defect healing
Clin Biomech: 16 839-840. 2001
- Lill H., Hepp P., Hoffmann J.E., Laborowicz J., Korner J., Josten C. & Duda G.N.:
Neue Implantate zur Stabilisierung proximaler Humerusfrakturen. Eine vergleichende in-vitro Studie
Osteosynthese Int: 9 85-93. 2001
- Hünerbein M., Totkas S., Khodadadyan-Klostermann C. & Schlag P.M.:
Potential Applications of Microendoscopy
Surg Technol Int: IX. 105-109. 2001
- Mittlmeier T. & Ewert A.:
Injuries of the knee joint extensor system
Unfallchirurg: 104(4) 344-56; quiz 356. 2001
- Raschke M., Kolbeck S., Bail H., Schmidmaier G., Flyvbjerg A., Lindner T., Dahne M., Roenne I. & Haas N.:
Homologous growth hormone accelerates healing of segmental bone defects.
Bone: 29(4) 368-73. 2001
- Scheffler S.U., Clineff T.D., Papageorgiou C.D., Debski R.E., Benjamin C. & Woo S.L.:
Structure and function of the healing medial collateral ligament in a goat model.
Ann Biomed Eng: 29(2) 173-80. 2001
- Scheffler S.U., Clineff T.D., Ma C.B., Papageorgiou C.D., Debski E.D., Woo S.L.:
A biomechanical and histological evaluation of the healing goat medial collateral ligament (MCL)
Ann Biomed Eng: 29 173-80, 2001
- Schmidmaier G., Wildemann B., Bail H., Lucke M., Fuchs T., Stemberger A., Flyvbjerg A., Haas N.P. & Raschke M.:
Local application of growth factors (insulin-like growth factor-1 and transforming growth factor-beta1) from a biodegradable poly(D,L-lactide) coating of osteosynthetic implants accelerates fracture healing in rats.
Bone: 28(4) 341-50. 2001

- Schmidmaier G., Wildemann B., Stemberger A., Haas N.P. & Raschke M.:
Biodegradable poly(D,L-lactide) coating of implants for continuous release of growth factors.
J Biomed Mater Res: 58(4) 449-55. 2001
- Schütz M., Müller M., Krettek C., Höntzsch D., Regazzoni P., Ganz R. & Haas N.P.:
Minimally invasive fracture stabilization of distal femoral fractures with the LISS: A prospective multicenter study. Results of a clinical study with special emphasis on difficult cases
Injury: 32, Supplement 3 S-C-48-54. 2001
- Schütz M. & Haas N.P.:
LISS: Internal Plate Fixator
Kongressbd Dtsch Ges Chir Kongr: 118 375-9. 2001
- Shakibaei M., Schulze-Tanzil G., de Souza P., John T., Rahmanzadeh M., Rahmanzadeh R. & Merker H.J.:
Inhibition of mitogen-activated protein kinase kinase induces apoptosis of human chondrocytes.
J Biol Chem: 276(16) 13289-94. 2001
- Stähelin A.C., Südkamp N.P. & Weiler A.:
Anatomic double-bundle posterior cruciate ligament reconstruction using hamstring tendons.
Arthroscopy: 17(1) 88-97. 2001
- Stöckle U., König B., Hofstetter R., Nolte L.P. & Haas N.P.:
[Navigation assisted by image conversion. An experimental study on pelvic screw fixation]
Unfallchirurg: 104(3) 215-20. 2001
- Strobel M.J., Castillo R.J. & Weiler A.:
Reflex extension loss after anterior cruciate ligament reconstruction due to femoral "high noon" graft placement.
Arthroscopy: 17(4) 408-11. 2001
- Südkamp N.P.:
[Rotator cuff rupture]
Zbl Chir: 126(3) 177-83. 2001
- Tempka A.:
Is "unjustified admission" in trauma surgery preventable?
Unfallchirurg: 104(7) 678-80. 2001
- Thomale U., Schaser K., Unterberg A.W. & Stover J.F.:
Visualization of rat pial microcirculation using the novel orthogonal polarized spectral (OPS) imaging after brain injury.
J Neurosci Meth: 108(1) 85-90. 2001

- Tingart M., Höher J., Bouillon B. & Tilling T.:
Meniscus repair: suture or arrow?
Unfallchirurg: 104(6) 507-12. 2001
- Warner M.D., Taylor W.R. & Cliff S.E.:
Finite element biphasic indentation of cartilage: a comparison of
experimental indenter and physiological contact geometries.
P I Mech Eng H: 215(5) 487-96. 2001
- Weiler A., Peters G., Mäurer J., Unterhauser F.N. & Südkamp N.P.:
Biomechanical properties and vascularity of an anterior cruciate ligament
graft can be predicted by contrast-enhanced magnetic resonance imaging.
A two-year study in sheep.
Am J Sport Med: 29(6) 751-61. 2001
- Weiler A., Richter M., Schmidmaier G., Kandziora F. & Südkamp N.P.:
The EndoPearl device increases fixation strength and eliminates construct
slippage of hamstring tendon grafts with interference screw fixation.
Arthroscopy: 17(4) 353-9. 2001
- Weisskopf M., Reindl R., Schröder R., Hopfenmuller P. & Mittlmeier T.:
CT scans versus conventional tomography in acute fractures of the
odontoidprocess.
Eur Spine J.: 10(3) 250-6. 2001

2002

- Bail H.J., Kolbeck S., Krummrey G., Schmidmaier G., Haas N.P. & Raschke M.J.:
Systemic application of growth hormone for enhancement of secondary and
intramembranous fracture healing.
Horm Res: 58 Suppl 3 39-42. 2002
- Bail H.J., Kolbeck S., Krummrey G., Weiler A., Windhagen H.J., Hennies K.,
Raun K. & Raschke M.J.:
Ultrasound can predict regenerate stiffness in distraction osteogenesis.
Clin Orthop Relat R: (404) 362-7. 2002
- Bail H.J., Raschke M.J., Kolbeck S., Krummrey G., Windhagen H.J., Weiler A.,
Raun K., Mosekilde L. & Haas N.P.:
Recombinant species-specific growth hormone increases hard callus
formation in distraction osteogenesis.
Bone: 30(1) 117-24. 2002
- Duda G.N., Mandruzzato F., Heller M., Kassi J.P., Khodadadyan C. & Haas N.P.:
Mechanical conditions in the internal stabilization of proximal tibial defects.
Clin Biomech: 17(1) 64-72. 2002

- Duda G.N., Sollmann M., Sporrer S., Hoffmann J.E., Kassi J.P., Khodadadyan C. & Raschke M.:
Interfragmentary motion in tibial osteotomies stabilized with ring fixators.
Clin Orthop Relat R: 2002(396) 163-72. 2002
- Duda G.N., Henßler A., Negele A., Kreidler J. & Claes L.:
Physiologische Belastung von Unterkieferosteosynthesen: Entwicklung eines
neuartigen Kieferbelastungssimulators
Biomed Technik (Bln): 47(11) 272-277. 2002
- Govender S., Csimma C., Genant H.K., Valentin-Opran A., Amit Y., Arbel R.,
Aro H., Atar D., Bishay M., Borner M.G., Chiron P., Choong P., Cinats J.,
Courtenay B., Feibel R., Geulette B., Gravel C., Haas N., Raschke M.,
Hammacher E., Van Der Velde D., Hardy P., Holt M., Josten C., Ketterl R.L.,
Lindeque B., Lob G., Mathevon H., McCoy G., Marsh D., Miller R., Munting E.,
Oevre S., Nordsetten L., Patel A., Pohl A., Rennie W., Reynders P., Rommens
P.M., Rondia J., Rossouw W.C., Daneel P.J., Ruff S., Ruter A., Santavirta S.,
Schildhauer T.A., Gekle C., Schnettler R., Segal D., Seiler H., Snowdowne R.B.,
Stapert J., Taglang G., Verdonk R., Vogels L., Weckbach A., Wentzensen A. &
Wisniewski T.:
Recombinant human bone morphogenetic protein-2 for treatment of open
tibial fractures: a prospective, controlled, randomized study of four hundred
and fifty patients.
J Bone Joint Surg Am: 84-A(12) 2123-34. 2002
- Gerber A. & Gogolewski S.:
Treatment of large diaphyseal bone defects using polylactide membranes in
combination with autogeneic cancellous bone. An experimental study.
Injury: 33(Suppl.2) 43-57. 2002
- Gerber A. & Warner J.J.P.:
Thermal capsulorrhaphy to treat shoulder instability.
Clin Orthop: 40 :105-116. 2002
- Haas N.P.:
The trauma centre: now and in the future.
J Bone Joint Surg Br: 84(5) 627-30. 2002
- Kaab M.J., Rahn B.A., Weiler A., Curtis R., Perren S.M. & Schneider E.:
Osseous integration of poly-(L-co-D/L-lactide) 70/30 and titanium suture
anchors: an experimental study in sheep cancellous bone.
Injury: 33 Suppl 2 B37-42. 2002
- Kaab M.J., Weiler A., Schaser K., Sudkamp N.P. & Haas N.P.:
Coincidence of recurrent arthritis and Behcet's disease following anterior
cruciate ligament reconstruction.
Arthroscopy: 18(3) E15. 2002

- Kandziora F., Bail H., Schmidmaier G., Schollmeier G., Scholz M., Knispel C., Hiller T., Pflugmacher R., Mittlmeier T., Raschke M. & Haas N.P.:
Bone morphogenetic protein-2 application by a poly(D,L-lactide)-coated interbody cage: in vivo results of a new carrier for growth factors.
J Neurosurg: 97(1 Suppl) 40-8. 2002
- Kandziora F., Neumann L., Schnake K.J., Khodadadyan-Klostermann C., Rehart S., Haas N.P. & Mittlmeier T.:
Atlantoaxial instability in Dyggve-Melchior-Clausen syndrome. Case report and review of the literature.
J Neurosurg: 96(1 Suppl) 112-7. 2002
- Kandziora F., Pflugmacher R., Ludwig K., Duda G., Mittlmeier T. & Haas N.P.:
Biomechanical comparison of four anterior atlantoaxial plate systems.
J Neurosurg: 96(3 Suppl) 313-20. 2002
- Kandziora F., Pflugmacher R., Scholz M., Knispel C., Hiller T., Schollmeier G., Bail H., Schmidmaier G., Duda G., Raschke M. & Haas N.P.:
Comparison of BMP-2 and combined IGF-I/TGF- β 1 application in a sheep cervical spine fusion model.
Eur Spine J.: 11(5) 482-93. 2002
- Kandziora F., Pflugmacher R., Scholz M., Schafer J., Schollmeier G., Schnake K.J., Bail H., Duda G. & Haas N.P.:
[Experimental fusion of the sheep cervical spine. Part I: Effect of cage design on interbody fusion]
Chirurg: 73(9) 909-17. 2002
- Kandziora F., Pflugmacher R., Kleemann R., Duda G., Wise D.L., Trantolo D.J. & Lewandrowski K.U.:
Biomechanical analysis of biodegradable interbody fusion cages augmented With poly(propylene glycol-co-fumaric acid).
Spine: 27(15) 1644-51. 2002
- Kandziora F., Schmidmaier G., Schollmeier G., Bail H., Pflugmacher R., Gorke T., Wagner M., Raschke M., Mittlmeier T. & Haas N.P.:
IGF-I and TGF- β 1 application by a poly-(D,L-lactide)-coated cage promotes intervertebral bone matrix formation in the sheep cervical spine.
Spine: 27(16) 1710-23. 2002
- Kandziora F., Schollmeier G., Scholz M., Schaefer J., Scholz A., Schmidmaier G., Schroder R., Bail H., Duda G., Mittlmeier T. & Haas N.P.:
Influence of cage design on interbody fusion in a sheep cervical spine model.
J Neurosurg: 96(3 Suppl) 321-32. 2002
- Kandziora F., Scholz M., Pflugmacher R., Krummrey G., Schollmeier G., Schmidmaier G., Schnake K.J., Duda G., Raschke M. & Haas N.P.:
[Experimental fusion of the sheep cervical spine. Part II: Effect of growth factors and carrier systems on interbody fusion]
Chirurg: 73(10) 1025-38. 2002

- Khodadadyan-Klostermann C., Liebig T., Melcher I., Raschke M. & Haas N.P.:
Osseous integration of hydroxyapatite grafts in metaphyseal bone defects of the proximal tibia (CT-study).
Acta Chir orthop Traum: 69(1) 16-21. 2002
- Khodadadyan-Klostermann C., Raschke M., Fontes R., Melcher I., Sossan A., Bagchi K. & Haas N.:
Treatment of complex proximal humeral fractures with minimally invasive fixation of the humeral head combined with flexible intramedullary wire fixation - introduction of a new treatment concept.
Langenbeck Arch Surg: 387(3-4) 153-60. 2002
- Klein P., Schell H., Streitparth F., Kandziora F., Heller M. & Duda G.
Frakturheilstadium am Schaf – Entwicklung und Validierung eines muskuloskelettalen Modells des Schafshinterlaufes
Tierlaboratorium: 24 21-29. 2002
- Lill H., Hepp P., Gowin W., Oestmann J.W., Korner J., Haas N.P., Josten C. & Duda G.N.:
[Age- and gender-related distribution of bone mineral density and mechanical properties of the proximal humerus]
Rofo Fortschr Rontg: 12 99-99, 2002
- Muller M., Käab M., Villiger C. & Holzach P.:
Osteolysis after open shoulder stabilization using a new bio-resorbable bone anchor: A prospective, non-randomized clinical trial
Injury: 33(Suppl. 2) 30-36, 2002
- Pufe T., Wildemann B., Petersen W., Mentlein R., Raschke M. & Schmidmaier G.:
Quantitative measurement of the splice variants 120 and 164 of the angiogenic peptide vascular endothelial growth factor in the time flow of fracture healing: a study in the rat.
Cell Tissue Res: 309(3) 387-92. 2002
- Raschke M., Wildemann B., Inden P., Bail H., Flyvbjerg A., Hoffmann J., Haas N.P. & Schmidmaier G.:
Insulin-like growth factor-1 and transforming growth factor-beta1 accelerates osteotomy healing using polylactide-coated implants as a delivery system: a biomechanical and histological study in minipigs.
Bone: 30(1) 144-51. 2002
- Schaser K.D., Bail H.J., Haas N.P. & Melcher I.:
[Treatment concepts of benign bone tumors and tumor-like bone lesions]
Chirurg: 73(12) 1181-90. 2002
- Scheffler S.U., Sudkamp N.P., Gockenjan A., Hoffmann R.F. & Weiler A.:
Biomechanical comparison of hamstring and patellar tendon graft anterior cruciate ligament reconstruction techniques: The impact of fixation level and fixation method under cyclic loading.
Arthroscopy: 18(3) 304-15. 2002

- Schmidmaier G., Wildemann B., Schwabe P., Stange R., Hoffmann J., Sudkamp N.P., Haas N.P. & Raschke M.:
A new electrochemically graded hydroxyapatite coating for osteosynthetic implants promotes implant osteointegration in a rat model.
J Biomed Mater Res: 63(2) 168-72. 2002
- Schmidmaier G., Wildemann B., Heeger J., Gabelein T., Flyvbjerg A., Bail H.J. & Raschke M.:
Improvement of fracture healing by systemic administration of growth hormone and local application of insulin-like growth factor-1 and transforming growth factor-beta 1.
Bone: 31(1) 165-72. 2002
- Schmidmaier G., Wildemann B., Cromme F., Kandziora F., Haas N.P. & Raschke M.:
Bone morphogenetic protein-2 coating of titanium implants increases biomechanical strength and accelerates bone remodeling in fracture treatment: a biomechanical and histological study in rats.
Bone: 30(6) 816-22. 2002
- Stockle U., Hoffmann R., Sudkamp N.P., Reindl R. & Haas N.P.:
Treatment of complex acetabular fractures through a modified extended iliofemoral approach.
J Orthop Trauma: 16(4) 220-30. 2002
- Stockle U., Konig B., Dahne M., Raschke M. & Haas N.P.:
[Computer assisted pelvic and acetabular surgery. Clinical experiences and indications]
Unfallchirurg: 105(10) 886-92. 2002
- Strobel M.J., Weiler A., Schulz M.S., Russe K. & Eichhorn H.J.:
Fixed posterior subluxation in posterior cruciate ligament-deficient knees: diagnosis and treatment of a new clinical sign.
Am J Sport Med: 30(1) 32-8. 2002
- Taylor W.R., Roland E., Ploeg H., Hertig D., Klabunde R., Warner M.D., Hobatho M.C., Rakotomanana L. & Cliff S.E.:
Determination of orthotropic bone elastic constants using FEA and modal analysis.
J Biomech: 35(6) 767-73. 2002
- Thomale U.W., Kroppenstedt S.N., Beyer T.F., Schaser K.D., Unterberg A.W. & Stover J.F.:
Temporal profile of cortical perfusion and microcirculation after controlled cortical impact injury in rats.
J Neurotraum: 19(4) 403-13. 2002
- Thomale U.W., Schaser K., Kroppenstedt S.N., Unterberg A.W. & Stover J.F.:
Cortical hypoperfusion precedes hyperperfusion following controlled cortical impact injury.
Acta Neurochir Suppl Wien: 81 229-31. 2002

- Weiler A., Hoffmann R.F., Bail H.J., Rehm O. & Sudkamp N.P.:
Tendon healing in a bone tunnel. Part II: Histologic analysis after biodegradable interference fit fixation in a model of anterior cruciate ligament reconstruction in sheep.
Arthroscopy: 18(2) 124-35. 2002
- Weiler A., Peine R., Pashmineh-Azar A., Abel C., Sudkamp N.P. & Hoffmann R.F.:
Tendon healing in a bone tunnel. Part I: Biomechanical results after biodegradable interference fit fixation in a model of anterior cruciate ligament reconstruction in sheep.
Arthroscopy: 18(2) 113-23. 2002
- Weiler A., Unterhauser F.N., Bail H.J., Huning M. & Haas N.P.:
Alpha-smooth muscle actin is expressed by fibroblastic cells of the ovine anterior cruciate ligament and its free tendon graft during remodeling.
J Orthopaed Res: 20(2) 310-7. 2002
- Weiler A., Scheffler S.U., Höher J.:
Transplantatauswahl für den primären Ersatz des vorderen Kreuzbandes
Orthopäde: 8(31) 731-740. 2002
- Windhagen H., Glockner R., Bail H., Kolbeck S. & Raschke M.:
Stiffness characteristics of composite hybrid external fixators.
Clin Orthop Relat R: 405 267-76. 2002

Awards

- **Gisela Sturm Award 2001, EFFORT, Rhodos**
M.O. Heller, G. Bergmann, G. Deuretzbacher, L. Dürselen, M. Pohl, L. Claes, N.P. Haas, G.N. Duda
Musculo-skeletal loading conditions at the hip during walking and stair climbing
- **Arthur-Vick-Preis 2001 der Assoziation für Orthopädische Rheumatologie**
F. Kandziora, F. Kerschbaumer, M. Starker, T. Mittlmeier
Biomechanical assessment of transoral plate fixation for atlantoaxial instability
- **New Investigator Recognition Award 2002, Orthopaedic Research Society**
G. Schmidmaier, B. Wildemann, F. Cromme, F. Kandziora, N. Haas, M. Raschke
BMP-2 coating of titanium implants increases biomechanical strength and accelerates bone remodelling in fracture treatment
- **Ferdinand Sauerbruch Forschungspreis 2002**
M. Schütz, A. Schmeling, K. Ho, H. Bail, E. Schneider, N.P. Haas
Neue Stabilisierungskonzepte mit Fixateur intern Systemen bei der Versorgung von Frakturen langer Röhrenknochen
- **S. M. Perren Award 2002, The European Society of Biomechanics**
J.P. Kassi, M. O. W. Heller, U. Stöckle, C. Perka, G.N. Duda
Muscle activity is essential for a realistic pre-clinical evaluation of primary stability in THA
- **Hans-Liniger-Preis 2002 der Deutschen Gesellschaft für Unfallchirurgie**
F. Kandziora, R. Pflugmacher, M. Scholz, J. Schäfer, G. Schollmeier, K.J. Schnake, H. Bail, G. Duda, N.P. Haas
Experimentelle Spondylodese der Schafshalswirbelsäule
- **Forumspreis experimentelle Unfallchirurgie 2002 der Deutschen Gesellschaft für Unfallchirurgie**
S.U. Scheffler, V. Schönfelder, P. Hunt, H. Chwastek, N.P. Südkamp, A. Weiler
Untersuchung des Langzeiteffekts von thermischer Schrumpfung des chronisch relaxierten vorderen Kreuzbandes am Schafsmode

Research Guests

Dr. Eric S. Steenlage, Haddonfield NJ, USA

Prof. Dr. Li Zhang, Fujian University, China

PD. Dr. Helmut Lill, Universitätsklinikum Leipzig, Germany

Dr. Pierre Hepp, Universitätsklinikum Leipzig, Germany

Students

Akman, Özcan

Ali, Majid

Alquiza, Miguel

Bamdad, Peymam

Baumgartner, Axel

Beyer, Thomas

Blank, Jessica

Bodman, Georg

Brenner, Niki

Cem Yetimoglu

Chwastek, Heike

Crnogorac, Vladan

Cromme, Felix

Daniel Ostapowicz

Demitter, Lutz

Dukic, Mirela

Dustmann, Moritz

Eckert, Nils

Endres, Michaela

Esser, Klaus-Tilman

Exner, Christine

Faensen, Benjamin

Falcke, Gotthard

Falk, Roman

Frahnow, Silke

Fuchs, Thomas

Funk, Julia

Gäblein, Tobias

Gangéy, Insa

Geisen, Bärbel

Gießel, Claudia

Großhauser, Johannes

Gumnior, Sarah

Haebler, Christine

Hartenstein, Katarina

Heeger, Joanna

Holmer, Christoph

Hügler, Susanne

Inden, Philipp

Izadpanah, Kaywan

Jasper, Maria

Jung, Tobias

Kadow-Romacker, Anke

Kähler, Britta

Karen Baehr	Ramme, Andreas
Keil, Judith	Reuther, Theresa
Keil, Stefanie	Rotter, Andreas
Kleis, Alexa	Sadoni, Sebastian
Kliche, Alexander	Sander, André
Knies, Moritz	Scherler, Jörn
Knispel, Christian	Schill, Alexander
König, Christian	Schleicher, Philip
Koristka, Anja	Schlichting, Karin
Kretschmar, Martin	Schmidt, Tanja
Kröller-Helen, Anna	Schneider, Constanze
Kuhn, Henrike Franziska	Scholz, Alexandra
Leonhardt, Uwe	Schwabe, Philip
Malzacher, Heidrun	Schwarzkopf, Joerg
Margariti, Rodanthe	Schwarzlose, Cathleen
Marten, Alexander	Sollmann, Michael
Melis, Björn	Sperfeld, Marc
Mladek, Markus	Sporrer, Simon
Mohr, Svenja	Spranger, Nicolai
Muchow, Sarah	Streitparth, Florian
Oevermann, Philip	Surke, Carsten
Opitz, Mark	Teschner, Steffi
Ordell, Sebastian	Voigt, Jutta
Palasdiess, Natalie	von Cramon, Lotta
Parwani, Abdul	Wagner, Martin
Pirschel, Daniela	Weber, Jörg
Pohlmann, Paula	Weiss, Markus
Pütz, Andrej	Wolf, Claudia
Quandte, Steffanie	

Congresses – Symposia

- **2. LCP Meeting**
05. und 06. Oktober 2001, Berlin
Thema: Neue winkelstabile Implantate, Vorträge und Falldiskussionen
- **CAB 2002, Chirurgische Arbeitsgemeinschaft Biomaterialien**
Jahrestagung 2001/2002, 19. Januar 2002, Berlin
Thema: Oberflächeneigenschaften und Methoden der Beschichtung von Biomaterialien
- **BCG 2002, 26. Berliner Chirurgetreffen**
Berliner Chirurgische Gesellschaft, Vereinigung der Chirurgen Berlins und Brandenburgs
21. bis 23. Februar 2002, Berlin
Thema: Komplikationsmanagement in der Chirurgie
- **3. LCP Meeting**
27. und 28. September 2002, Berlin
Thema: Neue winkelstabile Implantate, Vorträge und Falldiskussionen
- **3. Arbeitsseminar für niedergelassene Chiruginnen und Chirurgen Berlin**
21. und 22. Juni 2002, Berlin
Handchirurgie mit Live Ops
- **Specialty Day Berlin**
18. September 2002, Berlin
Thema: Spezielle Aspekte der vorderen Kreuzbandverletzung

Equipment

Mechanical Testing

- Zwick 1455 material testing, axial / torsional
- Instron 8871 servohydraulic material testing, axial
- 2 Novel emed force plate ST4
- Goniometer, Penny and Giles
- Intramedullary pressure sensor, Mammendorfer Institute
- Qualisys PCReflex 3-camera system
- Vicon 3-camera system
- Polhemus 'Motiontracker' (3 sensors)
- HBM MGC Amplifier with 4 slots
- HBM Spider & CatMan32, 4 amplifier with 4 slots
- Strain gauges to bone
- Ultrasound equipment
- CAD environment
- Vicon System

Histology, Immunhistology

- Exakt Cutting System
- Leica Microtome
- Exakt Micro Grinding System
- Exakt Light Polymerisation
- Wirtz Hand Grinding Machine
- Zeiss Kontron KS 400 Image analysis, incl. 2 working units
- Leica DMR mit 3 Chip CCD Camera, Fluoreszenz, Polarisation
- Intravital microscopy

Computer Simulation

- SGI Octane 2, SGI Octane, SGI O2, HP 715/80
- Marc 7 / Mentat 3.1 & Truegrid
- 30 Pentium IV NT workstations

Access to Animal Experiment Facilities